

Elucidating different aspects of protocell emergence on the early Earth

A thesis

Submitted in partial fulfillment of the requirements

Of the degree of

Doctor of Philosophy

By

Manesh Prakash Joshi
20163437



INDIAN INSTITUTE OF SCIENCE EDUCATION AND RESEARCH PUNE

2022

CERTIFICATE

Certified that the work incorporated in the thesis entitled “**Elucidating different aspects of protocell emergence on the early Earth**” submitted by Manesh Prakash Joshi was carried out by the candidate, under my supervision. The work presented here or any part of it has not been included in any other thesis submitted previously for the award of any degree or diploma from any other University or institution.



Dr. Sudha Rajamani
(Thesis Supervisor)

Date: 11th July, 2022

DECLARATION

I declare that this written submission represents my ideas in my own words and where others' ideas have been included; I have adequately cited and referenced the original sources. I also declare that I have adhered to all principles of academic honesty and integrity and have not misrepresented or fabricated or falsified any idea/data/fact/source in my submission. I understand that violation of the above will be cause for disciplinary action by the Institute and can also evoke penal action from the sources that have not been properly cited or from whom proper permission has not been taken when needed.



Manesh Prakash Joshi

Roll no. 20163437

Date: 11th July, 2022

ACKNOWLEDGEMENTS

This entire Ph.D. tenure was an incredible expedition and a whole new learning experience for me. This journey wouldn't have been possible without the generous help, support, and motivation I received at different stages. Therefore, I take this opportunity to acknowledge the same.

First and foremost, I thank God for everything. Then I would like to express my sincere thanks to my Ph.D. advisor, Dr. Sudha Rajamani, for giving me the opportunity to work with her. She was extremely helpful and supportive both on a personal and professional level. She was very patient and always backed me up when I struggled with work-life balance. She was always open to new ideas and encouraged me to drive my own project from the very beginning, which played a vital role in nurturing the independent researcher in me. I would also like to acknowledge my research advisory committee (RAC) members, Dr. Saikrishnan Kayarat, Dr. Nishad Matange, and Dr. Sayam Sen Gupta, for their constructive comments and valuable suggestions, which helped a lot to shape my Ph.D. project. I sincerely thank our collaborators for their help with the geochemical analysis of the hot spring water samples-Dr. Gyana Ranjan Tripathy at IISER Pune, his lab members Dr. Anupam Samanta and Rakesh Kumar Rout; and Prof. Martin J. Van Kranendonk and Luke Steller at UNSW, Australia. I am very grateful to Dr. David Deamer, Dr. Tony Jia, and Dr. Irena Mamajanov for all the scientific discussions and their crucial inputs on my research.

I would also like to thank all the present and past COoL lab people. It was great fun to work with them. I thank Chaitanya and Niraja for being very supportive senior colleagues and mentoring me during the early days of my Ph.D. A special thanks to Anupam, Shikha, and Susovan for being with me as friends and great colleagues throughout this time. Thank you, Souradeep, Gauri, Raya, Kushan, and all the current and past undergraduate lab members for maintaining such a lively environment in the lab.

I thank the Biology and Chemistry departments at IISER Pune for providing all the facilities and financial support. I would like to acknowledge in particular, the microscopy, HRMS, LC-MS, and NMR facilities at IISER Pune, which were crucial for accomplishing this work. A special thanks to Vijay Vitthal and Sandeep Kanade for their help during the microscopy and HRMS data acquisition respectively. I would also like to thank all the staff

members of the IISER academic office and Bio-admin, especially Kalpesh, Piyush, Mahesh, Rupali, and Mrinalini, for their help with all the academic stuff. I sincerely thank UGC and IISER Pune for the fellowship support.

I would like to conclude these acknowledgments by thanking my family and friends. I wouldn't have been what I am today without my family. I thank my parents, my brother and his family, and my wife for their unconditional love and support, and their constant faith in me, which motivated and immensely helped me to follow my dreams. Thank you, my little angel, for making my life beautiful. Finally, I would like to thank all my friends at IISER, especially, Vibishan, Abinaya, Alakananda, and Neelay, for all the fun and great memories.

TABLE OF CONTENTS

CERTIFICATE.....	2
DECLARATION.....	3
ACKNOWLEDGEMENTS.....	4
LIST OF FIGURES	7
LIST OF TABLES	9
SYNOPSIS.....	10
CHAPTER 1 – INTRODUCTION	17
CHAPTER 2 – THE EFFECT OF A MEMBRANE-FORMING AMPHIPHILE ON ABIOTIC PEPTIDE SYNTHESIS UNDER WET-DRY CYCLES.....	30
Introduction	31
Materials and methods.....	33
Results.....	36
Discussion.....	52
References.....	53
CHAPTER 3 – EXPLORATION OF N-ACYL AMINO ACIDS AS A NEW MODEL PROTOAMPHIPHILE SYSTEM.....	59
Introduction	60
Materials and methods	61
Results	66
Discussion.....	85
References.....	88
CHAPTER 4 – TESTING THE PREBIOTIC MEMBRANE ASSEMBLY PROCESS IN NATURAL, EARLY EARTH ANALOGUE HOT SPRING CONDITIONS	93
Introduction	94
Materials and methods	97
Results.....	99
Discussion.....	110
References.....	112
CHAPTER 5 SUMMARY AND CONCLUSIONS.....	115
PUBLICATIONS	118
COPYRIGHT LICENSCE PERMISSIONS.....	119

LIST OF FIGURES

Figure	Page
Figure 1.1 Different approaches used to explain the origin and evolution of life on Earth	19
Figure 1.2 Protocell: A crucial intermediate step during the abiotic to biotic transition	20
Figure 1.3 Wet-dry cycles and their role in protocell emergence	22
Figure 1.4 Formation of new amphiphiles via amphiphile-co-solute interactions in a prebiotic soup	24
Figure 1.5 Importance of validating laboratory outcomes under natural Conditions	25
Figure 2.1 Formation of Gly oligomers in the presence of POPC under wet-dry cycles and the effect of POPC on their overall yield	37
Figure 2.2 Effect of POPC on the yield of individual Gly oligomers	38
Figure 2.3 Effect of POPC on Gly oligomer yield with varying Gly to POPC ratios	38
Figure 2.4 Effect of POPC on overall glycine oligomer yield at 130°C	39
Figure 2.5 TLC analysis of Gly (G) + POPC (P) reaction mixture	40
Figure 2.6 Effect of POPC concentration and wet-dry cycles on the formation of new product as analysed by TLC	41
Figure 2.7 Formation of NAAs in the Gly + POPC reaction	42
Figure 2.8 Detection of phosphocholine-based hydrolysis products in the POPC control reaction	43
Figure 2.9 Confirmation of NAA formation in the Gly + POPC reaction by HRMS/MS and NMR analysis	45
Figure 2.10 NAA formation by other amino acids and phospholipids	47
Figure 2.11 Reaction mechanism for the NAA formation from amino acids and phospholipids	50
Figure 2.12 Mechanism of the amide bond formation in peptides versus in the NAAs	51
Figure 3.1 Conversion of GMO to NOG in the presence of Gly under wet-dry cycles	67
Figure 3.2 Control reactions for the NOG synthesis experiment	68
Figure 3.3 The ¹ H NMR analysis of GMO + OA + Gly wet-dry cycling reaction	69

Scheme 3.1 A plausible mechanism for NAA synthesis from GMO and amino acid through an ester-amide exchange reaction	70
Figure 3.4 NAAs self-assemble into vesicles on their own under acidic conditions	71
Figure 3.5 Encapsulation of calcein in NAA vesicles	72
Figure 3.6 Temperature-dependent phase behavior of NOG and NOS	73
Figure 3.7 Vesicle formation by NOG + GMO mixed system	74
Figure 3.8 Vesicle formation behavior of the NOG + OA mixed system	75
Figure 3.9 Effect of Mg^{2+} on pure NOG and NOG + GMO mixed vesicles	77
Figure 3.10 Re-formation of vesicles from magnesium-induced aggregates after the addition of a chelator	79
Figure 3.11 Effect of Na^+ on the stability of NOG-based vesicles	79
Figure 3.12 Schematic representation of the reaction of NOG with amino acids to form N-acylated peptide amphiphiles	80
Scheme 3.2 Acid-amine coupling reaction between NOG and amino acid, generating N-acylated peptides	81
Figure 3.13 Formation of Gly-containing lipopeptides by the reaction between NOG and Gly	81
Figure 3.14 Effect of temperature on the maximum length of the peptide chain generated on the NOG head group	83
Figure 3.15 Reaction of NOG with an amino acid other than Gly results in the formation of N-acylated heteropeptides	84
Figure 4.1 Different fatty acids and their derivatives used in fatty acid-based experiments	100
Figure 4.2 Vesicle formation behavior of oleic acid-based amphiphile systems in the laboratory “buffered” versus “natural” hot spring water sample	101
Figure 4.3 Vesicle formation behavior of oleic acid-based amphiphile systems in CH and PA hot spring water samples	102
Figure 4.4 UDA + UDG binary system generates vesicles in all hot spring water samples	103
Figure 4.5 DA + GMD binary system generates vesicles in all hot spring water samples	104
Figure 4.6 Vesicle formation behavior of DA + DOH + GMD tertiary system in the laboratory buffered versus hot spring water samples	105

Figure 4.7 Vesicle formation behavior of NOG-based amphiphile systems in hot spring water samples	109
Figure 4.8 Vesicle formation behavior of NOG + OOH mixed system in hot spring water samples	110

LIST OF TABLES

Table	Page
Table 2.1 Masses corresponding to different amphiphiles that were detected during the HRMS analysis of the Gly + POPC and the only POPC control reactions	44
Table 2.2 Different NAA masses observed during the HRMS analysis of the amino acid and lipid variation reactions	48
Table 4.1 A summary of the vesicle formation behavior of different fatty acid-based systems in bicine buffer and different hot spring water samples	106
Table 4.2 Geochemical analysis of hot spring water samples used in fatty acid-based experiments	107
Table 4.3 Geochemical analysis of the hot spring water samples used in NAA-based experiments	108

Synopsis

Chapter 1: Introduction

A cell is the basic unit of life, which itself is a highly organized chemical system where many molecules and their assemblies work in harmony to give a particular cell its unique identity. However, it is not yet fully understood how the first cells might have originated from a complex mixture of chemical compounds (also called a prebiotic soup) on the early Earth, which remains one of the biggest scientific questions of all time. It has been postulated that this transition from prebiotic chemistry to modern biology likely followed a fundamental step of protocell formation. A protocell is considered a primitive cell-like structure containing informational and functional molecules encapsulated in a membrane compartment. Two processes are thought to have been crucial for protocell formation; 1. Membrane assembly from single-chain amphiphiles (SCAs), and 2. Abiotic synthesis of oligomers like nucleic acids and peptides from their respective monomers. Given that both membrane assembly and abiotic oligomerization processes might have co-occurred in a common milieu and resulted in protocells, it is imperative to check how these processes would have affected each other under prebiotically-plausible conditions. In this context, certain features of terrestrial hot springs, such as their low ionic strength, high temperature, a diverse range of pH, and wet-dry cycles, are thought to have facilitated the above-mentioned crucial events during the origin of cellular life. Especially the wet-dry cycle is an interesting feature wherein a chemical system would experience consecutive dry and aqueous phases due to natural events like day-night cycles, seasonal changes, etc. Among the two oligomerization processes mentioned above, earlier studies mainly looked at the effect of membrane-forming amphiphiles on the abiotic nucleic acid synthesis under wet-dry cycling conditions [1,2]. However, it is not known how amphiphiles influence abiotic peptide synthesis under geologically-relevant wet-dry cycles. Therefore, we first investigated this important and still unanswered question in the origin of life research.

Chapter 2: The effect of membrane-forming amphiphiles on abiotic peptide synthesis under wet-dry cycles.

We checked how lipid's presence affects abiotic peptide synthesis under wet-dry cycles in terms of their formation and overall yield and also investigated the underpinning mechanism behind the effect we observed. For this, we used 1-palmitoyl-2-oleoyl-sn-glycero-3-phosphocholine (POPC) as a proxy for membrane-forming lipid and checked its effect on glycine (Gly) oligomerization under wet-dry cycles. Upon LC-MS analysis, Gly oligomers up to hexamers were detected in the Gly + POPC reaction. However, the overall peptide yield was lower in the presence of POPC when compared to the control reaction that did not contain POPC. A plausible reason for this effect might have been a cross-reaction between Gly & POPC that could have resulted in the formation of a new product. Preferential utilization of Gly for this cross-reaction would have rendered fewer Gly molecules available for peptide synthesis, thereby decreasing the overall peptide yield. A preliminary TLC analysis of the reaction mixture indeed showed a new spot on the TLC plate. Further HRMS analysis led to the identification of two new compounds: N-palmitoyl glycine and N-oleoyl glycine (NOG). They belong to an intriguing class of single-chain amphiphiles called N-acyl amino acids (NAAs), which contain an amino acid head group attached to a fatty acid chain via an amide linkage. Notably, the formation of NAA was also observed with other amino acids and phospholipids, indicating the generality of this reaction. Mechanistically, it can be explained as an example of an ester-amide exchange phenomenon, where the nucleophilic amino group of an amino acid attacks one of the ester linkages of the phospholipid to form an alcohol and an amide (which is NAA in this case). To our knowledge, this is the first experimental demonstration of ester-amide exchange occurring between amino acids and lipids under prebiotically-plausible wet-dry cycling conditions. In the Gly + POPC reaction, the kinetically favorable NAA synthesis would have outcompeted the peptide synthesis for the utilization of the free Gly, which caused the lowering of the Gly oligomer yield in the presence of POPC. These results highlight the necessity of adopting a systematic and unbiased approach while exploring the interdependence between the above-mentioned (and other) prebiotic processes. It could lead to identifying hitherto undescribed chemical species, which might have important implications for the emergence of life processes.

Chapter 3: Exploration of N-acyl amino acids as a new model protoamphiphile system

N-acyl amino acid, identified as a novel product in our earlier reaction, is a hybrid molecule of fatty acid and amino acid. This amalgamation of two prebiotically important molecules within a single chemical species might have allowed NAAs to exploit properties of both amino acids and fatty acids, as well as to acquire new emergent properties. Therefore, it would be interesting to explore NAAs as model protoamphiphiles (prebiotically-plausible SCAs that might have constituted protocell membranes on early Earth), which has not been done to date. Towards this, we systematically evaluated different aspects pertaining to this amphiphile system, including; 1. their synthesis from prebiotically-relevant reactants under early Earth conditions, 2. their ability to self-assemble into vesicles, and also the pH and metal ion stability of NAA-based vesicles, and 3. the potential of NAA to act as a substrate for peptide chain growth, thereby generating different lipopeptides. We mainly used N-oleoyl glycine (NOG) as the representative NAA amphiphile for all these experiments.

Earlier, we showed the synthesis of NAAs from phospholipids and amino acids under wet-dry cycling conditions. However, phospholipids themselves are structurally complex diacyl lipids that depend on SCA precursors for their synthesis both in biosynthetic [3] and potentially prebiotic enzyme-free reactions [4]. Therefore, we checked whether chemically simpler, prebiotically-relevant, ester linkage-containing SCAs like monoglycerides, could react with amino acids via ester-amide exchange to generate NAAs. Towards this, a mixture of glycerol 1-monooleate (GMO), oleic acid (OA), and Gly was subjected to wet-dry cycles under previously standardized conditions for a phospholipid-amino acid reaction. TLC and HRMS analyses indeed showed the conversion of GMO to NOG upon wet-dry cycling, and this monoglyceride to NAA conversion was also observed with other amino acids. To our knowledge, this describes a new prebiological route for NAA synthesis, which supports their potential availability on the early Earth.

Subsequently, we checked whether NAAs could self-assemble into vesicles on their own, which would have been an essential property for them to act as protocell compartments. Unlike phospholipids, SCAs preferentially form vesicles when the pH of the solution is around the apparent pKa of their head group [5]. Using DIC and fluorescence microscopy, we showed that NAAs like NOG could indeed form vesicles in the acidic pH range around pH 5 to 6. This vesicle formation behavior is markedly different from what we see in fatty acid-based

conventional model protoamphiphiles that form vesicles only at neutral to alkaline pH. Furthermore, admixing NOG with other amphiphiles like GMO and OA dramatically increased the vesicle formation range of the mixed system, with the mixture of NOG and GMO forming vesicles from pH 4 to 11, while that of NOG and OA resulted in vesicles from pH 5 to 9. The latter result is particularly intriguing as blending NOG and OA enabled this mixed system to form vesicles over a wider pH range compared to its individual components. These results nicely demonstrate how amphiphiles affect each other's physicochemical properties in a mixture. They also highlighted the ability of NOG to generate robust membranes over a diverse pH range when mixed with other amphiphiles, which would have provided a significant advantage for protocell compartments incorporating these moieties. Furthermore, we also evaluated the metal ion stability of NOG-based vesicles, as metal ions have been shown to play a crucial role in other prebiotic reactions, especially those pertaining to the RNA world [6,7]. However, high concentrations of such metal ions tend to destabilize negatively charged SCA vesicles by inducing their aggregation. Nonetheless, the addition of surfactants like monoglycerides has been shown to increase the stability of the resultant mixed vesicles towards metal ions. Given this backdrop, we evaluated the metal ion stability of NOG vesicles using DIC microscopy and also checked whether the addition of monoglycerides like GMO could provide a further stabilizing effect in the presence of metal ions. For divalent cations like Mg^{2+} , magnesium-induced aggregates of pure NOG vesicles were observed when the Mg^{2+} concentration exceeded the NOG concentration. However, the addition of GMO significantly increased the Mg^{2+} stability of NOG + GMO mixed vesicles, and this overall effect was consistent even for monovalent cations like Na^+ . Notably, the intrinsic stability of NOG vesicles was almost 100-fold higher in the presence of sodium (a monovalent cation) than in magnesium. These results highlight the ability of NAAs to generate metal-ion tolerant membranes, whose robustness further increases when admixed with monoglycerides.

Finally, we checked the ability of NAAs to act as a substrate for peptide chain growth by reacting with amino acids, where the addition of subsequent amino acids to the free carboxyl terminus of the NAA head group can generate different lipopeptides. Towards this, a mixture of NOG and an amino acid was subjected to a single wet-dry cycle at 130 °C, and peptide chain extension products were detected by HRMS. The reaction between NOG and Gly led to the formation of N-oleoyl glycine peptides with up to three Gly additions on to the NOG. However,

the addition of only a single amino acid was observed for the reactions of NOG with other amino acids (Lys, Ala, Val, and Ser). These results show the potential of NAAs to generate N-acylated peptide amphiphiles under prebiotically-pertinent wet-dry cycling conditions. Such membrane-anchored short peptides could have enabled protocell membranes to perform active catalysis on their surface, and might have allowed them to act as ‘signaling’ moieties allowing protocell communication.

In summary, these results together demonstrate NAAs as a promising model protoamphiphile system and underscore their importance in the emergence and evolution of early cellular life on Earth.

Chapter 4: Testing prebiotic membrane assembly process in water samples collected from early Earth analogue hot spring sites

In this chapter, we discuss a new and slightly unorthodox approach recently adopted to better understand the origin of life conundrum. Most of the discoveries in the origin of life research are an outcome of experiments performed in the laboratory using highly pure reagents and solvents, and under stringently controlled reaction conditions. There is a tacit assumption that the outcome will be similar under natural conditions as well, which are incredibly complex and diverse in nature. To validate this assumption, one could either perform these experiments directly in the field, but that in itself is a very challenging task for several practical reasons. Alternatively, one could collect samples from such natural, early Earth analogue sites and use them to perform experiments in the laboratory. It will essentially give a more realistic sense of how prebiotic processes might advent under natural conditions compared to stringently controlled laboratory conditions. Towards this, we tested the prebiotic membrane assembly process in water samples collected from active hot springs situated in certain astrobiologically relevant sites (e.g., Ladakh in India, Tikitere in New Zealand). It also enabled us to evaluate the conduciveness of terrestrial hot springs for the prebiotic membrane assembly process, which in turn allows testing their potential as a plausible niche for the origin of life on Earth. Towards this, the vesicle formation behavior of both fatty acid-based and NAA-based amphiphile systems was studied in different hot spring water samples. Considering the pH range at which these amphiphiles form vesicles under laboratory buffered conditions, we used hot spring water samples having neutral to alkaline pH for fatty acid-based systems and those with acidic to neutral pH for NAA-based systems. In fatty acid-based experiments, different combinations of

OA and its derivatives like GMO and oleyl alcohol readily formed vesicles under laboratory buffered conditions. However, in the hot spring water samples, only a mixture of OA and GMO could form vesicles. Also, there was a positive correlation between the overall vesicle forming propensity and the ionic strength of the different hot spring samples. These results were consistent over different fatty acid types irrespective of their chain length and the presence of unsaturation. Subsequently, we performed similar experiments with NAA-based systems, wherein both pure NOG and NOG + GMO mixed systems were able to self-assemble into vesicles in hot spring samples. Together, these results demonstrated that hot spring waters could overall support the prebiotic membrane assembly process. Furthermore, they could also act as a selection pressure, where certain amphiphile combinations preferentially formed vesicles over the others, which also highlights the importance of validating laboratory outcomes under natural conditions.

Chapter 5: Summary and conclusions

In this chapter, we summarize the major findings of this Ph.D. work and discuss the implications of these results in a broad context of the origin of life research.

References

1. Rajamani, S.; Vlassov, A.; Benner, S.; Coombs, A.; Olasagasti, F.; Deamer, D. Lipid-assisted Synthesis of RNA-like Polymers from Mononucleotides. *Orig. Life Evol. Biosph.* **2008**, *38*, 57–74.
2. Mungi, C. V; Rajamani, S. Characterization of RNA-Like Oligomers from Lipid-Assisted Nonenzymatic Synthesis: Implications for Origin of Informational Molecules on Early Earth. *Life (Basel, Switzerland)* **2015**, *5*, 65–84.
3. Vance, J.E.; Vance, D.E. Phospholipid biosynthesis in mammalian cells. *Biochem. Cell Biol.* **2004**, *82*, 113–128.
4. Liu, L.; Zou, Y.; Bhattacharya, A.; Zhang, D.; Lang, S.Q.; Houk, K.N.; Devaraj, N.K. Enzyme-free synthesis of natural phospholipids in water. *Nat. Chem.* **2020**, *12*, 1029–1034.

5. Mansy, S.S. Model protocells from single-chain lipids. *Int. J. Mol. Sci.* **2009**, *10*, 835–43.
6. Inoue, A.; Takagi, Y.; Taira, K. Importance of magnesium ions in the mechanism of catalysis by a hammerhead ribozyme: strictly linear relationship between the ribozyme activity and the concentration of magnesium ions. *Magnes. Res.* **2003**, *16*, 210–7.
7. Bapat, N. V.; Rajamani, S. Templated replication (or lack thereof) under prebiotically pertinent conditions. *Sci. Rep.* **2018**, *8*, 15032.

Chapter 1
INTRODUCTION

1.1 Origin of life: The big question

How did life originate and evolve on Earth? This remains one of the biggest and most fundamental scientific questions to date. Starting with a complex pool of chemical compounds (also known as a prebiotic soup), the specific set of events that led to this transition from chemistry to biology about 3.8-4 billion years ago [1] remains elusive. But before going into further details, one needs to scientifically define “Life” to distinguish between living and non-living. In this context, several operational definitions of life have been proposed in the literature [2], the most popular being the one defined by the NASA exobiology program, which is as follows:

“Life is a self-sustained chemical system capable of undergoing Darwinian evolution” [3]. Keeping this conceptual framework in mind, researchers have used a variety of approaches to explain the origin and evolution of life on Earth (Figure 1.1). Among these, the three major approaches are the prebiotic RNA world-based approach, the compartmentalization-centric approach, and the metabolism-first approach. The prebiotic RNA world-based approach [4] exploits the ability of RNA to work both as a catalyst and an information storage molecule. It considers a self-replicating ribozyme as being the molecule central to the origin of life. This ribozyme then could have subsequently given rise to DNA and the protein machinery, where proteins took over the responsibility of catalysis, and DNA became the genetic material, as is observed in extant living systems.

The compartmentalization-centric approach, also known as the lipid world hypothesis, is based on a basic observation that most of the extant cellular life has some form of the compartment, which separates it from the surrounding environment and gives a particular cell its distinct identity. Therefore, the main assumption underlying this approach is that compartmentation would have also been a central phenomenon during the emergence of life, which further facilitated other processes required for the non-life to life transition [5]. This approach is supported by the fact that prebiotically-plausible amphiphiles can spontaneously self-assemble to generate cell-like compartments (vesicles) [6].

A third approach, popularly called the “metabolism-first approach,” states that primitive metabolic pathways, such as the reductive citric acid cycle, would have served as an initial step for the origin of life. These simple metabolic pathways then would have eventually given rise to other biomacromolecules at a later stage [7]. Furthermore, some other theories are also proposed in addition to the three theories mentioned above, such as the “peptide-RNA world hypothesis,” which considers mutualism between small peptides and RNAs to be crucial for the emergence of life on Earth [8]. Another theory called the “Iron-Sulfur World hypothesis” postulates the chemo-autotrophic origin of life on the iron sulfide mineral surfaces of deep hydrothermal vents [9,10]. This approach underscores the catalytic role played by Iron,

nickel, and other transition metal centers during the conversion of simple inorganic substrates to complex macromolecules.

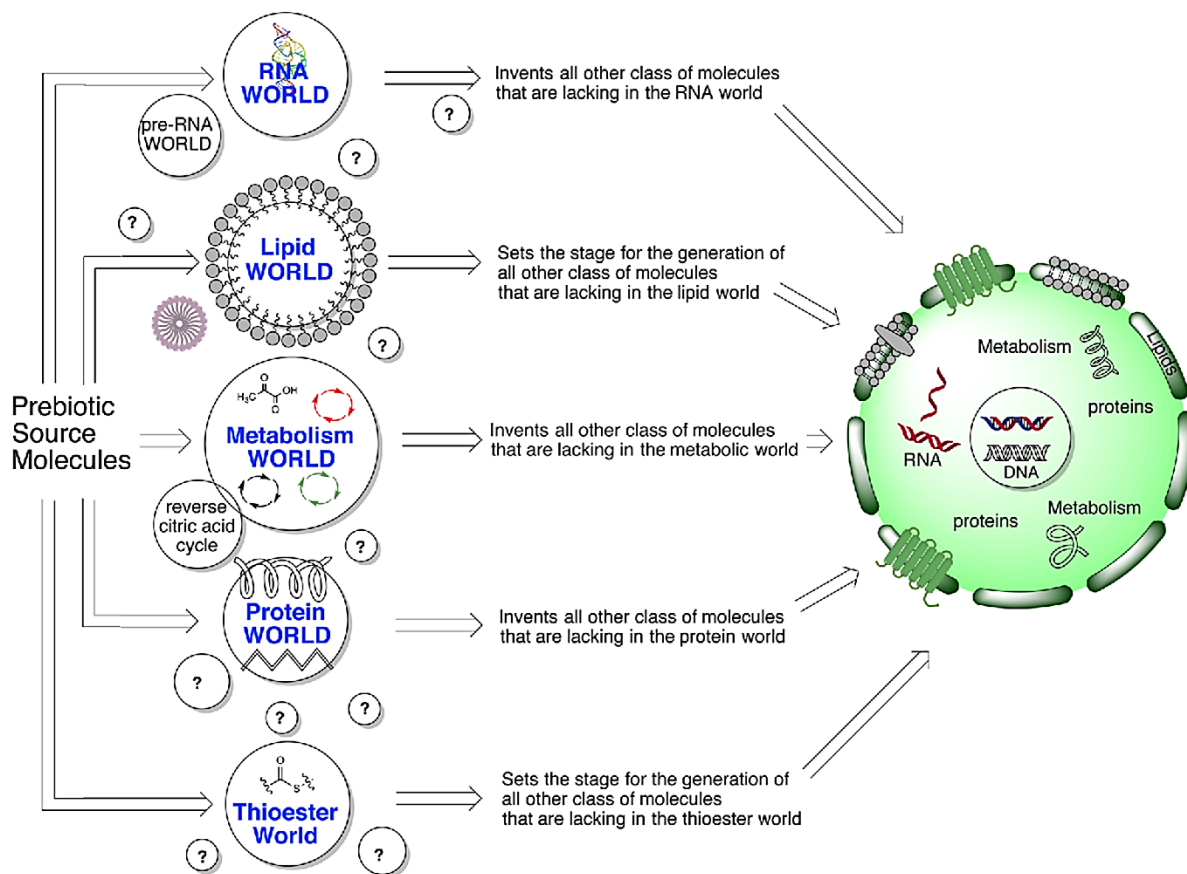


Figure 1.1 Different approaches used to explain the origin and evolution of life on Earth.

Image reproduced from Krishnamurthy, R. (2017) *Acc. Chem. Res.* [11]

Nonetheless, these individual approaches haven't yet provided a comprehensive picture of the abiotic to biotic transition. More recently, a "systems chemistry" approach has been gathering traction in the field, which emphasizes studying the networks of interacting molecules at a systems level rather than studying them in isolation [12,13]. This approach also stands logical from a prebiotic perspective as the "prebiotic soup" would have contained a diverse set of chemical species concurrently interacting with each other. Pursuing this approach further might lead to the identification of some new emergent properties/molecules originating from the set of interacting molecules at different hierarchical levels. It could facilitate a better understanding of life's origin, which itself is considered an emergent phenomenon. Notably, a recent study from Sutherland's group provides experimental support to the underlying principles of the systems chemistry approach. In this study, the authors reported the unexpected emergence of lipidated species of nucleotides and amino acids along with oligonucleotides

and peptides when they set up a single-pot reaction containing nucleotides, amino acids, and lipids in the presence of methyl isocyanide as an activating agent [14].

Nonetheless, despite having differences, all the approaches mentioned above assume that the formation of a protocell would have been a fundamental step during the emergence of life on Earth.

1.2 Protocell: A vital intermediate step during the abiotic to biotic transition

Protocell essentially serves as a hypothetical link between a complex mixture of chemical compounds in a prebiotic soup and the earliest life forms that are thought to have emerged from this mixture (Figure 1.2). In this context, a protocell formation is considered a stage where concurrent interactions between chemical compounds would have given rise to an ensemble with life-like properties. From an RNA world point of view, the protocell is defined as a cell-like entity wherein informational polymers capable of replication and catalysis (self-replicating ribozymes) are encapsulated in a replicating membrane compartment [15]. Another, more generalized definition of a protocell explains it as any experimental or theoretical model containing a self-assembled compartment linked to chemical processes occurring around or within it [16]. These chemical processes could vary from simple single-step reactions to more complex chemical pathways, which would have also involved the reactions that produced the building blocks of protocells themselves. Nonetheless, two processes are thought to have been fundamental for the formation of a protocell, namely membrane assembly of amphiphiles to form compartments, and the abiotic oligomerization of monomers to form polymers [5]. The prebiotic oligomerization reactions mainly pertain to the formation of nucleic acids (informational and/or catalytic polymers) from mononucleotides and the formation of peptides from amino acids (catalytic polymers).

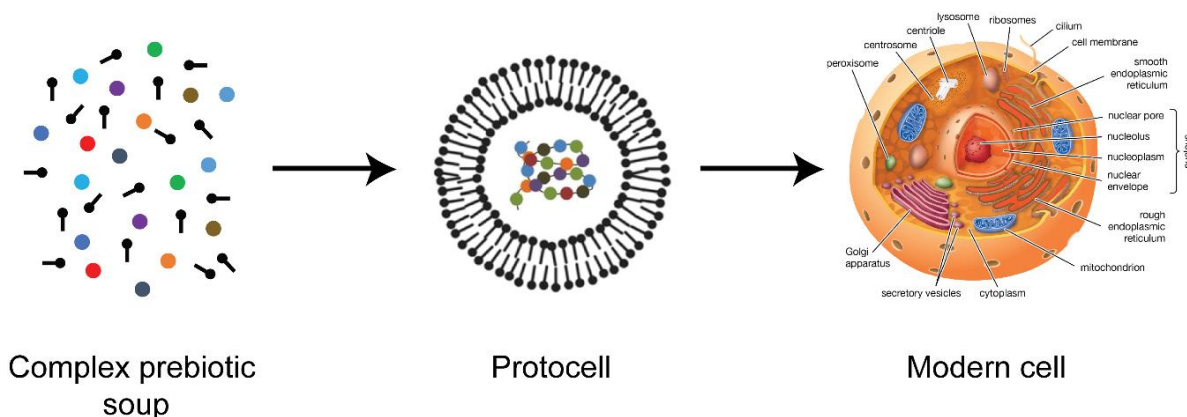


Figure 1.2 Protocell: A crucial intermediate step during the abiotic to biotic transition.

Content adapted from: Mansy, S.S. (2009) *Int. J. Mol. Sci.*[17], and <https://www.britannica.com/science/cell-biology#/media/1/101396/112877>

1.3 Defining the problem

Given that protocell formation would have involved a simultaneous occurrence of membrane assembly and abiotic oligomerization processes being facilitated in a common milieu, it raises several important questions:

- 1) How would these two processes have affected each other, and what type of environmental/geological setting(s) would have supported the simultaneous occurrence of these processes?
- 2) Can such interactions generate new chemical species that might have been potentially advantageous to the protocells themselves?
- 3) How would these prebiotically-pertinent processes have behaved under natural conditions instead of the stringently-controlled laboratory conditions under which we test them today?

In my Ph.D. work, I set out to address these key questions related to the emergence of protocells on the early Earth. In the following sections of this chapter, I will provide a brief context for each of the questions mentioned above, which define the subsequent chapters of this thesis. A more detailed introduction of these specific topics and relevant background literature are provided in the individual chapters.

1.4 Membrane assembly and abiotic oligomerization occurring under hot spring conditions: A plausible scenario for the emergence of protocells

Terrestrial hot springs are widely considered a promising niche for the origin of life [18]. This is mainly because of their pertinent features that can support both membrane assembly and abiotic oligomer synthesis, and also the encapsulation of the resultant oligomers into membrane compartments to form protocell-like structures. Unlike extant cellular membranes, which are mainly composed of phospholipids and proteins, the protocellular membranes are thought to have been made of relatively simpler single-chain amphiphiles (SCAs) [17]. These SCAs can spontaneously self-assemble into vesicles under certain conditions of temperature, pH, and ionic strength [19]. Typically, the overall low ionic strength of hot springs is thought to have been conducive to protocell membrane assembly from SCAs. Also, the diverse pH range observed for these hot springs could have provided pertinent pH regimes that favor SCA self-assembly.

In addition to being supportive of membrane assembly from SCAs, terrestrial hot springs, with their other features like high temperature and wet-dry cycles, would have also facilitated abiotic oligomerization processes. Wet-dry cycles (also known as dehydration-rehydration cycles) are a very interesting, geologically driven feature of hot spring pools, which enable a chemical system to undergo

consecutive aqueous and dry phases (Figure 1.3a). A dry phase occurs due to water evaporation because of sunlight (day-night cycles) and the temperature of the hot spring. It is followed by a wet/aqueous phase, where events like precipitation (driven by seasonal changes), dewing, or the groundwater coming out of the hot spring replenish the water content. Reduced water activity and high temperature during the dry phase can drive oligomerization reactions like RNA synthesis via ester bond formation and peptide synthesis via amide bond formation. Both of these are condensation reactions involving the removal of a water molecule. The subsequent wet phase allows the efficient remixing of both reactants and products. Importantly, these wet-dry cycling events can also allow some cooperative interactions between membrane assembly and abiotic oligomer synthesis, and the formation of protocell-like entities (Figure 1.3b). Specifically, the dry phase causes the formation of multilamellar sheets of membranes wherein monomers can get concentrated and react more efficiently with each other to form higher oligomers. The water replenishment during a wet phase causes the spontaneous formation of vesicles from these multilamellar sheets, which could encapsulate the resultant oligomers, thereby generating protocell-like structures.

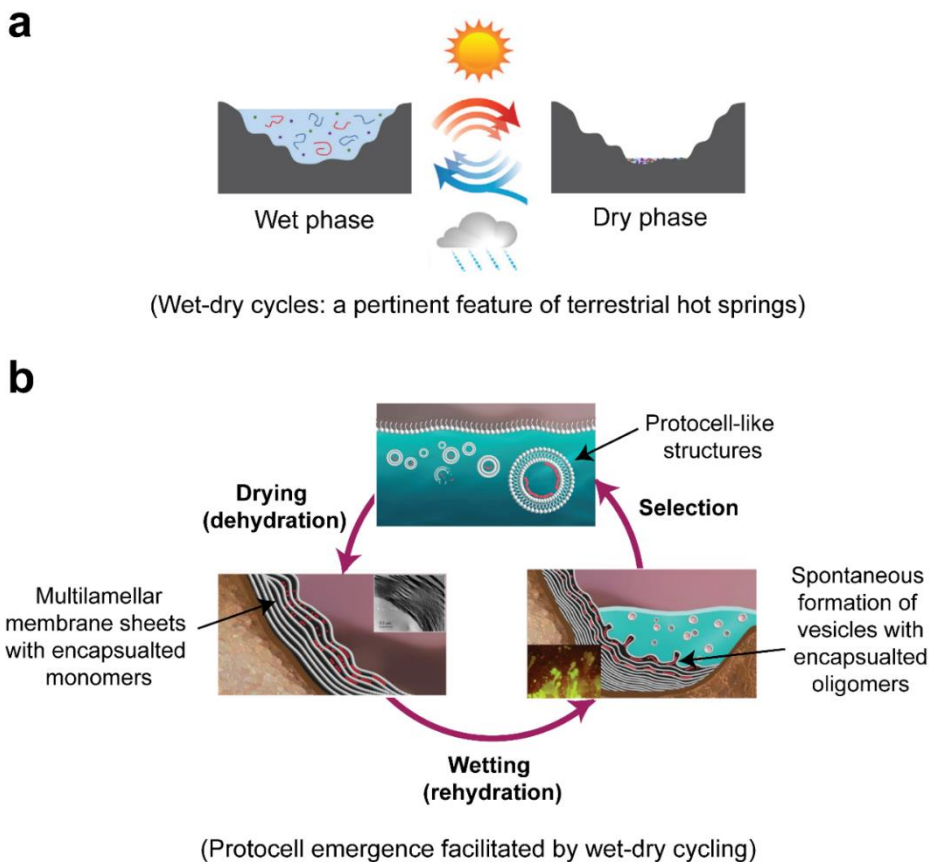


Figure 1.3 Wet-dry cycles and their role in protocell emergence. (a) Wet-dry cycle is an important feature of terrestrial hot springs. A dry phase occurs due to water evaporation because of sunlight and the

temperature of the hot spring. It is followed by a wet/aqueous phase, where events like precipitation, dewing, etc., replenish the water content. (b) Wet-dry cycles can facilitate important steps of protocell emergence. Reduced water activity and high temperature during the dry phase facilitate the abiotic oligomerization process, which can be further enhanced in the presence of multilamellar sheets of membranes where monomers get concentrated and react more efficiently. The water replenishment during a wet phase causes the spontaneous formation of vesicles from these multilamellar sheets, which could encapsulate the resultant oligomers, thereby generating protocell-like structures.

Content adapted from: Fares et al. (2020) *Nat. commun.* [22], YU et al. (2017) *Macromolecules* [23], and Damer and Deamer (2015) *Life* [24]

The phenomena mentioned above have been experimentally tested mainly in the context of lipids and RNA under hot spring-like conditions. Rajamani et al. in 2008 showed that the presence of lipids could assist the formation of RNA-like polymers under wet-dry cycles at high temperatures [20]. Another study by Topozini et al. demonstrated the formation of multilamellar lipid sheets during a dry phase, which organizes nucleotide monomers in close proximity [21]. Both these studies used phospholipids as a proxy for membrane-forming amphiphiles and checked their effect on abiotic RNA synthesis under wet-dry cycles. However, it is not yet known how peptide synthesis might get affected in the presence of membrane-forming amphiphiles, especially under hot spring-like conditions. These unanswered questions form the basis of the second chapter of my thesis, where I will discuss our systematic efforts toward elucidating the effect of membrane-forming amphiphiles on abiotic peptide synthesis under wet-dry cycling conditions.

1.5 The emergence of new amphiphiles through amphiphile-co-solute interactions and their potential role as a model protoamphiphile system

An important assumption underlying both membrane assembly and abiotic oligomerization processes is that the building blocks required for these processes were readily available on early Earth. This supposed “prebiotic availability” of these building blocks is usually justified by two means. 1) Their presence in extra-terrestrial objects like meteorites indicating the possibility of their exogenous delivery on Earth through meteorite bombardment. 2) The endogenous synthesis of these molecules from simple precursors under prebiotically-plausible conditions. For example, single-chain amphiphiles like fatty acids that are considered plausible constituents of protocell membranes, have been synthesized under hydrothermal conditions from simple precursors like formic acid or oxalic acid via Fischer-Tropsch-type reaction [25]. Moreover, their presence has also been detected in meteorite samples [26]. In addition to the above-mentioned conventional routes, there is also a possibility that reactions of existing SCAs with

other co-solutes in a complex prebiotic soup might have also led to the formation of new amphiphilic species (Figure 1.4). These co-solutes could have been of varying chemical nature and would have also included those that acted as precursors of abiotic oligomerization processes, such as nucleotides and amino acids. The generation of a new class of amphiphilic molecules via such interactions would have further diversified the amphiphile inventory on the prebiotic Earth [27,28]. Importantly, some of these newly-formed amphiphiles could also have implications for the formation, stability, and functioning of protocell membranes. Therefore, to better understand the origin and early evolution of protocell membranes, different amphiphile-co-solute interactions should be systematically evaluated for their potential to generate new classes of amphiphilic molecules. Furthermore, different physicochemical properties of the novel amphiphiles generated from such interactions should also be studied to discern their significance as protocellular membranes.

Earlier literature contains some proof-of-concept studies supporting this overall phenomenon. In 2005, Apel and Deamer reported the formation of a monoglyceride from fatty acid and glycerol under prebiotically-relevant wet-dry cycling conditions [29]. Such monoglycerides have been shown to provide several advantages to fatty acid vesicles. They reduce the critical vesicle concentration (CVC) of fatty acids, allowing them to self-assemble into vesicles at a lower concentration [30]. They also allow fatty acids to form vesicles over a wider pH range [30] and provide stability to these vesicles in the presence of metal ions [30–32]. Another case study comes from monoacyl cyclophospholipids, which have been synthesized from fatty acid, glycerol, and phosphate, in the presence of a prebiotically-relevant phosphorylating agent called diamidophosphate [33]. Vesicles generated by these cyclophospholipid-based amphiphile systems are more robust than conventional fatty acid vesicles in terms of membrane assembly over a broad pH range, and their stability in the presence of high metal ion concentrations [34].

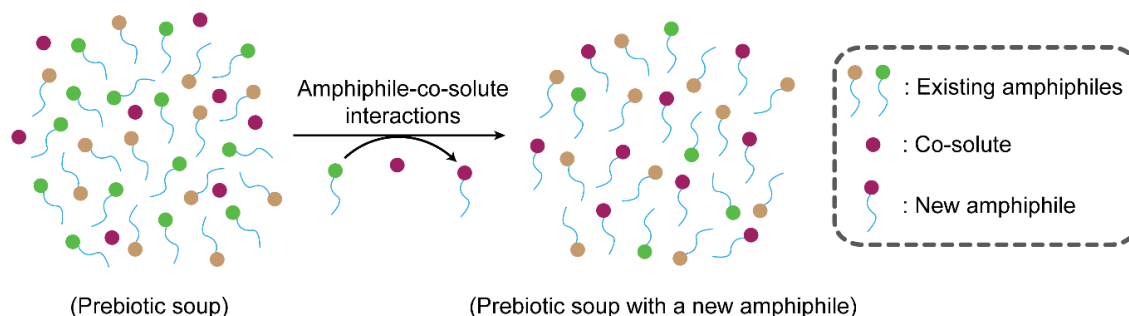


Figure 1.4 Formation of new amphiphiles via amphiphile-co-solute interactions in a prebiotic soup.

Interestingly, our systematic efforts toward understanding the effect of membrane-forming amphiphiles on abiotic peptide synthesis under wet-dry cycles led to the serendipitous discovery of a new type of amphiphilic species in the system called N-acyl amino acids (NAAs), which were generated

through lipid-amino acid interactions. NAA constitutes an intriguing class of SCAs containing fatty acid and amino acid linked via an amide linkage. Their resemblance with fatty acids in terms of their amphiphilic nature, and the presence of an amino acid as a head group makes NAAs a unique system to be pursued as a model protoamphiphilic system. Protoamphiphiles are prebiotically-plausible amphiphiles that might have constituted protocell membranes on early Earth [28]. However, to our knowledge, NAAs themselves have not been explored as protoamphiphilic molecules. In the third chapter of this thesis, I will discuss our systematic assessment of NAAs as a model protoamphiphile candidate and their potential role in generating robust and functional protocell membranes.

1.6 Testing prebiotic membrane assembly process under natural, early Earth analogue conditions

The conventional approach usually followed in the origin of life research involves mimicking early Earth conditions in the laboratory and performing prebiotically-pertinent experiments under such conditions. It also includes reactions pertaining to the emergence of protocells under hot spring-like conditions that were discussed in earlier sections. This approach comes with an implicit assumption that such reactions will behave similarly and give comparable results under natural conditions as well. However, it should be noted that experiments performed in the laboratory involve the usage of pure reagents and solvents, and are usually stringently controlled and optimized for the reaction of interest. Therefore, results obtained under laboratory conditions may subject to change if such reactions occur under natural conditions that are incredibly complex and have a diverse set of molecules (Figure 1.5).

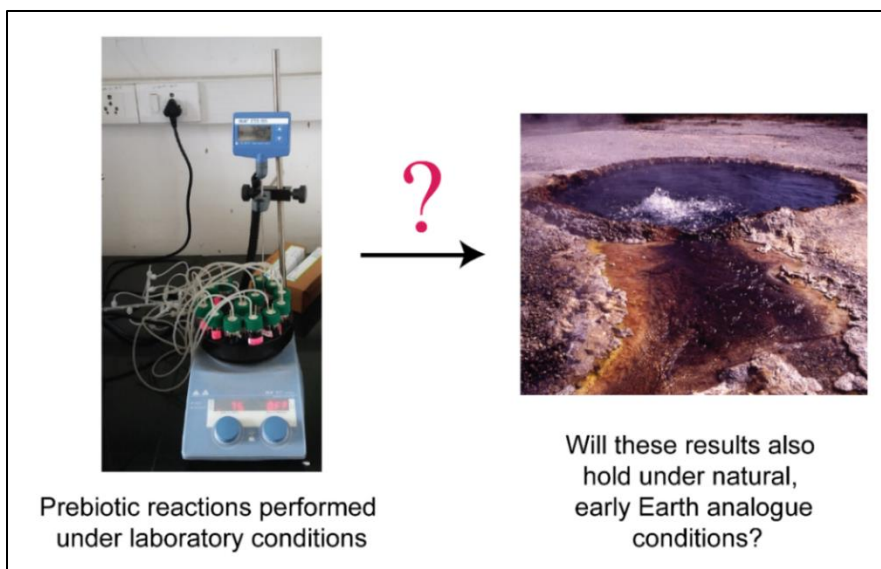


Figure 1.5 Importance of validating laboratory outcomes under natural conditions.

Content adapted from: Alkaline spring image (Shoshone Lake Geysir Basin, Yellowstone National Park) by Bob Lindstrom, 1996; source: National Park Service (2013).

Therefore, one needs to systematically validate the laboratory outcomes of prebiotic reactions under natural conditions to get a more “realistic” and comprehensive understanding of the emergence of life phenomenon. After all, life started in nature and not in the laboratory.

In this context, Dr. David Deamer’s group performed some prebiotically-pertinent experiments directly in hot spring pools in the field [35], as these geological settings are considered a potential niche where life might have originated. However, the authors mention many practical limitations and challenges while pursuing this approach. To tackle these problems, we have adopted an alternative approach with Dr. Deamer and a few other researchers, where we collect samples from such natural, early Earth analogue sites, and use them to perform experiments in the laboratory. This will give a more realistic sense of how prebiotic processes might occur in natural conditions compared to stringently-controlled laboratory conditions. In the fourth chapter of this thesis, I will discuss some systematic experiments that we have performed in this regard, where we collected water samples from natural hot spring sites in two countries, having features analogous to early Earth conditions. These samples were used to study the prebiotic membrane assembly process from different protoamphiphilic systems to glean “more realistic” insights into how protocell membranes would have been generated under terrestrial hot spring conditions.

References

1. Pearce, B.K.D.; Tupper, A.S.; Pudritz, R.E.; Higgs, P.G. Constraining the Time Interval for the Origin of Life on Earth. *Astrobiology* **2018**, *18*, 343–364.
2. Benner, S.A. Defining life. *Astrobiology* **2010**, *10*, 1021–30.
3. Domagal-Goldman, S.D.; Wright, K.E.; Adamala, K.; Arina de la Rubia, L.; Bond, J.; Dartnell, L.R.; Goldman, A.D.; Lynch, K.; Naud, M.-E.; Paulino-Lima, I.G.; et al. The Astrobiology Primer v2.0. *Astrobiology* **2016**, *16*, 561–653.
4. Robertson, M.P.; Joyce, G.F. The origins of the RNA world. *Cold Spring Harb. Perspect. Biol.* **2012**, *4*, a003608.
5. Luisi, L.P. The Emergence of Life. From Chemical Origins to Synthetic Biology. By Pier Luigi Luisi. *Angew. Chemie Int. Ed.* **2007**, *46*, 823–824.
6. Deamer, D.; Dworkin, J.P.; Sandford, S.A.; Bernstein, M.P.; Allamandola, L.J. The First Cell Membranes. *Astrobiology* **2002**, *2*, 371–381.
7. Morowitz, H.J.; Kostelnik, J.D.; Yang, J.; Cody, G.D. The origin of intermediary metabolism. *Proc. Natl. Acad. Sci. U. S. A.* **2000**, *97*, 7704–8.

8. van der Gulik, P.; Speijer, D. How Amino Acids and Peptides Shaped the RNA World. *Life* **2015**, *5*, 230–246.
9. Wächtershäuser, G. Iron-Sulfur World. *Wiley Encycl. Chem. Biol.* **2008**, 1–8.
10. Wächtershäuser, G. Groundworks for an evolutionary biochemistry: The iron-sulphur world. *Prog. Biophys. Mol. Biol.* **1992**, *58*, 85–201.
11. Krishnamurthy, R. Giving Rise to Life: Transition from Prebiotic Chemistry to Protobiology. *Acc. Chem. Res.* **2017**, *50*, 3, 455–459.
12. Altamura, E.; Fiore, M. The Origin and Early Evolution of Life: (Prebiotic) Systems Chemistry Perspective. *Life* **2022**, *12*, 710.
13. Phillips, M.L. The Origins Divide: Reconciling Views on How Life Began. *Bioscience* **2010**, *60*, 675–680.
14. Bonfio, C.; Russell, D.A.; Green, N.J.; Mariani, A.; Sutherland, J.D. Activation chemistry drives the emergence of functionalised protocells. *Chem. Sci.* **2020**, *11*, 10688–10697.
15. Schrum, J.P.; Zhu, T.F.; Szostak, J.W. The origins of cellular life. *Cold Spring Harb. Perspect. Biol.* **2010**, *2*, a002212.
16. Ruiz-Mirazo, K. Protocell. *Encycl. Astrobiol.* **2011**, 1353–1354.
17. Mansy, S.S. Model protocells from single-chain lipids. *Int. J. Mol. Sci.* **2009**, *10*, 835–43.
18. Mulkidjanian, A.Y.; Bychkov, A.Y.; Dibrova, D. V; Galperin, M.Y.; Koonin, E. V Origin of first cells at terrestrial, anoxic geothermal fields. *Proc. Natl. Acad. Sci. U. S. A.* **2012**, *109*, E821-30.
19. Walde, P.; Namani, T.; Morigaki, K.; Hauser, H.; Namani, T.; Morigaki, K.; Hauser, H. Formation and Properties of Fatty Acid Vesicles (Liposomes). In *Liposome Technology*; CRC Press, 2018; pp. 23–42.
20. Rajamani, S.; Vlassov, A.; Benner, S.; Coombs, A.; Olasagasti, F.; Deamer, D. Lipid-assisted Synthesis of RNA-like Polymers from Mononucleotides. *Orig. Life Evol. Biosph.* **2008**, *38*, 57–74.
21. Topozini, L.; Dies, H.; Deamer, D.W.; Rheinstädter, M.C. Adenosine Monophosphate Forms Ordered Arrays in Multilamellar Lipid Matrices: Insights into Assembly of Nucleic Acid for Primitive Life. *PLoS One* **2013**, *8*, e62810.

22. Fares, H.M.; Marras, A.E.; Ting, J.M.; Tirrell, M. V.; Keating, C.D. Impact of wet-dry cycling on the phase behavior and compartmentalization properties of complex coacervates. *Nat. Commun.* **2020**, *11*, 1–13.
23. Yu, S.S.; Solano, M.D.; Blanchard, M.K.; Soper-Hopper, M.T.; Krishnamurthy, R.; Fernández, F.M.; Hud, N. V.; Schork, F.J.; Grover, M.A. Elongation of Model Prebiotic Proto-Peptides by Continuous Monomer Feeding. *Macromolecules* **2017**, *50*, 9286–9294.
24. Damer, B.; Deamer, D. Coupled Phases and Combinatorial Selection in Fluctuating Hydrothermal Pools: A Scenario to Guide Experimental Approaches to the Origin of Cellular Life. *Life* **2015**, *5*, 872–887.
25. McCollom, T.M.; Ritter, G.; Simoneit, B.R. Lipid synthesis under hydrothermal conditions by Fischer-Tropsch-type reactions. *Orig. Life Evol. Biosph.* **1999**, *29*, 153–66.
26. Lawless, J.G.; Yuen, G.U. Quantification of monocarboxylic acids in the Murchison carbonaceous meteorite. *Nature* **1979**, *282*, 396–398.
27. Maurer, S.E.; Deamer, D.W.; Boncella, J.M.; Monnard, P.A. Chemical evolution of amphiphiles: glycerol monoacyl derivatives stabilize plausible prebiotic membranes. *Astrobiology* **2009**, *9*, 979–987.
28. Joshi, M.P.; Sawant, A.A.; Rajamani, S. Spontaneous emergence of membrane-forming protoamphiphiles from a lipid–amino acid mixture under wet–dry cycles. *Chem. Sci.* **2021**, *12*, 2970–2978.
29. Apel, C.L.; Deamer, D.W. The Formation Of Glycerol Monodecanoate By A Dehydration Condensation Reaction: Increasing The Chemical Complexity Of Amphiphiles On The Early Earth. *Orig. Life Evol. Biosph.* **2005**, *35*, 323–332.
30. Sarkar, S.; Dagar, S.; Verma, A.; Rajamani, S. Compositional heterogeneity confers selective advantage to model protocellular membranes during the origins of cellular life. *Sci. Rep.* **2020**, *10*, 1–11.
31. Chen, I.A.; Salehi-Ashtiani, K.; Szostak, J.W. RNA Catalysis in Model protocell Vesicles. *J. Am. Chem. Soc.* **2005**, *127*, 13213–13219.
32. Monnard, P.-A.; Apel, C.L.; Kanavarioti, A.; Deamer, D.W. Influence of Ionic Inorganic Solutes on Self-Assembly and Polymerization Processes Related to Early Forms of Life: Implications for a Prebiotic Aqueous Medium. *Astrobiology* **2002**, *2*, 139–152.

33. Gibard, C.; Bhowmik, S.; Karki, M.; Kim, E.K.; Krishnamurthy, R. Phosphorylation, oligomerization and self-assembly in water under potential prebiotic conditions. *Nat. Chem.* **2018**, *10*, 212–217.
34. Toparlak, Ö.D.; Karki, M.; Egas Ortuno, V.; Krishnamurthy, R.; Mansy, S.S. Cyclophospholipids Increase Proto-cellular Stability to Metal Ions. *Small* **2019**, 1903381.
35. Deamer, D. Where Did Life Begin? Testing Ideas in Prebiotic Analogue Conditions. *Life* **2021**, *Vol. 11*, Page 134 **2021**, *11*, 134.

Chapter 2

THE EFFECT OF A MEMBRANE-FORMING AMPHIPHILE ON ABIOTIC PEPTIDE SYNTHESIS UNDER WET-DRY CYCLES

Adapted from: *Chemical Science* (2021) 12, 2970-2978

2.1 Introduction

Proteins constitute more than half of the cell membrane in extant biology [1] and play a vital role in maintaining its structural integrity and functionality [2]. This remarkable synergy observed between proteins and membranes in modern cells is likely to be a relic of the co-evolution of membrane assembly and peptide synthesis processes that would have occurred during the early history of life's origin. Importantly, these co-evolutionary processes would have played a crucial role in the formation of first protocells on the early Earth [3]. Therefore, several aspects of the interdependence between peptide synthesis and membrane assembly have been pursued in the field of prebiotic chemistry [4–9]. However, one of the fundamental questions that need to be addressed to understand this interplay is, what are the possible ways in which membrane-forming amphiphiles would have influenced nonenzymatic peptide synthesis? A membrane-forming amphiphile may affect peptide synthesis at a systems level, wherein amphiphiles assemble into vesicles and facilitate peptide formation either by concentrating monomers through encapsulation [10], preventing the hydrolysis of activated precursors [11], or via surface catalysis through non-covalent interactions [12–16]. A relatively less explored alternative possibility is that the amphiphile may affect peptide synthesis at a molecular level, where it could covalently interact with an amino acid, thereby generating a new chemical species having properties of both an amphiphile and an amino acid. This is an interesting possibility to consider because such novel compounds, emerging via this chemical cross-talk, would not only have diversified the prebiotic soup, but could have also conferred some form of selective advantage for the protocell formation process.

Previous studies exploring the effect of amphiphiles on peptide synthesis have mainly investigated the oligomerization of activated amino acids in the presence of model membranes [11–16]. However, given the inherent instability associated with oligomer assembly involving activation chemistry, this process would have been less feasible under high temperature geochemical settings [17], such as terrestrial hot springs and submarine hydrothermal vents; which are widely considered as plausible niches for the origin of life [18–20]. Particularly, N-carboxyanhydrides (NCAs) of amino acids have been shown to predominantly form cyclic peptides at high temperature, which hinders further growth of the polypeptide chain making them unsuitable to form longer peptides in the above-mentioned niches [21].

Therefore, it is important to evaluate the effect of amphiphiles on peptide synthesis using non-activated amino acids, under prebiotically plausible conditions. However, considering the kinetic [22] and thermodynamic [23] constraints on peptide bond formation, peptide synthesis from non-activated amino acids in the absence of sophisticated enzymatic machinery on the early Earth is thought to have been a challenging task. As a potential solution to this problem, several prebiotically plausible routes have been proposed which can facilitate the formation of peptides from non-activated amino acids [24–33], many of which use wet-dry cycling at high temperature. Peptide bond formation between non-activated amino acids involves the removal of a water molecule, which is facilitated by reduced water activity in the dry phase. A subsequent rehydration during the wet phase allows for the mixing and redistribution of, both, the reactants and products. Also, the elevated temperature provides the necessary activation energy required for this process to occur [34]. Thus, wet-dry cycling is an efficient process for the generation of peptides from non-activated amino acids [27]. Furthermore, as mentioned earlier, these wet-dry cycles and high temperature would have been prevalent features of terrestrial hot springs, which is a highly probable candidate niche for the origin of life on Earth [18,19]. Interestingly, wet-dry cycling has also been known to facilitate the synthesis of nucleic acids, and several studies have evaluated the effect of lipids as a co-solute on the abiotic nucleic acid synthesis under wet-dry cycling conditions [35–38]. However, to our knowledge, the effect of amphiphiles on peptide synthesis under wet-dry cycles has yet to be explored.

In this chapter, I will discuss our systematic investigation on the effect of phospholipid as a model membrane-forming amphiphile, on the peptide synthesis from non-activated glycine (Gly), under wet-dry cycles at high temperature. We demonstrate a molecular level effect of the amphiphile, wherein the peptide synthesis reaction is accompanied by a parallel competing reaction involving the covalent interaction between the amino acid and phospholipid to form an N-acyl amino acid. The NAA synthesis also occurs with several other amino acids and phospholipids showing the generality of this reaction. I will also discuss the plausible mechanism for the formation of NAA from an amino acid and a phospholipid, and the potential competing nature of peptide synthesis and NAA synthesis reactions.

2.2 Materials and Methods

2.2.1 Materials

All the phospholipids and NAA standards were purchased from Avanti polar lipids (USA). The rest of the chemicals and reagents, including amino acids, were bought from Sigma-Aldrich (India). All reagents were of analytical grade and used without further purification.

2.2.2 Setting up the wet-dry cycling reaction

In a typical reaction, adequate volume of 25 mg/ml lipid (1-palmitoyl-2-oleoyl-sn-glycero-3-phosphocholine (POPC)) chloroform stock, required to prepare 200 μ l of 8 mM POPC solution, was taken in a glass vial. The chloroform was evaporated to form a dry lipid film, which was rehydrated with 200 μ l of 80 mM Gly pH 9.8 solution to get a mixture of the Gly and the POPC in 10:1 ratio. This solution was then subjected to wet-dry cycles at 90 °C on a heating block (RCT basic, IKA). Each wet-dry cycle duration was 24 hours, where a solution was allowed to evaporate to dryness at 90 °C and again rehydrated after 24 hours with 200 μ l of ultrapure water, and vortexed briefly to remix the components. The same procedure was followed for multiple wet-dry cycles. At the end of wet-dry cycling, the reaction was rehydrated with 200 μ l of ultrapure water, vortexed and stored at 4 °C until further analysis. Other reactions like only Gly (80 mM) and only POPC (8 mM) control reactions, and those with other amino acids and phospholipids, were also performed under the same reaction conditions, excepting for a few variations in some reactions. In POPC concentration variation experiments, the concentration of Gly was maintained at 80 mM while that of POPC was varied as 4 mM, 8 mM and 16 mM to get Gly to POPC ratios of 20:1, 10:1 and 5:1, respectively. In the Lys + POPC reaction, pH was set to 9.1 in order to account for the lower pKa of α -amino group of Lys (8.9). In the Asp + POPC reaction, 30 mM Asp and 3 mM POPC (10:1 ratio) was used due to the low solubility of Asp in water. In the Gly + POPC reaction under acidic conditions, the pH was 3.

2.2.3 Separation of lipids from Gly oligomers in a reaction mixture

Before mass analysis, lipids were separated from Gly oligomers using the butanol-hexane (BH) extraction. Briefly, 100 μ l of the reaction mixture was diluted by adding 200 μ l of ultrapure water. To this diluted sample, 300 μ l of butanol was added and vortexed briefly. The solution was then centrifuged at 13,000 rpm for 1 minute. The upper butanol layer was collected in a

separate vial and the butanol extraction step was repeated once again. Then, 150 μ l of hexane was added to the aqueous layer. This solution was vortexed and centrifuged at 13,000 rpm for 1 minute. The upper hexane layer was removed carefully and stored separately at 4 °C. The remaining solution was evaporated to dryness at 30 °C in CentriVap DNA vacuum concentrator (Labconco). The dry layer was dissolved in 100 μ l of ultrapure water to reconstitute the aqueous phase containing free Gly and its oligomers, which was analysed by LC-MS. Whereas, the butanol phase containing all the lipids was analysed using HRMS. For experiments involving the quantification of Gly oligomers, a control reaction containing 80 mM Gly without POPC was also subjected to BH extraction to account for the loss of Gly oligomers during the extraction process.

2.2.4 Detection and quantification of Gly oligomers

Gly oligomers formed in the Gly control and the Gly + POPC reactions were analysed by Liquid Chromatography-Mass Spectrometry (LC-MS; ExionLC coupled with X500R-QTOF MS; SCIEX). Samples were prepared from the aqueous phase of the BH extraction mixture, with 1:10 dilution in ultrapure water and acidified with 0.1% v/v formic acid, to which 10 nmoles of dialanine was added as an internal standard. 50 μ l aliquots of Samples were passed through a reversed phase C₁₈ column (Phenomenex Luna 5 μ m C18(2) 100 Å, 250 \times 4.6 mm) attached to a guard column (Phenomenex Luna 5 μ m C18(2) 100 Å, 50 \times 4.6 mm) at 0.5 ml/min flow rate with a linear gradient mixture of solvents A (water + 0.1% v/v formic acid) and B (100% acetonitrile + 0.1% v/v formic acid) over 32 minutes as follows: 0 min, 100% A; 4 min, 100% A; 14 min, 35% B; 15 min, 100% B; 23 min, 100% B; 24 min, 100% A; 32 min, 100% A.

For the TOFMS and MS/MS analysis, following parameters were used: ion source temperature = 400 °C, ion polarity was positive, ionspray voltage = 5500 V, declustering potential = 70 V, collision energy (CE) was 5 eV for MS analysis and a collision energy spread of 20 eV was used during MS/MS analysis to induce optimum fragmentation. The identity of Gly oligomers was confirmed by checking for the expected oligomer mass in MS spectra, and their respective fragmentation patterns upon MS/MS analysis. Data acquisition and analysis was done using SCIEX OS software. The peak area of the internal standard (dialanine) was used to normalize the peak areas of Gly oligomers, which were then summed up to get the overall

oligomer yield. All quantitation experiments were performed in at least 3 to 4 replicates, while the rest of the experiments were repeated independently at least two times.

2.2.5 Detection and identification of NAAs using thin-layer chromatography (TLC) and high resolution mass spectrometry (HRMS)

The Gly + POPC and other control reactions were analysed by TLC using a normal phase silica plate (Merck) using chloroform, methanol, and water (65:25:4) as a solvent system, and visualized by staining with either iodine or primuline. During the BH extraction of Gly + POPC and other control reactions, the butanol phase containing all the lipidic species in the reaction was collected separately. The butanol was then evaporated under vacuum, and the dry lipid film was re-suspended into methanol and analysed by HRMS (SYNAPT G2 High Definition Mass Spectrometer equipped with QTOF mass analyzer; Waters) through direct injection of the samples. Molecules were ionized using electrospray ionization (ESI) method in negative ion mode with capillary voltage of 3 kV. Sometimes positive ion mode was also used for the detection of POPC and its degradation products. The NAAs corresponding to other amino acids and phospholipids were also analysed similarly. For getting highly accurate mass data (≤ 5 ppm), LockMass correction was applied using Leucine enkephalin as an internal standard. The ppm error was calculated using the following formula:

$$\text{ppm error} = ((\text{observed mass} - \text{theoretical mass}) \div \text{theoretical mass}) * 1000000$$

The MS/MS analysis of NOG and NPG standards and reaction products was performed similarly in negative ion mode using a collision energy of 10 eV to induce fragmentation. Data acquisition and analysis was done using MassLynx software from Waters.

2.2.6 NMR analysis of NAA standards and reaction products

NMR samples were prepared by drying the butanol phases that were collected separately during the BH extraction of Gly + POPC (10:1) and 8 mM POPC control reactions. The dry lipid film was then dissolved in 750 μl of DMSO- d_6 . For NOG and NPG standards, 1 mg of the dry powder of the corresponding NAA was directly dissolved in 600 μl of DMSO- d_6 . All these samples were subjected to ^1H NMR analysis on a Bruker 400 MHz Spectrometer at IISER Pune NMR facility, and the corresponding NMR spectra were analysed using Mnova software from Mestrelab.

2.3 Results

2.3.1 Formation of glycine oligomers under wet-dry cycles in the presence of phospholipid

Earlier studies have shown that peptides could efficiently form under wet-dry cycles at high temperature and alkaline pH from non-activated amino acids, using Gly oligomerization as a model reaction [27,39]. We used similar conditions to explore the effect of a model membrane-forming amphiphile on peptide synthesis, by studying the Gly oligomerization reaction in the presence of POPC. Phospholipids such as POPC are often used to study the effect of membrane-forming amphiphiles on prebiotically pertinent processes[15,38,40]. This is mainly because they are the major constituents of contemporary cell membranes and have also been shown to get synthesized under certain prebiotically relevant conditions [41–44]. Furthermore, they could readily form stable vesicles under varied experimental conditions, making it easy to monitor the effect of membrane on the reaction of interest. As a first step, we asked whether Gly oligomers (peptides) are produced in the presence of POPC and, if yes, what their overall yield might be.

Towards this, we subjected 80 mM Gly solution of pH 9.8, containing 4 mM POPC (20:1 ratio of Gly to POPC), to five wet-dry cycles at 90 °C, with each cycle being a duration of 24 hours. The POPC was then separated from the reaction mixture using Butanol-Hexane extraction method, where POPC preferentially goes into the butanol (organic) phase while free Gly and its corresponding oligomers will remain in the aqueous phase. Upon LC-MS analysis (positive ion mode) of the aqueous phase, we observed the formation of Gly oligomers in the presence of POPC (Figure 2.1a). However, the overall oligomer yield was lower in the presence of POPC than in the control reaction containing only Gly (Figure 2.1b). We also note that the formation of Gly oligomers under wet-dry cycles followed a typical pattern consistent with earlier studies [27], where the yield of shorter oligomers was higher than the longer ones. This overall pattern seemed to remain same even in the presence of amphiphiles. Therefore, although the individual yields of different oligomers were lower in the presence of amphiphiles, the shorter oligomers were more abundant than the longer ones (Figure 2.2). We also detected diketopiperazine (DKP), a cyclic dipeptide of Gly, in the reaction, whose yield was lower in the presence of POPC. However, we did not include it while quantifying the total oligomer yield, as DKP is usually considered a dead-end byproduct in the peptide synthesis process. Other variations of Gly to POPC ratios, like 10:1 and 5:1, were also investigated where the Gly concentration was 80 mM

and POPC concentrations were 8 mM and 16 mM, respectively, where we observed a decrease in the oligomer yield even at these POPC concentrations (Figure 2.3). Gly oligomerization has been shown to be more efficient at higher temperatures like 130 °C, both in terms of the overall yield and the formation of longer oligomers [27]. Therefore, we also studied Gly oligomerization in the presence of 4 mM POPC (20:1 ratio of Gly to POPC) at 130 °C. It was observed that although the overall yield and the length of the oligomers formed were both better at 130 °C than 90 °C, the effect of POPC was similar to that of the 90 °C reaction, where the oligomer yield was lower in the Gly + POPC reaction (Figure 2.4). This indicated that the observed decrease in the oligomer yield at 90 °C in the presence of POPC was not merely due to the lower reaction temperature. Also, temperatures below 100 °C would have been more consistent with temperatures of terrestrial hot springs than those exceeding the boiling point of water [45]. Therefore, we decided to use 90 °C as the reaction temperature for further investigation of these results.

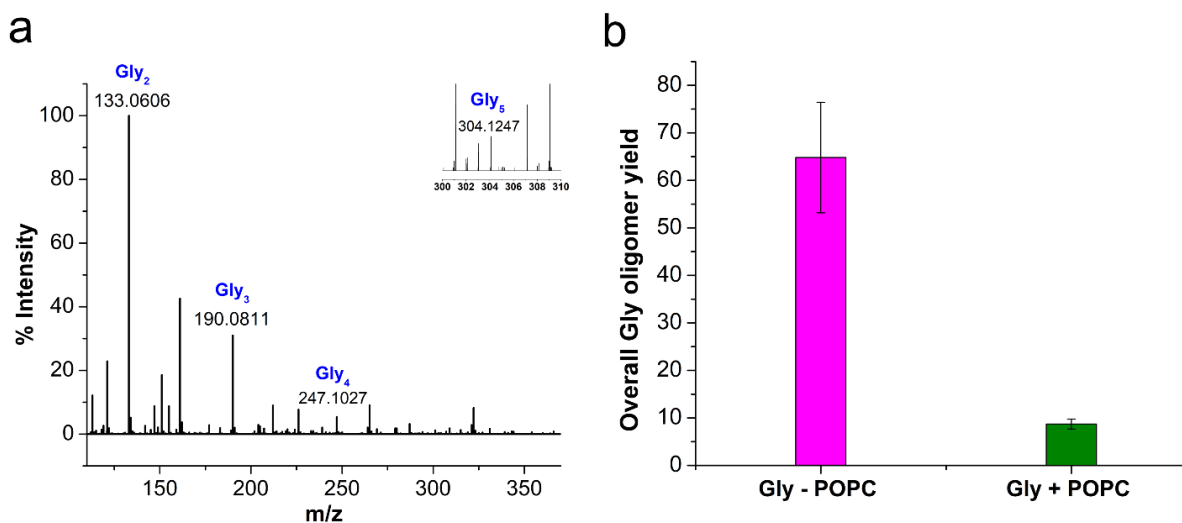


Figure 2.1 Formation of Gly oligomers in the presence of POPC under wet-dry cycles and the effect of POPC on their overall yield. (a) Gly + POPC reaction, which was subjected to five wet-dry cycles at 90 °C, showed the presence of Gly oligomers. The concentrations of Gly and POPC are 80 mM and 4 mM respectively (Gly to POPC ratio is 20:1). (b) Relative abundances of individual oligomers are summed up to give the overall oligomer yield, which was found to be lower in the presence POPC (Gly + POPC) than that of the 80 mM Gly control (Gly – POPC) reaction. All glycine peptides were detected and quantified using LC-MS in positive ion mode (see methods for more details). The error bars represent standard deviation (N = 4).

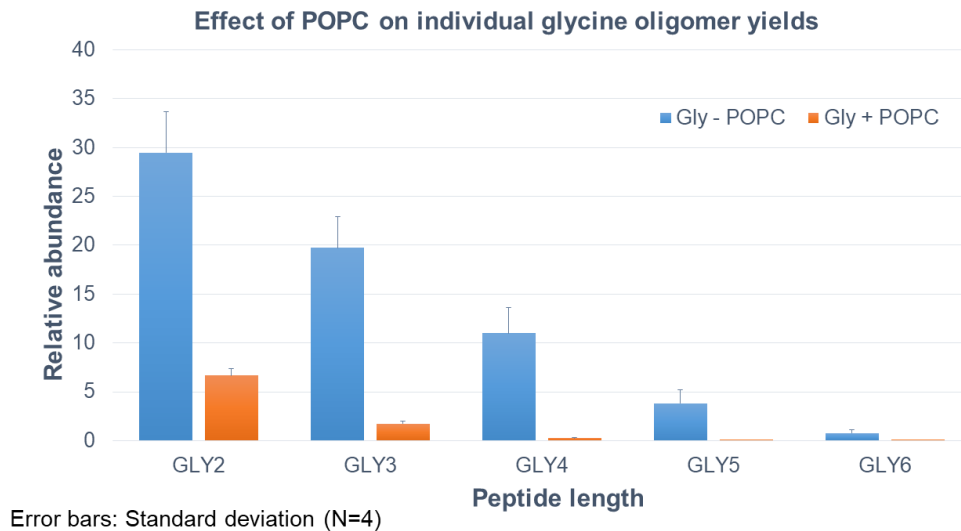


Figure 2.2 Effect of POPC on the yield of individual Gly oligomers. Although the yield of individual oligomers decreases the presence of POPC, The shorter oligomers are still more abundant than the longer ones. The reaction conditions were same as that mentioned in Figure 2.1.

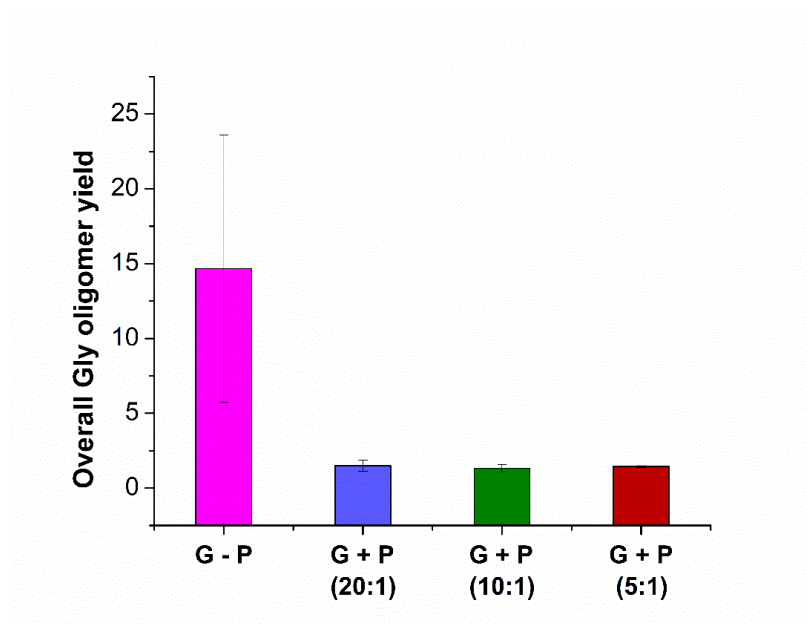


Figure 2.3 Effect of POPC on Gly oligomer yield with varying Gly to POPC ratios. The observed effect of POPC on Gly oligomer yield is consistent over different concentrations of POPC, where the overall yield decreases in the presence of POPC. The Gly concentration is 80 mM and the POPC concentration is varied as 4 mM (G + P; 20:1), 8 mM (G + P; 10:1), and 16 mM (G + P; 5:1), respectively. G – P represents the control reaction, which contains only Gly (80 mM). The overall yield was quantified using LC-MS in a positive ion mode. Error bars represent standard deviation (N = 3).

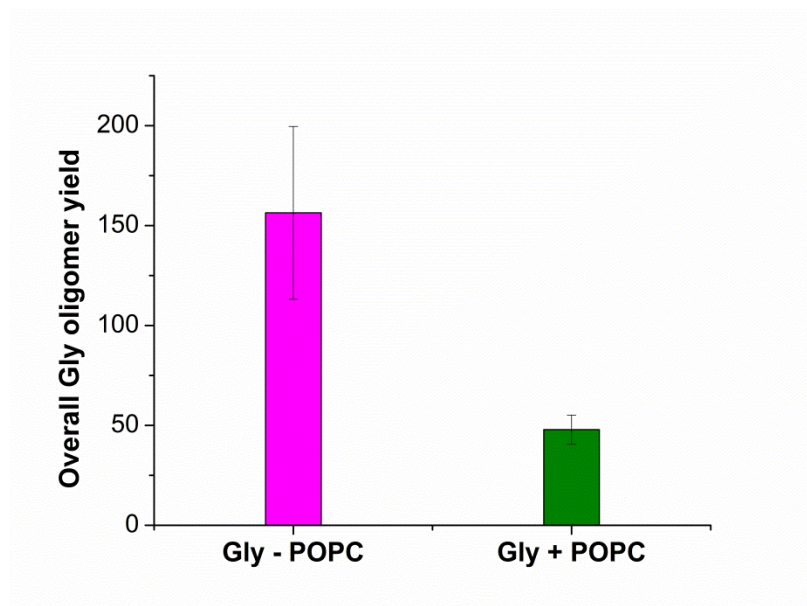


Figure 2.4 Effect of POPC on overall glycine oligomer yield at 130°C. The effect was similar to that of the 90°C reaction, wherein the yield is lower in the presence of POPC (Gly + POPC) as compared to the control reaction (Gly – POPC). The concentrations of Gly and POPC are 80 mM and 4 mM respectively (Gly to POPC ratio is 20:1). Oligomers were quantified using LC-MS in a positive ion mode. Error bars represent standard deviation (N = 4).

2.3.2 Formation of NAAs in the reaction containing glycine and POPC

Intrigued by the lower yield of Gly oligomers in the presence of POPC, we hypothesized that one of the plausible reasons for getting these results might be a reaction of free Gly with the POPC, potentially forming a new chemical species. Preferential utilization of Gly for this alternative reaction might have caused the decrease in oligomer yield in the presence of POPC. Therefore, we started exploring whether any new product had formed in the Gly + POPC reaction, in addition to the Gly oligomers. As a preliminary check, we analysed reaction samples using thin-layer chromatography. The chromatographic separation indeed revealed the formation of a new product only in the Gly + POPC reaction that underwent wet-dry cycling (Figure 2.5). The new product seemed to be more non-polar than POPC, as it moved ahead of the POPC band on the TLC plate (Figure 2.5). It also preferentially went into the butanol phase during BH extraction indicating its plausible lipidic nature, and was not stained by ninhydrin suggesting the absence of a free amino group in it. It was further observed that the intensity of the new band

increased with increasing POPC concentration (Figure 2.6a), and almost a complete conversion of POPC to the new product occurred by the end of five wet-dry cycles at 90 °C (Figure 2.6b). Therefore, we decided to use Gly + POPC in 10:1 ratio and five wet-dry cycles at 90 °C as standard reaction conditions for further identification and characterization of this new product.

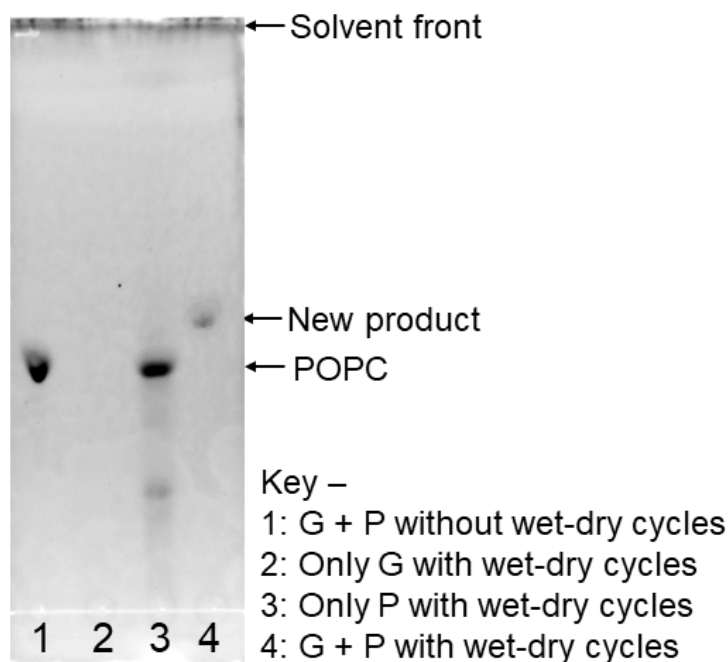


Figure 2.5 TLC analysis of Gly (G) + POPC (P) reaction mixture. The reaction was subjected to five wet-dry cycles at 90°C. A new spot is observed in lane 4, which is absent in other control reactions (lanes 1-3), indicating the formation of a new product upon wet-dry cycling in the Gly + POPC reaction. R_f values for the POPC and the new product are 0.31 and 0.38 respectively. TLC analysis was performed on a normal phase silica plate using chloroform, methanol, and water (65:25:4) as the solvent system, and spots were visualized by staining with the fluorescent dye primuline, whose fluorescence increases in the presence of molecules containing long hydrocarbon chains.

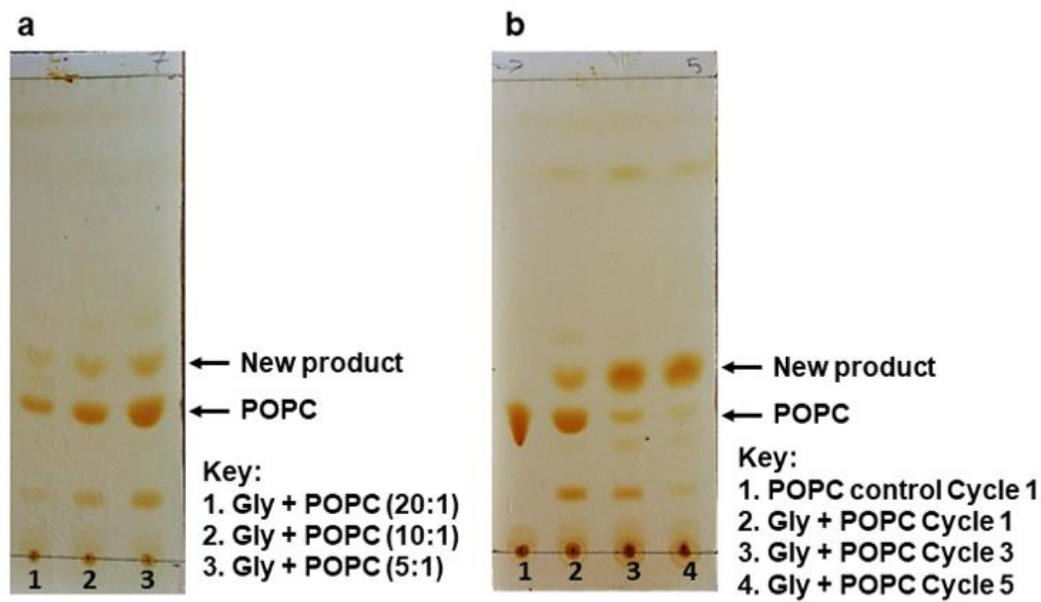


Figure 2.6 Effect of POPC concentration and wet-dry cycles on the formation of new product as analysed by TLC. (a) The intensity of the new spot increases with increasing POPC concentration (lanes 1-3). The Gly concentration is 80 mM while the POPC concentration varies as 4 mM (Gly + POPC; 20:1), 8 mM (Gly + POPC; 10:1), and 16 mM (Gly + POPC; 5:1), respectively. **(b)** The conversion of POPC to the new product increases with increasing wet-dry cycles (lanes 2-4), and almost all of the POPC gets converted to the new product by the end of five wet-dry cycles (lane 4). There are few other spots observed in the Gly + POPC reaction (lanes 2 and 3), which are also present in the TLC in panel **a**. These spots possibly correspond to the transient species formed during the conversion of POPC to the new product, which almost disappear over five wet-dry cycles (lane 4). The TLC analysis was performed on a normal phase silica plate using chloroform, methanol, and water (65:25:4) as the solvent system, and the spots were visualized with iodine staining.

As the majority of the new product was recovered in the butanol phase during the BH extraction of the Gly + POPC reaction, the butanol phase was analyzed using high resolution mass spectrometry. Upon HRMS analysis (negative ion mode), we observed two predominant masses corresponding to N-palmitoylglycine (NPG) and N-oleoylglycine (NOG) (Figure 2.7a, Table 2.1), which were absent in the POPC alone control reaction (Figure 2.7b, Table 2.1). These results corroborated our hypothesis about the formation of a new chemical species by the reaction of Gly and POPC, along with Gly oligomers, in the Gly + POPC reaction (Figure 2.7c). We also observed phosphocholine-based hydrolysis products in our POPC control reaction when it was analyzed by HRMS in positive ion mode (Figure 2.8).

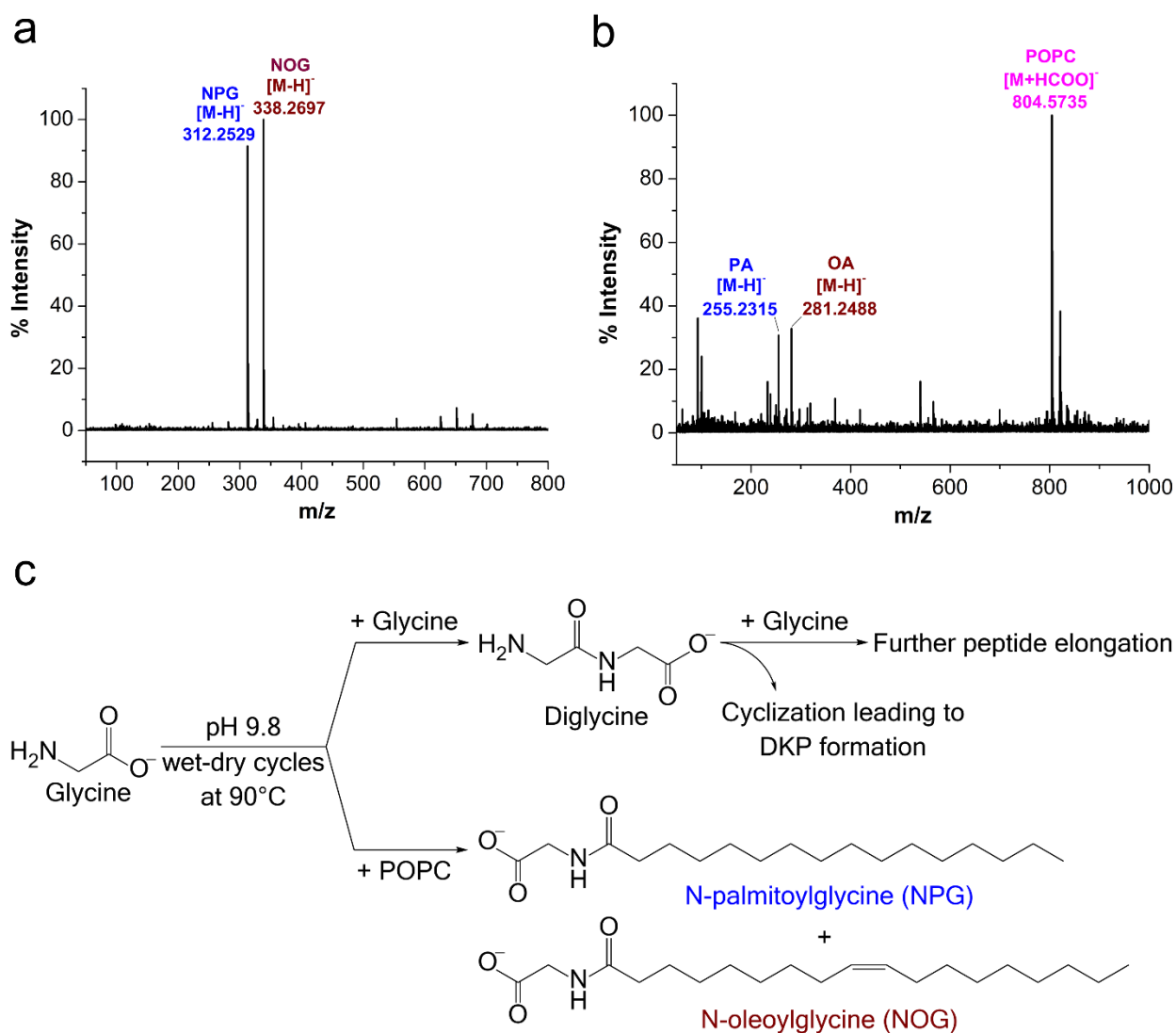


Figure 2.7 Formation of NAAs in the Gly + POPC reaction. (a) HRMS analysis (negative ion mode) of the butanol phase collected during BH extraction of the Gly + POPC wet-dry cycling reaction shows two predominant peaks with masses corresponding to NAAs namely, NPG ($[M-H]^- = 312.2529$) and NOG ($[M-H]^- = 338.2697$). (b) HRMS analysis (negative ion mode) of the butanol phase of the only POPC control reaction shows masses corresponding to POPC and its hydrolysis products, but not that of NPG and NOG. The hydrolysis products of POPC include free fatty acids like palmitic acid (PA) and oleic acid (OA). The reaction was subjected to five wet-dry cycles at 90°C and the concentration of POPC was 8 mM. (c) An overview of the reactions occurring in the Gly + POPC mixture, under wet dry cycles. Gly can either react with another Gly molecule to form diglycine or it can react with POPC to generate NAAs (NPG and NOG). Diglycine may undergo further elongation to form higher oligomers or cyclize to form DKP.

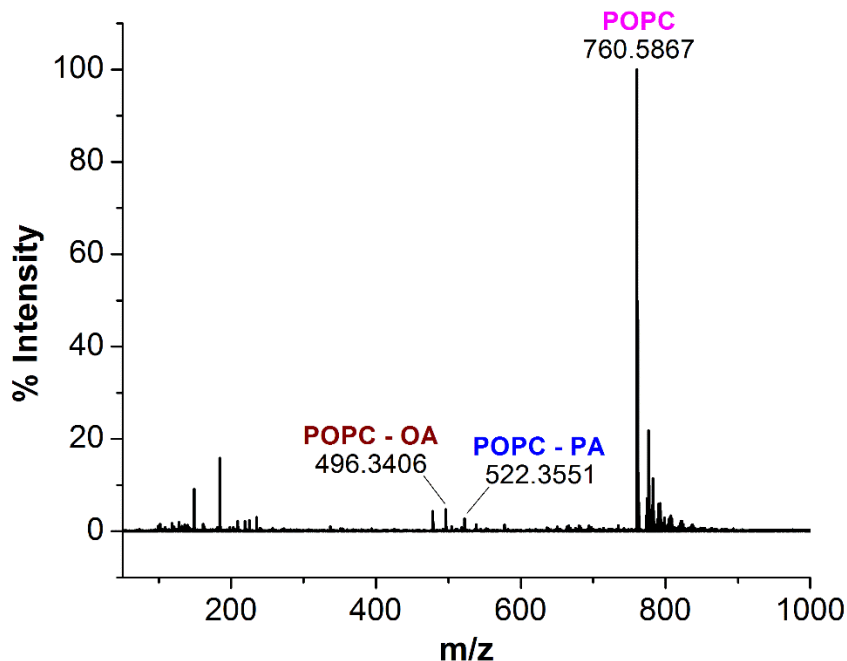


Figure 2.8 Detection of phosphocholine-based hydrolysis products in the POPC control reaction. The HRMS analysis of the butanol phase of the only POPC control reaction in positive ion mode shows masses corresponding to intact POPC and its hydrolysis products lacking one fatty acyl chain (POPC – OA and POPC – PA).

As the polarity of NPG and NOG is similar, they did not separate on a TLC plate and were observed as a co-spot upon TLC analysis, thereby giving the initial impression of the formation of a single new product in the reaction. The identity of NPG and NOG was further confirmed by HRMS/MS and NMR analysis. Upon MS/MS analysis, the fragmentation patterns of NPG and NOG formed in the reaction were observed to be overlapping with those produced by commercially purchased NPG and NOG standards, respectively (Figure 2.9a and 2.9b). The ^1H NMR analysis of the butanol phase of Gly + POPC reaction (Figure 2.9c), which contained NPG and NOG, but not the Gly peptides, showed a signature peak at around 8 ppm for the exchangeable hydrogen attached to the nitrogen atom of the amide linkage present in both NPG and NOG. It was in good agreement with similar peaks observed in the ^1H NMR analysis of NPG and NOG standards analyzed under the same conditions (Figure 2.9c). Notably, this peak was absent in the ^1H NMR spectrum of the POPC control reaction (Figure 2.9c). These results confirmed that the new product formed in the Gly + POPC reaction was a mixture of NPG and NOG, both of which belong to a class of amphiphiles called N-acyl amino acids. The NAA, also

known as a lipoamino acid, is a conjugate of an amino acid and a fatty acid that are joined by an amide linkage. Considering their plausible prebiotic availability, NAAs along with fatty acids and other related amphiphiles, can together be designated as protoamphiphiles; a group of prebiotically pertinent amphiphiles that would have served as components of membrane compartments of primitive cells on the early Earth.

Table 2.1 Masses corresponding to different amphiphiles that were detected during the HRMS analysis of the Gly + POPC and the only POPC control reactions.

Reaction type	Chemical species observed	Exact mass	Ion type	Theoretical mass	Observed mass	Error (ppm)
Gly + POPC	NPG	313.2617	[M-H] ⁻	312.2544	312.2529	-4.8
	NOG	339.2773		338.2701	338.2697	-1.2
Only POPC	PA	256.2402	[M-H] ⁻	255.233	255.2315	-5.9
	OA	282.2559		281.2486	281.2488	0.7
	POPC	759.5778	[M+HCOO] ⁻	804.576	804.5735	-3.1
			[M+H] ⁺	760.5851	760.5867	2.1
	POPC – PA	521.3481	[M+H] ⁺	522.3554	522.3551	-0.6
	POPC – OA	495.3325		496.3398	496.3406	1.6

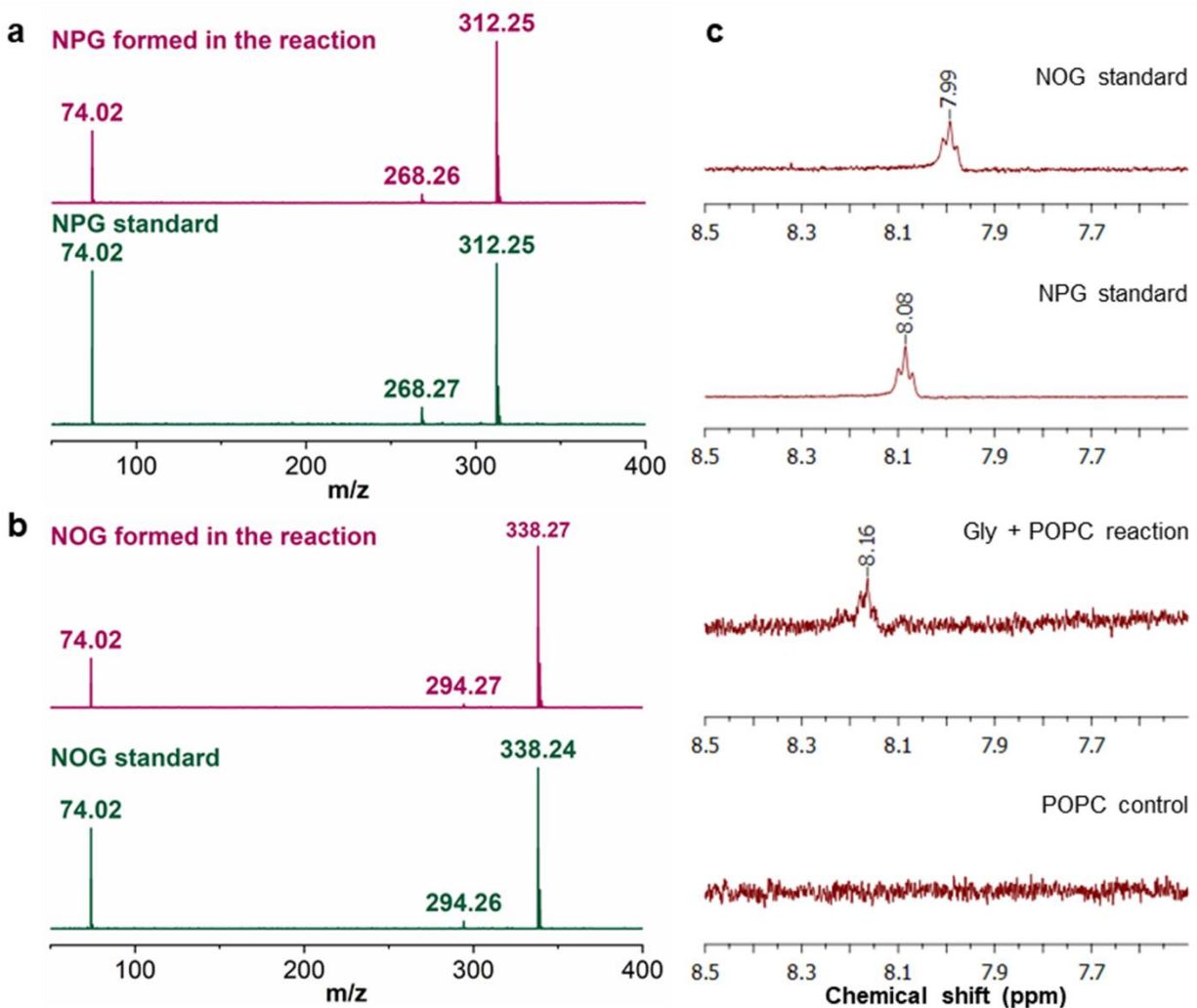


Figure 2.9 Confirmation of NAA formation in the Gly + POPC reaction by HRMS/MS and NMR analysis. HRMS/MS analysis of (a) NPG and (b) NOG, formed in the Gly + POPC reaction, whose fragmentation pattern overlaps with those produced by commercially purchased NPG and NOG standards, respectively. The analysis was performed in the negative ion mode. (c) The ^1H NMR analysis of the butanol phase collected during the BH extraction of Gly + POPC reaction (3rd trace from the top) shows a signature peak corresponding to the hydrogen atom involved in the amide linkage at around 8 ppm. This peak is also present in ^1H NMR spectra of NPG and NOG standards (top two traces). However, this peak is not observed in the ^1H NMR spectrum of the POPC control reaction (last trace).

2.3.3 NAAs formed by other amino acids and phospholipids

After confirming the formation of NAAs in the Gly + POPC reaction, we sought to explore whether this reaction is specific to only Gly and POPC, or if it could be extended to other amino acids and phospholipids as well. Towards this, two sets of experiments were performed. Firstly, the amino acid component was varied by setting up reactions of POPC with Alanine (Ala) and Valine (Val), which are considered among the most prebiotically abundant proteinaceous amino acids other than Gly [46–49]. Secondly, the lipid component was varied by performing reactions of Gly with short-chain phospholipids, namely 1, 2-didecanoyl-sn-glycero-3-phosphocholine (C10 PC) and 1, 2-dioctanoyl-sn-glycero-3-phosphocholine (C8 PC). These phospholipids were specifically selected to check if short-chain NAAs could also form under wet-dry cycling conditions. This is an important phenomenon to be validated because short-chain amphiphiles are of particular interest as plausible membrane components of protocells, owing to their prebiotic abundance [50,51]. All the variation experiments were performed under the same standard set of reaction conditions mentioned above for the Gly + POPC reaction (amino acid to lipid ratio of 10:1, pH 9.8, and five wet-dry cycles at 90 °C). The resultant reaction mixtures were then subjected to BH extraction followed by HRMS analysis of the butanol phase, to check for the presence of NAAs. In the amino acid variation experiments, we did observe masses corresponding to NAAs containing Ala and Val (Figure 2.10a and Figure 2.10b, Table 2.2).

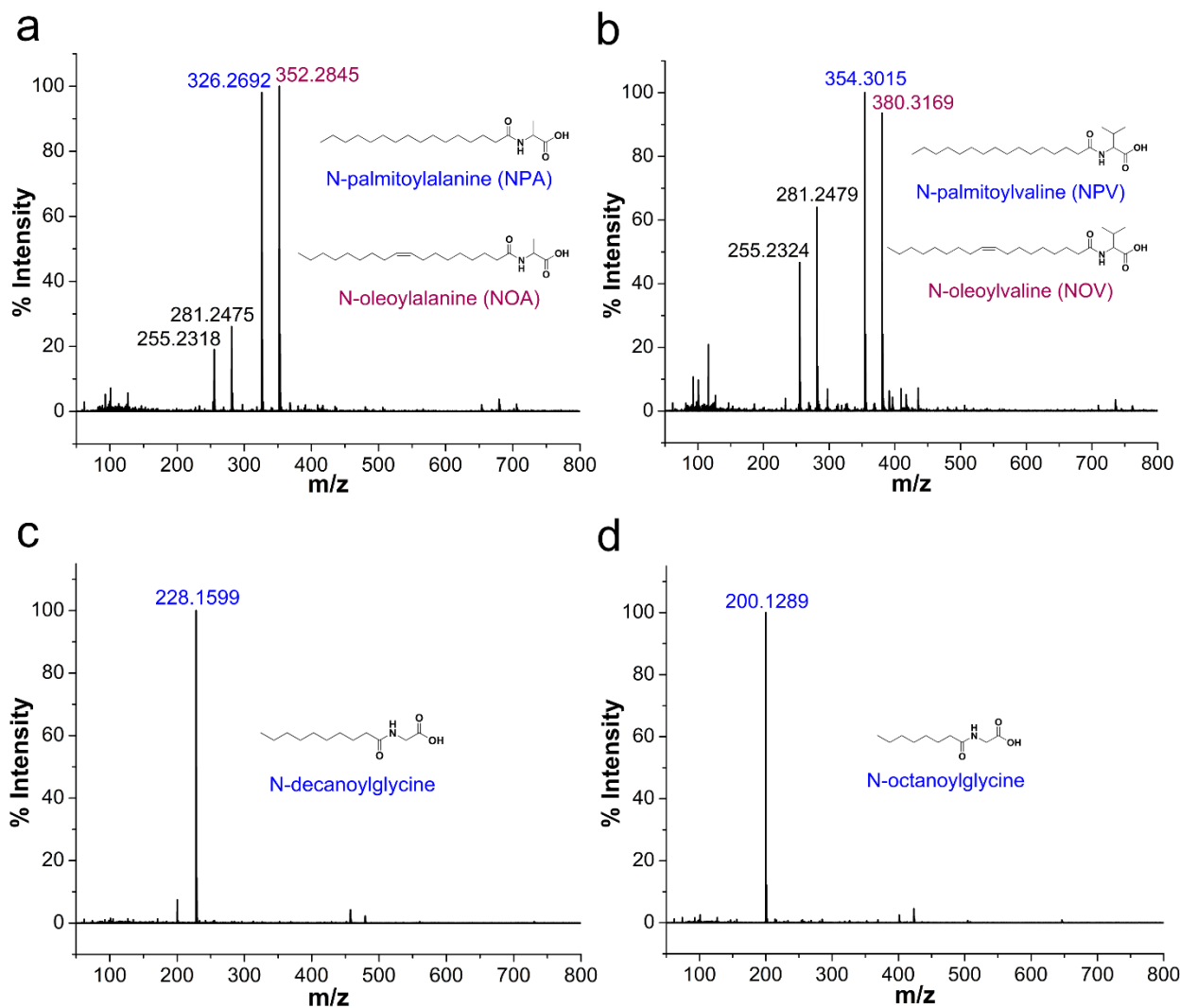


Figure 2.10 NAA formation by other amino acids and phospholipids. HRMS analysis (negative ion mode) of butanol phase of **(a)** Alanine + POPC reaction shows the formation of N-palmitoylalanine (NPA; $[M-H]^- = 326.2692$) and N-oleoylalanine (NOA; $[M-H]^- = 352.2845$), **(b)** Valine + POPC reaction shows the formation of N-palmitoylvaline (NPV; $[M-H]^- = 354.3015$) and N-oleoyl valine (NOV; $[M-H]^- = 380.3169$). In both Alanine and Valine reactions, we also observed peaks corresponding to free fatty acids, namely palmitic acid (255.23) and oleic acid (281.24), with significant intensities. **(c)** The reaction of Gly with C10 PC shows the formation of N-decanoylglycine. **(d)** The reaction of Gly with C8 PC shows the formation of N-octanoylglycine.

Table 2.2 Different NAA masses observed during the HRMS analysis of the amino acid and lipid variation reactions.

NAA	Acronym	Exact mass	Theoretical mass	Observed mass	Error
			[M-H] ⁻	[M-H] ⁻	(ppm)
N-palmitoylalanine	NPA	327.2773	326.2701	326.2692	-2.8
N-oleoylalanine	NOA	353.293	352.2857	352.2845	-3.4
N-palmitoylvaline	NPV	355.3086	354.3014	354.3015	0.3
N-oleoylvaline	NOV	381.3243	380.317	380.3169	-0.3
N-decanoylglycine	-	229.1678	228.1605	228.1599	-2.6
N-octanoylglycine	-	201.1365	200.1292	200.1289	-1.5

Encouraged by these results, we also tried POPC reaction with amino acids having different side chains properties like Lysine (positively charged), Aspartic acid (negatively charged) and Serine (polar uncharged), to check the effect of amino acid side chain variation on NAA formation. We observed NAA formation from these amino acids as well, which indicates that different amino acids can indeed react with a phospholipid under wet-dry cycles to form corresponding NAAs. However, the efficiency of NAA formation by amino acids other than Gly appeared to be lower than that for Gly, potentially owing to the increased complexity of their side chain. This is particularly reflected in their mass spectrum, where significant peaks of free fatty acids (PA and OA) that were generated during the hydrolysis of POPC, are detected (Figures 2.10a and 2.10b). As these amino acids react less efficiently with POPC, the NAA formation would be overridden by POPC hydrolysis, which is a plausible alternative fate for POPC under alkaline, high temperature conditions as observed in the POPC control reaction without any amino acid (Figure 2.7b and Figure 2.8). In the lipid variation experiments, the formation of N-decanoylglycine and N-octanoylglycine was detected in Gly + C10 PC and Gly + C8 PC reactions, respectively (Figures 2.10c and 2.10d, Table 2.2), demonstrating the synthesis of short-chain NAA under wet-dry cycling conditions. Overall, these results confirmed that amino acids and phospholipids, other than Gly and POPC, could also react under prebiotic conditions to generate corresponding NAAs, reiterating the complexity inherent to the prebiotic soup.

2.3.4 A plausible reaction mechanism

The formation of NAAs by the reaction between amino acids and phospholipids, which contain fatty acyl chains linked to the glycerol backbone via an ester linkage, could be explained mechanistically as a classic example of an ester-amide exchange process. Under alkaline conditions, the nucleophilic amino group ($-\text{NH}_2$) of the amino acid attacks the carbonyl carbon of either of the two ester linkages present in the phospholipid to form the corresponding amide (NAA) (Figure 2.11). For example, if the nucleophilic attack by Gly occurs at the ester linkage joining the oleoyl group to the glycerol backbone of POPC, then the resultant product will be N-oleoylglycine. Similarly, an attack on the ester bond linking palmitoyl group to the glycerol backbone of POPC will form N-palmitoylglycine. This ester-amide exchange occurs more efficiently at higher temperatures[26], similar to what was used in this study. The reaction between Gly and POPC resulting in NAA was also found to be occurring at pH 3, albeit less

efficiently, possibly due to the decreased nucleophilicity of the amino group under acidic conditions. These results further support the putative mechanism mentioned above for the formation of NAAs via an ester-amide exchange. Also, NAA formation by other amino acids and phospholipids indicate the generality of this process.

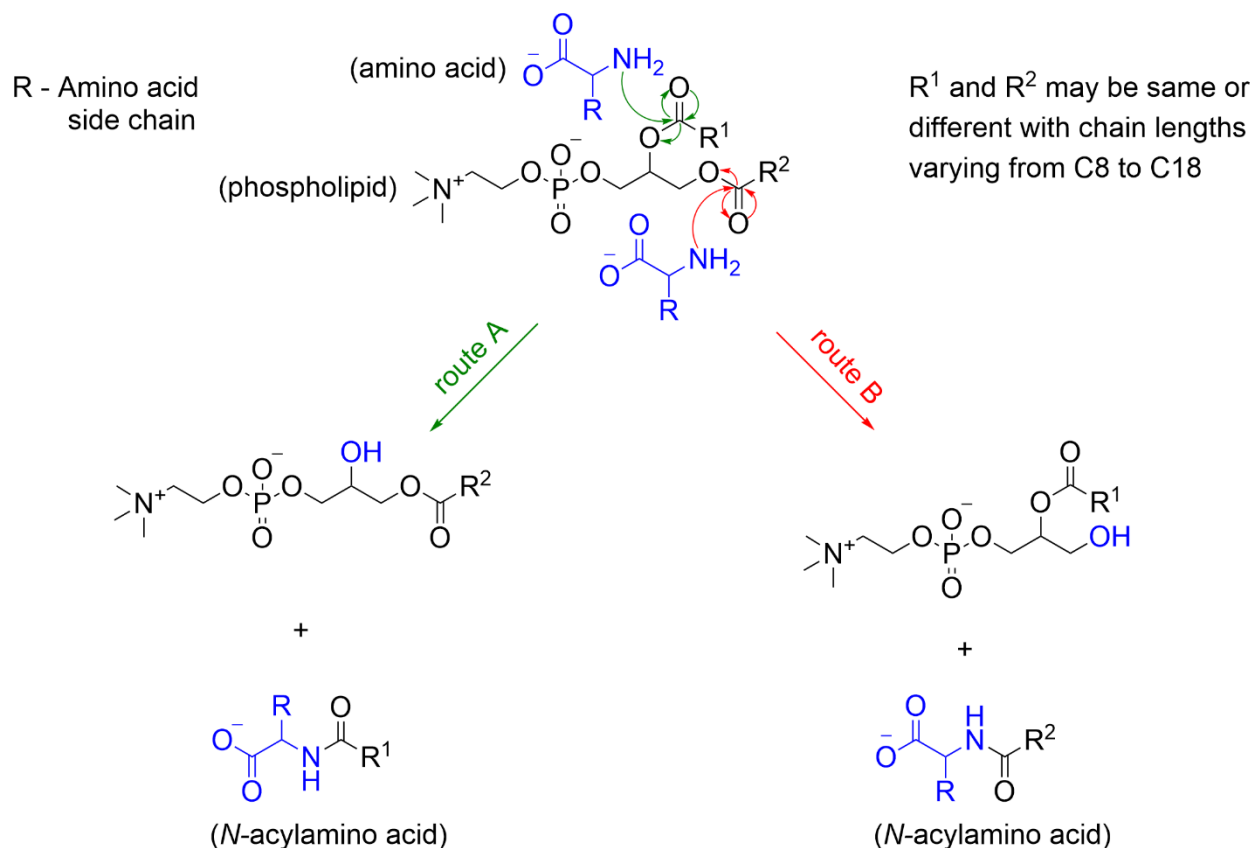


Figure 2.11 Reaction mechanism for the NAA formation from amino acids and phospholipids. At alkaline pH, the deprotonated, nucleophilic amino group of an amino acid attacks the carbonyl carbon of one of the ester linkages in a phospholipid (route A or B) to give the corresponding NAA, and a phospholipid with one less acyl chain. If both the acyl chains (R¹ and R²) of a phospholipid are the same (like in the C8 PC and in C10 PC) then only one type of NAA will be produced. However, a phospholipid with two different acyl chains (like in POPC) will give rise to two different types of NAAs in the reaction

In view of this mechanism, the observed decrease in the Gly oligomer yield in the presence of POPC (Figure 2.1b and Figure 2.2) can also be readily explained. In the Gly + POPC mixture, two types of reactions that mainly occur are peptide synthesis and NAA synthesis, both of which involve the formation of an amide linkage, although via different modes (Figure 2.12). In peptide synthesis, the amide bond is formed via an acid-amine coupling, while in the case of

NAA synthesis it is formed through an ester-amide exchange process. The latter reaction would be kinetically more favorable, as the ester-amide exchange involves $-OR$ as a leaving group, which is a better leaving group than the $-OH$ that is involved in the acid-amine coupling. This kinetic feasibility of amide bond formation via ester-amide exchange has been previously discussed in the context of depsipeptides [52]. Thus, NAA synthesis could outcompete peptide synthesis for the utilization of the free Gly under our reaction conditions, which would have caused the lowering of the Gly oligomer yield in the presence of POPC.

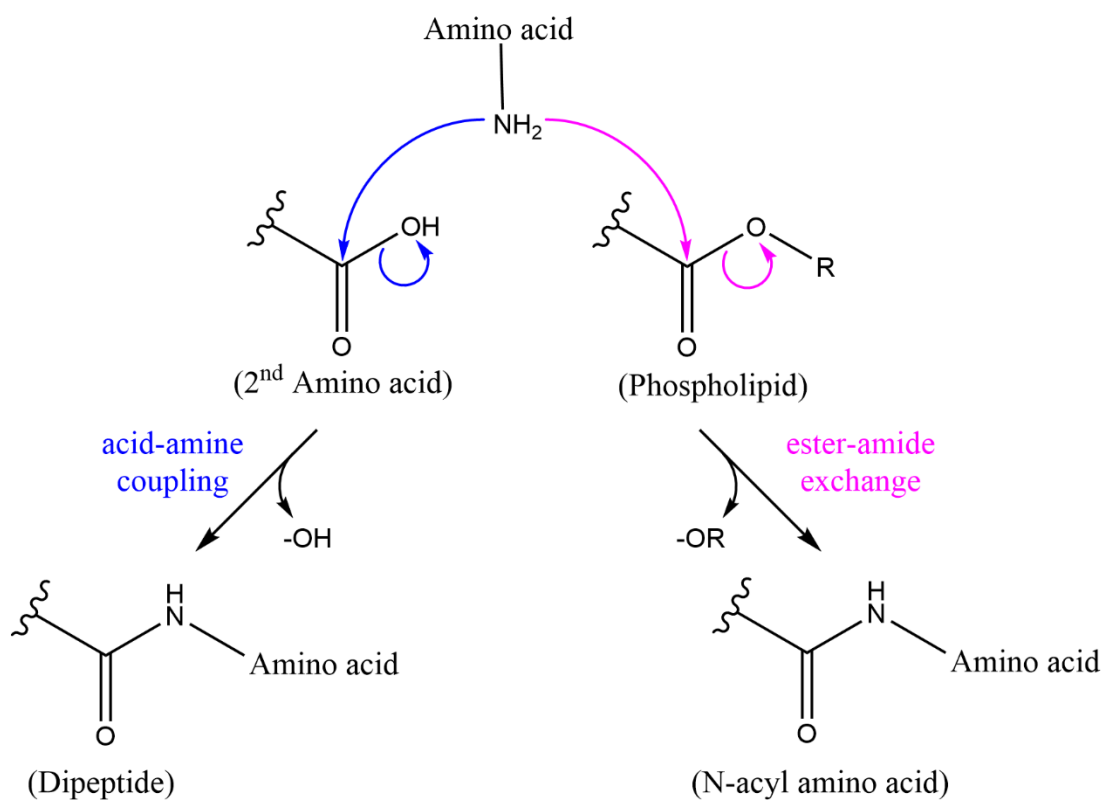


Figure 2.12 Mechanism of the amide bond formation in peptides versus in the NAAs. Two types of reactions that mainly occur in Gly + POPC reaction under wet-dry cycles are peptide synthesis and NAA synthesis, both of which involve the formation of an amide linkage, although via different modes. In peptide synthesis, the amide bond is formed via an acid-amine coupling that involves $-OH$ as a leaving group. In the case of NAA synthesis, amide bond formation occurs through an ester-amide exchange reaction that involves $-OR$ as a leaving group. The latter reaction would be kinetically more favorable than the first one, as $-OR$ is a better leaving group than $-OH$.

2.4 Discussion

In this study, we explored the dynamic interplay between membrane assembly and peptide synthesis under prebiotically pertinent conditions. This was done by investigating the effect of phospholipid as a model membrane-forming amphiphile, on the peptide synthesis process involving non-activated Gly monomers. These reactions were carried out under wet-dry cycles at high temperature, which are characteristic features of terrestrial geothermal pools/hot springs. In the presence of POPC, Gly underwent two types of concurrent yet competing reactions; one leading to the synthesis of Gly peptides via a conventional condensation reaction, while the other resulted in the formation of NAAs from Gly and POPC via an ester-amide exchange process. Both these reactions are dependent on the free Gly monomer pool in the reaction mixture, resulting in the simultaneous synthesis of peptides and amino acid containing protoamphiphiles, from a common set of reactants molecules. Recent studies report the synthesis of both peptides and NAAs in a common reaction, albeit using activated amino acids [53], and the generation of lipidated species of amino acids and peptides by adding external activating agent [54]. Our work demonstrates that this phenomenon can occur with non-activated amino acids and, importantly, without the help of any external activating moiety. They do so by simply relying on the reaction conditions like high temperature and wet-dry cycles, which are more prebiotically-pertinent. Nonetheless, such one-pot reactions are indicative of the intricate reaction network and kinetics, which would have been an inherent feature of a complex prebiotic soup. In this heterogeneous mixture, both cooperative and competitive types of reactions would have occurred simultaneously by utilizing a common pool of starting materials, resulting in different classes of product molecules with their own prebiotic implications.

We further showed that NAAs could also be formed by using different amino acids and phospholipids under wet-dry cycles, indicating the generality of this reaction. Significantly, the formation of NAAs by amino acids having diversity in their side chain highlights how such processes could contribute to increasing the amphiphile diversity on prebiotic Earth. We propose that the NAA synthesis from amino acids and phospholipids, likely followed an ester-amide exchange process. So far, this process has been discussed in a prebiotic context mainly during the formation of depsipeptides from a mixture of hydroxy acids and amino acids [26] (depsipeptides are considered as prebiotically plausible and relevant protopeptides). However, to

our knowledge, the process of ester-amide exchange has not been reported with amino acids and lipids in a prebiotic scenario. The formation of NAAs in our reaction is the first experimental demonstration of this process in a lipid-amino acid-based system under wet-dry cycles. This signifies the importance of ester-amide exchange in also facilitating the formation of protoamphiphiles (NAA), in addition to that of protopeptides.

The discovery of NAAs in the amino acid-lipid mixture allowed us explore new research directions in my PhD project. Although, being a very intriguing class of prebiotically-relevant single-chain amphiphiles, NAAs have not been systematically studied as a model protoamphiphile system. Therefore, we evaluated different aspects of NAAs as a model protoamphiphile candidate, and its potential role towards generating robust, functionally active protocell membranes, which will be discussed in detail in the next chapter of this thesis.

References

1. Guidotti, G. Membrane Proteins. *Annu. Rev. Biochem.* **1972**, *41*, 731–752.
2. Watson, H. Biological membranes. *Essays Biochem.* **2015**, *59*, 43–70.
3. Black, R.; Blosser, M. A Self-Assembled Aggregate Composed of a Fatty Acid Membrane and the Building Blocks of Biological Polymers Provides a First Step in the Emergence of Protocells. *Life* **2016**, *6*, 33.
4. De Kanti, S.; Chakraborty, A. Interaction of monomeric and self-assembled aromatic amino acids with model membranes: Self-reproduction phenomena. *Chem. Commun.* **2019**, *55*, 15109–15112.
5. Cornell, C.E.; Black, R.A.; Xue, M.; Litz, H.E.; Ramsay, A.; Gordon, M.; Mileant, A.; Cohen, Z.R.; Williams, J.A.; Lee, K.K.; et al. Prebiotic amino acids bind to and stabilize prebiotic fatty acid membranes. *Proc. Natl. Acad. Sci. U. S. A.* **2019**, *116*, 17239–17244.
6. Bomba, R.; Kwiatkowski, W.; Sánchez-Ferrer, A.; Riek, R.; Greenwald, J. Cooperative Induction of Ordered Peptide and Fatty Acid Aggregates. *Biophys. J.* **2018**, *115*, 2336–2347.
7. Mayer, C.; Schreiber, U.; Dávila, M.; Schmitz, O.; Bronja, A.; Meyer, M.; Klein, J.; Meckelmann, S. Molecular Evolution in a Peptide-Vesicle System. *Life* **2018**, *8*, 16.

8. Adamala, K.; Szostak, J.W. Competition between model protocells driven by an encapsulated catalyst. *Nat. Chem.* **2013**, *5*, 495–501.
9. Yanagawa, H.; Ogawa, Y.; Kojima, K.; Ito, M. Construction of protocellular structures under simulated primitive earth conditions. *Orig. Life Evol. Biosph.* **1988**, *18*, 179–207.
10. Furuuchi, R.; Imai, E.I.; Honda, H.; Hatori, K.; Matsuno, K. Evolving lipid vesicles in prebiotic hydrothermal environments. *Orig. Life Evol. Biosph.* **2005**, *35*, 333–343.
11. Grochmal, A.; Prout, L.; Makin-Taylor, R.; Prohens, R.; Tomas, S. Modulation of Reactivity in the Cavity of Liposomes Promotes the Formation of Peptide Bonds. *J. Am. Chem. Soc.* **2015**, *137*, 12269–12275.
12. Murillo-Sánchez, S.; Beaufils, D.; González Mañas, J.M.; Pascal, R.; Ruiz-Mirazo, K.; Plasson, R.; Pascal, R. Fatty acids' double role in the prebiotic formation of a hydrophobic dipeptide. *Chem. Sci.* **2016**, *7*, 3406–3413.
13. Zepik, H.H.; Rajamani, S.; Maurel, M.-C.; Deamer, D. Oligomerization of Thioglutamic Acid: Encapsulated Reactions and Lipid Catalysis. *Orig. Life Evol. Biosph.* **2007**, *37*, 495–505.
14. Blocher, M.; Liu, D.; Luisi, P.L. Liposome-assisted selective polycondensation of α -amino acids and peptides: the case of charged liposomes. *Macromolecules* **2000**, *33*, 5787–5796.
15. Hitz, T.; Luisi, P.L. Liposome-assisted selective polycondensation of α -amino acids and peptides. *Biopolymers* **2000**, *55*, 381–90.
16. Blocher, M.; Liu, D.; Walde, P.; Luisi, P.L. Liposome-assisted selective polycondensation of α -amino acids and peptides. *Macromolecules* **1999**, *32*, 7332–7334.
17. Ross, D.; Deamer, D. Prebiotic Oligomer Assembly: What Was the Energy Source? *Astrobiology* **2019**, *19*, 517–521.
18. Deamer, D.W.; Georgiou, C.D. Hydrothermal Conditions and the Origin of Cellular Life. *Astrobiology* **2015**, *15*, 1091–1095.
19. Mulkidjanian, A.Y.; Bychkov, A.Y.; Dibrova, D. V; Galperin, M.Y.; Koonin, E. V Origin of first cells at terrestrial, anoxic geothermal fields. *Proc. Natl. Acad. Sci. U. S. A.* **2012**,

- 109, E821-30.
20. Baross, J.A.; Hoffman, S.E. Submarine hydrothermal vents and associated gradient environments as sites for the origin and evolution of life. *Orig. Life Evol. Biosph.* **1985**, *15*, 327–345.
 21. Kricheldorf, H.R.; Lossow, C. V.; Lomadze, N.; Schwarz, G. Cyclic polypeptides by thermal polymerization of α -amino acid N-carboxyanhydrides. *J. Polym. Sci. Part A Polym. Chem.* **2008**, *46*, 4012–4020.
 22. Smith, R.M.; Hansen, D.E. The pH-rate profile for the hydrolysis of a peptide bond. *J. Am. Chem. Soc.* **1998**, *120*, 8910–8913.
 23. Martin, R.B. Free energies and equilibria of peptide bond hydrolysis and formation. *Biopolymers* **1998**, *45*, 351–353.
 24. Campbell, T.D.; Febrian, R.; McCarthy, J.T.; Kleinschmidt, H.E.; Forsythe, J.G.; Bracher, P.J. Prebiotic condensation through wet–dry cycling regulated by deliquescence. *Nat. Commun.* **2019**, *10*, 1–7.
 25. Erastova, V.; Degiacomi, M.T.; Fraser, D.G.; Greenwell, H.C. Mineral surface chemistry control for origin of prebiotic peptides. *Nat. Commun.* **2017**, *8*, 1–9.
 26. Forsythe, J.G.; Yu, S.-S.; Mamajanov, I.; Grover, M.A.; Krishnamurthy, R.; Fernández, F.M.; Hud, N. V. Ester-Mediated Amide Bond Formation Driven by Wet-Dry Cycles: A Possible Path to Polypeptides on the Prebiotic Earth. *Angew. Chemie* **2015**, *127*, 10009–10013.
 27. Rodriguez-Garcia, M.; Surman, A.J.; Cooper, G.J.T.; Suárez-Marina, I.; Hosni, Z.; Lee, M.P.; Cronin, L. Formation of oligopeptides in high yield under simple programmable conditions. *Nat. Commun.* **2015**, *6*, 8385.
 28. Mita, H.; Nomoto, S.; Terasaki, M.; Shimoyama, A.; Yamamoto, Y. Prebiotic formation of polyamino acids in molten urea. *Int. J. Astrobiol.* **2005**, *4*, 145–154.
 29. Imai, E.I.; Honda, H.; Hatori, K.; Brack, A.; Matsuno, K. Elongation of oligopeptides in a simulated submarine hydrothermal system. *Science (80-.)*. **1999**, *283*, 831–833.

30. Schwendinger, M.G.; Rode, B.M. Salt-induced formation of mixed peptides under possible prebiotic conditions. *Inorganica Chim. Acta* **1991**, *186*, 247–251.
31. Lahav, N.; White, D.; Chang, S. Peptide formation in the prebiotic era: Thermal condensation of glycine in fluctuating clay environments. *Science (80-.)*. **1978**, *201*, 67–69.
32. Chang, S.; Flores, J.; Ponnampereuma, C. Peptide formation mediated by hydrogen cyanide tetramer: a possible prebiotic process. *Proc. Natl. Acad. Sci. U. S. A.* **1969**, *64*, 1011–1015.
33. Rabinowitz, J.; Flores, J.; Krebsbach, R.; Rogers, G. Peptide formation in the presence of linear or cyclic polyphosphates. *Nature* **1969**, *224*, 795–796.
34. Damer, B.; Deamer, D. Coupled Phases and Combinatorial Selection in Fluctuating Hydrothermal Pools: A Scenario to Guide Experimental Approaches to the Origin of Cellular Life. *Life* **2015**, *5*, 872–887.
35. Bapat, N. V.; Rajamani, S. Templated replication (or lack thereof) under prebiotically pertinent conditions. *Sci. Rep.* **2018**, *8*, 15032.
36. Mungi, C. V; Rajamani, S. Characterization of RNA-Like Oligomers from Lipid-Assisted Nonenzymatic Synthesis: Implications for Origin of Informational Molecules on Early Earth. *Life (Basel, Switzerland)* **2015**, *5*, 65–84.
37. Olasagasti, F.; Kim, H.J.; Pourmand, N.; Deamer, D.W. Non-enzymatic transfer of sequence information under plausible prebiotic conditions. *Biochimie* **2011**, *93*, 556–561.
38. Rajamani, S.; Vlassov, A.; Benner, S.; Coombs, A.; Olasagasti, F.; Deamer, D. Lipid-assisted Synthesis of RNA-like Polymers from Mononucleotides. *Orig. Life Evol. Biosph.* **2008**, *38*, 57–74.
39. Sakata, K.; Kitadai, N.; Yokoyama, T. Effects of pH and temperature on dimerization rate of glycine: Evaluation of favorable environmental conditions for chemical evolution of life. *Geochim. Cosmochim. Acta* **2010**, *74*, 6841–6851.
40. Monnard, P.A.; Deamer, D.W. Nutrient uptake by protocells: A liposome model system.

In Proceedings of the Origins of Life and Evolution of the Biosphere; Springer, 2001; Vol. 31, pp. 147–155.

41. Liu, L.; Zou, Y.; Bhattacharya, A.; Zhang, D.; Lang, S.Q.; Houk, K.N.; Devaraj, N.K. Enzyme-free synthesis of natural phospholipids in water. *Nat. Chem.* **2020**, *12*, 1029–1034.
42. Gibard, C.; Bhowmik, S.; Karki, M.; Kim, E.K.; Krishnamurthy, R. Phosphorylation, oligomerization and self-assembly in water under potential prebiotic conditions. *Nat. Chem.* **2018**, *10*, 212–217.
43. Rao, M.; Eichberg, J.; Oró, J. Synthesis of phosphatidylethanolamine under possible primitive earth conditions. *J. Mol. Evol.* **1987**, *25*, 1–6.
44. HARGREAVES, W.R.; MULVIHILL, S.J.; DEAMER, D.W. Synthesis of phospholipids and membranes in prebiotic conditions. *Nature* **1977**, *266*, 78–80.
45. Rohlfsing, D.L. Thermal polyamino acids: Synthesis at less than 100°C. *Science (80-.)*. **1976**, *193*, 68–70.
46. Parker, E.T.; Cleaves, H.J.; Dworkin, J.P.; Glavin, D.P.; Callahan, M.; Aubrey, A.; Lazcano, A.; Bada, J.L. Primordial synthesis of amines and amino acids in a 1958 Miller H₂S-rich spark discharge experiment. *Proc. Natl. Acad. Sci. U. S. A.* **2011**, *108*, 5526–5531.
47. van der Gulik, P.; Massar, S.; Gilis, D.; Buhrman, H.; Rooman, M. The first peptides: The evolutionary transition between prebiotic amino acids and early proteins. *J. Theor. Biol.* **2009**, *261*, 531–539.
48. Ikehara, K. Possible steps to the emergence of life: The [GADV]-protein world hypothesis. *Chem. Rec.* **2005**, *5*, 107–118.
49. Kvenvolden, K.; Lawless, J.; Pering, K.; Peterson, E.; Flores, J.; Ponnampereuma, C.; Kaplan, I.R.; Moore, C. Evidence for extraterrestrial amino-acids and hydrocarbons in the murchison meteorite. *Nature* **1970**, *228*, 923–926.
50. McCollom, T.M.; Ritter, G.; Simoneit, B.R. Lipid synthesis under hydrothermal

- conditions by Fischer-Tropsch-type reactions. *Orig. Life Evol. Biosph.* **1999**, *29*, 153–66.
51. Lawless, J.G.; Yuen, G.U. Quantification of monocarboxylic acids in the Murchison carbonaceous meteorite. *Nature* **1979**, *282*, 396–398.
 52. Yu, S.S.; Krishnamurthy, R.; Fernández, F.M.; Hud, N. V.; Schork, F.J.; Grover, M.A. Kinetics of prebiotic depsipeptide formation from the ester-amide exchange reaction. *Phys. Chem. Chem. Phys.* **2016**, *18*, 28441–28450.
 53. Izgu, E.C.; Björkbom, A.; Kamat, N.P.; Lelyveld, V.S.; Zhang, W.; Jia, T.Z.; Szostak, J.W. N-Carboxyanhydride-Mediated Fatty Acylation of Amino Acids and Peptides for Functionalization of Protocell Membranes. *J. Am. Chem. Soc.* **2016**, *138*, 16669–16676.
 54. Bonfio, C.; Russell, D.A.; Green, N.J.; Mariani, A.; Sutherland, J.D. Activation chemistry drives the emergence of functionalised protocells. *Chem. Sci.* **2020**, *11*, 10688–10697.

Chapter 3

EXPLORATION OF N-ACYL AMINO ACIDS AS A NEW MODEL PROTOAMPHIPHILE SYSTEM

Adapted from: *ChemRxiv* (2022) and *Life* (2021) 11, 1413

3.1 Introduction:

Compartmentalization is one of the key features of cellular life and would have also been a crucial step during life's emergence on early Earth [1,2]. Before the advent of sophisticated enzymatic machinery to produce specialized lipids as per the cell's requirement, early protocell membranes would have been generated from amphiphiles in the surrounding environment. Such prebiotic amphiphiles, which might have served as membrane components of early protocells, are called protoamphiphiles [3]. In this context, single-chain amphiphiles (SCAs) serve as promising protoamphiphile candidates, given their ability to self-assemble into membranes [4] and their potential availability on early Earth [5,6]. Interestingly, some of these SCAs might have also reacted with other co-solutes present in a prebiotic soup to generate new amphiphiles, thereby further expanding the protoamphiphile inventory [3,7–9]. Early protocells would have explored a large array of such amphiphiles to generate their membrane compartments, and utilized different physicochemical properties of those amphiphiles to adapt to fluctuating environmental conditions on early Earth.

Although many SCAs can in principle be envisioned as protoamphiphiles, the focus has mainly remained on exploring fatty acids as a model protoamphiphile system [10–15]. This excess dependence on fatty acids essentially limits the environmental conditions under which protocell membranes could have formed. Importantly, it also overlooks other interesting features that different protoamphiphiles would have endowed to protocell membranes that might hold implications for their sustenance and function. Therefore, a systematic and unbiased approach would allow a better understanding of the origin and evolution of protocell membranes on early Earth. This involves identifying and characterizing new amphiphiles that are deemed fit to be protoamphiphiles.

N-acyl amino acids (NAAs) constitute one such intriguing class of SCAs, which are a hybrid molecule of a fatty acid and an amino acid linked via an amide bond. This amalgamation of two prebiotically important molecules within a single chemical species might have enabled NAAs to exploit the properties of both these molecules and acquire new emergent properties. In extant biology, NAAs are involved in several biological processes [16] and also have widespread commercial applications as antimicrobial agents [17] and as a drug delivery system [18]. In a prebiotic context, NAAs have been investigated for their ability to assist fatty acid-based

membranes towards vesicle growth and the localization of RNA on membrane surfaces [19,20]. However, to the best of our knowledge, NAAs themselves have not been systematically explored as a model protoamphiphile system. As discussed in chapter 2, we demonstrated the formation of NAAs in a phospholipid-amino acid system under prebiotically-pertinent wet-dry cycling conditions. This chapter will discuss our systematic assessment of NAAs as a model protoamphiphile system. Firstly, we showed a novel, prebiotically-plausible route for NAA synthesis from amino acids and ester linkage-containing single-chain amphiphile like glycerol 1-monooleate (GMO) under wet-dry cycling conditions, which supports their prebiotic availability. Then we showed that NAAs could assemble into vesicles on their own, which is one of the crucial parameters for ascertaining their ability to serve as model protocell membranes. They do so at an acidic pH range. Subsequently, we also demonstrated the robustness of NAA-based amphiphile systems in terms of their ability to form vesicles over a broad pH range, which can also tolerate high metal ion concentrations. Finally, we showed that NAAs could act as a substrate for peptide chain growth under wet-dry cycles, generating N-acylated peptide amphiphiles that could aid in the functionality of protocell membranes. We mainly used N-oleoyl glycine (NOG) as a representative NAA amphiphile for all these studies.

3.2. Materials and Methods

3.2.1 Materials

Glycerol-1-monooleate (GMO) and oleic acid (OA) were purchased from Nu-Chek-Prep (USA), whereas N-oleoyl glycine (NOG) and N-oleoyl serine (NOS) were purchased from Avanti polar lipids (USA). EDTA disodium salt dihydrate and trisodium citrate (Qualigens) were procured from HiMedia (Mumbai, India) and Thermo Fisher Scientific (Mumbai, India), respectively. The rest of the chemicals and reagents, including amino acids and different buffers, were bought from Sigma-Aldrich (India). These reagents and chemicals were bought in their most pure available form and used without further purification.

3.2.2 Synthesis of N-acyl amino acid from GMO and an amino acid under wet-dry cycling conditions

3.2.2.1 Setting up the reaction

Most of the protocol used in this study for NAA synthesis and analysis was adapted from our previously standardized protocol for NAA synthesis from phospholipids and amino acids, as

described in the previous chapter. In a typical reaction, adequate volumes of 10 mg/ml methanol stocks of GMO and OA were taken in a glass vial, and methanol was evaporated under a vacuum to form a dry lipid film. This film was then hydrated with 200 mM glycine (Gly) solution pH 9.8 to get a final 200 μ l reaction mixture containing 3 mM each of GMO and OA, and a 200 mM Gly. OA was used in the reaction mixture to increase the overall solubility of GMO, which is otherwise poorly soluble in water. Given the buffering capacity of Gly between pH 8.6 to 10.6 (pKa of the α -amino group of Gly is 9.6), a slightly higher concentration of Gly (200 mM) was used so that Gly can also maintain the reaction pH in addition to acting as one of the reactants. The reaction mixture was then subjected to three wet-dry cycles at 90 °C on a heating block (RCT basic, IKA). The duration of each wet-dry cycle was 24 hours, where water was allowed to evaporate to dryness at 90 °C. This dried mixture was rehydrated after 24 hours with 200 μ l of ultrapure water (18.2 M Ω -cm) to complete one wet-dry cycle. After rehydration, the solution was briefly vortexed to remix the reaction components. The same procedure was followed for subsequent wet-dry cycles. The final rehydration was done with 200 μ l of ultrapure water twice with vortexing to recover the entire reaction content. This reaction solution was then stored at 4 °C until further analysis. Similar reaction conditions and the experimental procedure were followed for NAA synthesis from GMO and other amino acids (alanine, valine, lysine, and serine), and also for the other control reactions, except for a few variations as mentioned below. For the GMO + Lys reaction, pH was set to 9.1 to account for the lower pKa of the α -amino group of Lys (8.9). For the control reaction that did not contain Gly, a solution of GMO + OA (3 mM each) was prepared in 200 mM CHES buffer pH 9.8, and subjected to three wet-dry cycles at 90 °C. For the OA + Gly control reaction, 3 mM OA solution was prepared in 200 mM Gly pH 9.8 and subjected to three wet-dry cycles at 90 °C.

3.2.2.2 Monitoring the conversion of GMO to NOG using thin-layer chromatography (TLC)

The conversion of GMO to NOG in the GMO + OA + Gly wet-dry cycling reaction was initially detected by TLC analysis on a normal phase silica plate (Merck) using a solvent system of toluene, chloroform, methanol (4:4:2) + 0.1 % glacial acetic acid. The reaction samples were loaded alongside commercially purchased OA, GMO, and NOG standards for comparing the TLC spots. The solvent front was 6 cm. Also, the solvent system was run twice with intermediate

drying for better resolution of TLC spots. Lipid species were visualized by staining with iodine. TLC analysis of other control reactions was also performed similarly.

3.2.2.3 Confirmation of NOG formation by HRMS and ^1H NMR analysis

Firstly, the lipid content of the reaction mixture was separated from other aqueous content (unreacted Gly and any Gly oligomers generated during wet-dry cycling alongside NOG) by butanol extraction. This lipid content was analysed using HRMS by direct infusion method, as described in chapter 2. ^1H NMR analysis protocol was also similar to that mentioned in chapter 2, except for the NMR solvent, which was Methanol- d_4 instead of DMSO- D_6 .

3.2.3. Studying the vesicle formation behavior of N-acyl amino acids (NOG and NOS)

The vesicle formation by NAAs was checked over a diverse pH range to find the optimum pH range for their vesicle self-assembly. In a typical reaction, an appropriate volume of NOG methanol stock (10 mg/ml) was taken in a microfuge tube. The methanol was evaporated under vacuum to form a dry lipid film, which was hydrated with 100 μl of 200 mM buffer of appropriate pH to get a 6 mM final concentration of NOG. A similar procedure was followed for NOS, except that the stock solution (1 mg/ml) was prepared by dissolving a dry powder of NOS in chloroform, methanol (8:2; v/v) solution followed by gentle heating and sonication. For different pH values, the following buffers were used: sodium phosphate for pH 3, acetate for pH 4 and 5, MES for pH 6, HEPES for pH 7, bicine for pH 8 and 9, and CHES for pH 10. After hydration of the lipid film with a buffer, the resultant solution was incubated at 60 $^\circ\text{C}$ on ThermoMixer C (Eppendorf) for one hour with constant shaking at 500 rpm, along with frequent mixing by vortexing and pipetting. This heating step is essential for generating vesicles by both NOG and NOS-based amphiphile systems because we observed that the chain-melting transition temperature of these NAAs is higher than room temperature. Also, this high temperature would be required to maintain NOG in a vesicle form. This was achieved by incubating vesicle solutions in ThermoMixer C with a temperature-controlling lid (ThermoTop; Eppendorf) that allows maintaining a constant temperature, both inside and outside of the microfuge tube, thereby avoiding volume changes due to evaporation and condensation. These heated amphiphile-containing solutions were immediately subjected to microscopy to check for vesicle formation (Axio Imager Z1, Carl Zeiss). Different higher-order structures, including vesicles, were visualized under 40X objective (NA = 0.75) using differential interference contrast (DIC)

and fluorescence microscopy. For fluorescence imaging, vesicles were stained with 10 μM of amphiphilic dye called Octadecyl Rhodamine B Chloride (R18) (Invitrogen), which was generously donated by Pucadyil lab at IISER Pune. Vesicle staining was performed by adding an appropriate volume of R18 dye methanol stock while making the dry lipid film of NAAs. Fluorescent vesicles were visualized using a filter set 43 HE (Ex: 550/25 nm, Em: 605/70 nm, Beamsplitter: FT 570). Image acquisition and processing were performed using AxioVision and ImageJ software, respectively.

3.2.4 Vesicle formation by NOG-based amphiphile systems over a broad pH range

For NOG + GMO mixed system, appropriate volumes of NOG and GMO methanol stocks (10 mg/ml each) were taken together in a microfuge tube and mixed with 10 μl of 50 μM R18 dye (for fluorescence imaging). The methanol was evaporated under vacuum at 35 $^{\circ}\text{C}$ to form a dry lipid film, which was hydrated with 50 μl of 200 mM buffer of a particular pH to get a 6 mM total amphiphile concentration, with NOG and GMO in a 2:1 ratio. Solutions of different pH values were prepared in ultrapure water (18.2 $\text{M}\Omega\text{-cm}$) using the following buffers: acetate for pH 4 and 5, MES for pH 6, HEPES for pH 7, bicine for pH 8 and 9, CHES for pH 10, and CAPS for pH 11. A similar procedure was followed for generating vesicles from NOG, OA, and NOG + OA mixed systems. The total amphiphile concentration was 6 mM for all these systems, with NOG and OA being in a 1:1 ratio (3 mM each) in the mixed system. Vesicles generated by NOG-based amphiphile systems were visualized under DIC and fluorescence microscopy as detailed in section 3.2.3.

3.2.5 Evaluating the metal ion stability of NOG-based vesicles

3.2.5.1 Vesicle Preparation

NOG-based vesicles were prepared similarly to that described in earlier sections. Typically, two types of vesicle systems were prepared in metal ion stability reactions. The pure NOG system contained vesicles made of only NOG, whereas the NOG + GMO mixed system contained NOG and GMO amphiphiles in a 2:1 ratio. A master mix solution was prepared for pure NOG and NOG + GMO mixed systems in 200 mM acetate buffer pH 5 (prepared in ultrapure water (18.2 $\text{M}\Omega\text{-cm}$)) to get a final total amphiphile concentration of 7.5 mM.

3.2.5.2 Setting up the metal ion stability experiments

Briefly, 40 μL aliquots of the NOG master mix vesicular solution were taken into separate microcentrifuge tubes. To these individual tubes, appropriate volumes of metal ion stock solution were externally added to get increasing concentrations of metal ion (usually in the range of 0 to 11 mM for Mg^{2+} and 0 to 600 mM for Na^+) while keeping the NOG concentration constant. After adding the metal ion stock solution into individual reaction vials, the final volume was adjusted to 50 μL using 200 mM acetate buffer pH 5 to get a 6 mM working concentration of NOG. The Control reaction contained only 6 mM NOG with no externally added metal ions. A similar procedure was followed for the NOG + GMO mixed system experiments. For the Mg^{2+} stability experiments, 100 mM MgCl_2 stock solution was used, while for the Na^+ stability experiments, 4 M NaCl stock solution was used. Both these stock solutions were prepared in 200 mM acetate buffer pH 5. After adding metal ions to vesicular solutions, the reactions were incubated for 30 min at 60 $^\circ\text{C}$ to allow the metal ion to interact with vesicles. As detailed above, all the amphiphile-based higher order structures like vesicles, droplets, and metal ion-induced aggregates were visualized under DIC microscopy.

3.2.5.3 Vesicle re-formation by the addition of magnesium chelators

Briefly, 6 mM pure NOG and NOG + GMO (2:1 ratio) vesicular solutions containing externally added 12 mM Mg^{2+} ions were prepared as mentioned above. This Mg^{2+} concentration was selected to ensure magnesium-induced aggregates formation in the pure NOG and the NOG + GMO mixed systems. Firstly, the presence of aggregates was confirmed by DIC microscopy. Then, a chelator (EDTA or citrate) was added in 1:1 mole equivalents to that of Mg^{2+} to the same aggregate-containing solution, followed by the incubation at 60 $^\circ\text{C}$ for 30 min. The dissociation of aggregates and the reappearance of vesicles was monitored using DIC microscopy.

3.2.6 NOG acting as a substrate for peptide chain growth under wet-dry cycles

In a typical reaction, the appropriate volume of 10 mg/ml methanol stock of NOG was taken in a glass vial, and methanol was evaporated under a vacuum to prepare a dry lipid film of NOG. This film was then hydrated with 200 μl of 200 mM of an amino acid solution of pH 9.8 (except for lysine, where the pH was 9.1) to get a 3 mM NOG solution, which was then subjected to a single wet-dry cycle of 24 hours duration at 130 $^\circ\text{C}$. These conditions were adapted from previously standardized conditions for peptide synthesis from non-activated amino

acids [3,21], as adding amino acids to the NOG terminus involves the formation of a peptide bond. In temperature variation experiments for NOG and Gly, the wet-dry cycling temperature was varied from 90 °C to 140 °C. The rehydration was done twice with 200 µl ultrapure water to recover the entire reaction content, which was then subjected to butanol extraction to extract the total lipid content of the reaction (unreacted NOG and N-oleoyl peptide products). This lipid content was analysed using HRMS via direct infusion of the sample as detailed in chapter 2, but in a positive mode, which was found to be more suitable for detecting N-oleoyl peptide products as compared to the negative mode. Both NOG and its extension products were mainly detected as sodium adducts.

All the experiments in this study were performed in at least two independent replicates.

3.3 Results

3.3.1 Synthesis of NAA from GMO and an amino acid under wet-dry cycling conditions

The NAA synthesis reported in our earlier study occurs via an ester-amide exchange reaction between phospholipids and amino acids [3]. However, phospholipids themselves are structurally complex lipids, which depend on SCA precursors for their synthesis both in biosynthetic [22] as well as potentially prebiotic enzyme-free reactions [23–26]. Therefore, we tested whether chemically simpler ester linkage-containing SCAs like monoglycerides can act as a lipid precursor for the synthesis of NAAs under prebiotically-relevant conditions using glycerol 1-monooleate (GMO) as a representative amphiphile. Towards this, a mixture of GMO and oleic acid (OA) (3 mM each) was subjected to three wet-dry cycles at 90°C in the presence of 200 mM glycine (Gly) at pH 9.8 (Figure 3.1a). A mixture of OA and GMO was used to increase the overall solubility of GMO in water. The formation of N-oleoyl glycine (NOG; a Gly containing NAA) was first evaluated by thin-layer chromatography (TLC), where we observed the complete disappearance of GMO spot with a concurrent appearance of a new spot comparable to that of the NOG standard, indicating the conversion of GMO to NOG (Figure 3.1b). Notably, this NOG spot did not appear in other control reactions (Figure 3.2). The NOG formation was also confirmed by analyzing the final lipid content of the reaction mixture using high-resolution mass spectrometry (HRMS), which showed a prominent peak corresponding to NOG with high accuracy (Figure 3.1c). The ¹H-NMR analysis of the final lipid mixture further corroborated these results, where we observed a signature peak for the amide hydrogen at 8.09 ppm, which

was in good agreement with the one observed for the NOG standard at 8.05 ppm (Figure 3.3). We also observed the formation of NAAs with different amino acid head groups when Gly was replaced with alanine, lysine, serine, and valine. The conversion of GMO to NAA in the presence of an amino acid likely follows an ester-amide exchange mechanism (Scheme 3.1), similar to that described for the phospholipid-amino acid reaction in the previous chapter. At an alkaline pH, the nucleophilic amino group of an amino acid attacks the carbonyl carbon of the ester linkage in GMO, thereby generating a corresponding NAA via amide bond formation. To our knowledge, this is a new, prebiotically-pertinent route for the formation of NAA, which supports their potential availability on early Earth.

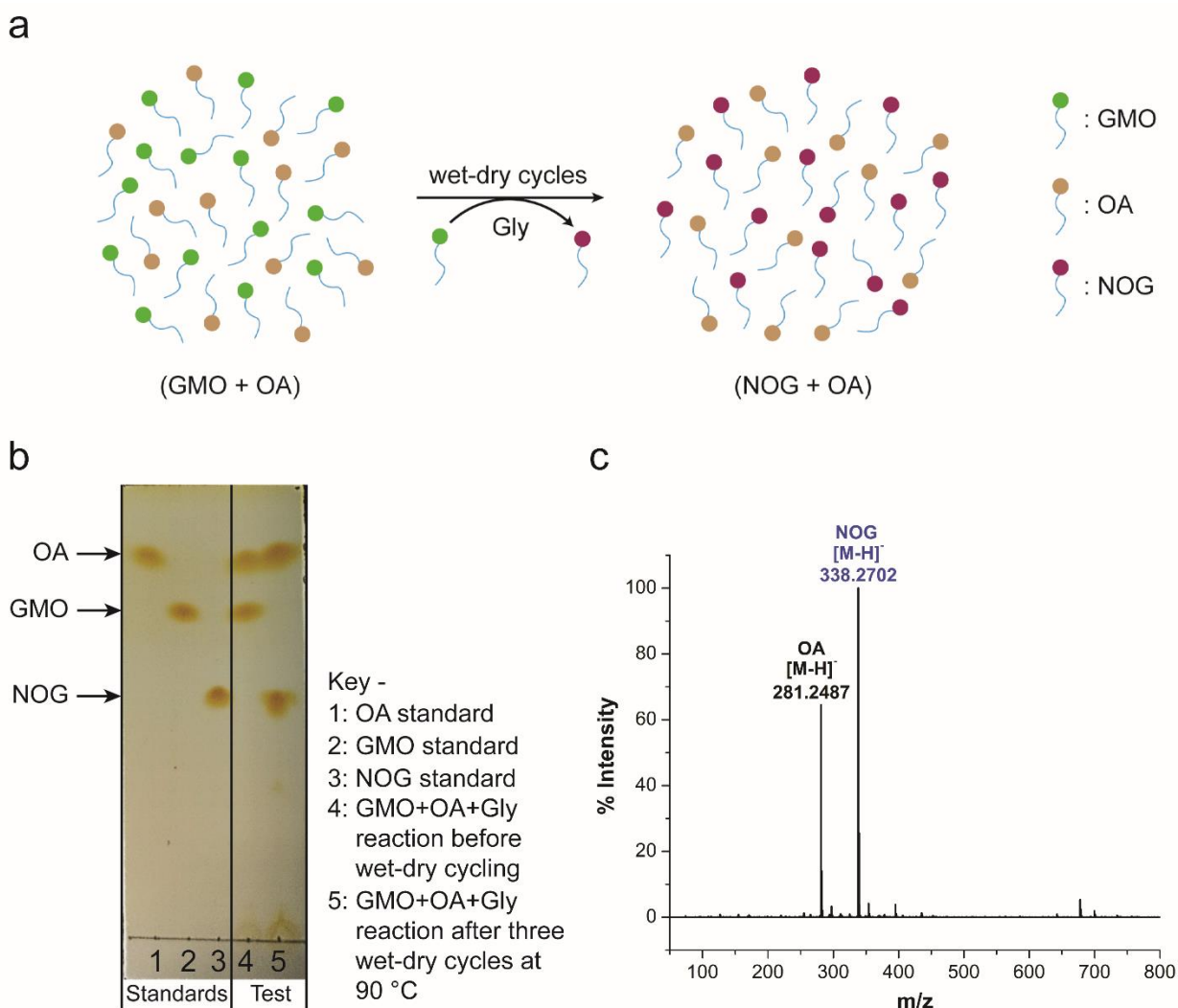


Figure 3.1 Conversion of GMO to NOG in the presence of Gly under wet-dry cycles. (a) A schematic overview of the reaction, where a mixture of GMO and OA (3 mM each) was subjected to three wet-dry

cycles at 90 °C in the presence of 200 mM Gly at pH 9.8, resulted in the formation of NOG by the reaction of GMO and Gly. **(b)** TLC analysis of the same reaction shows the complete disappearance of the GMO spot with a concurrent appearance of the NOG spot after wet-dry cycling (lane 5). **(c)** HRMS analysis (negative mode) of the final lipid content shows a prominent peak corresponding to NOG (calculated: 338.2701; observed: 338.2702; mass error = 0.3 ppm).

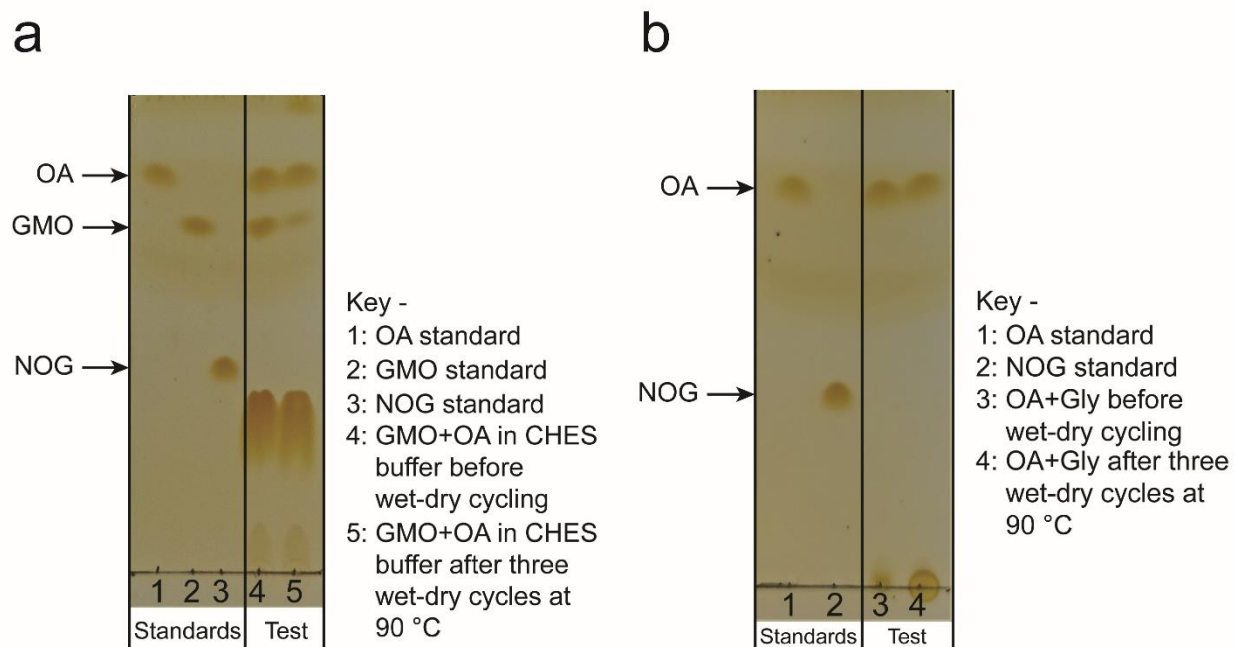


Figure 3.2 Control reactions for the NOG synthesis experiment. **(a)** GMO + OA mixture in the absence of Gly does not form NOG. The reaction was set up in 200 mM CHES buffer pH 9.8 and subjected to three wet-dry cycles at 90 °C. A spot corresponding to NOG did not appear after wet-dry cycling (compare lanes 3 and 5). The intensity of the GMO spot also decreased after wet-dry cycling, potentially indicating the degradation of GMO due to alkaline hydrolysis. A large spot in both lanes 4 and 5 towards the bottom side of the TLC is likely coming from the CHES buffer. **(b)** Only OA in the presence of Gly does not form NOG. A TLC analysis of the reaction containing 3 mM OA in 200 mM Gly pH 9.8, which was subjected to three wet-dry cycles at 90 °C, did not show the NOG spot after wet-dry cycling (compare lanes 2 and 4), indicating that OA itself does not react with Gly to form NOG under these reaction conditions.

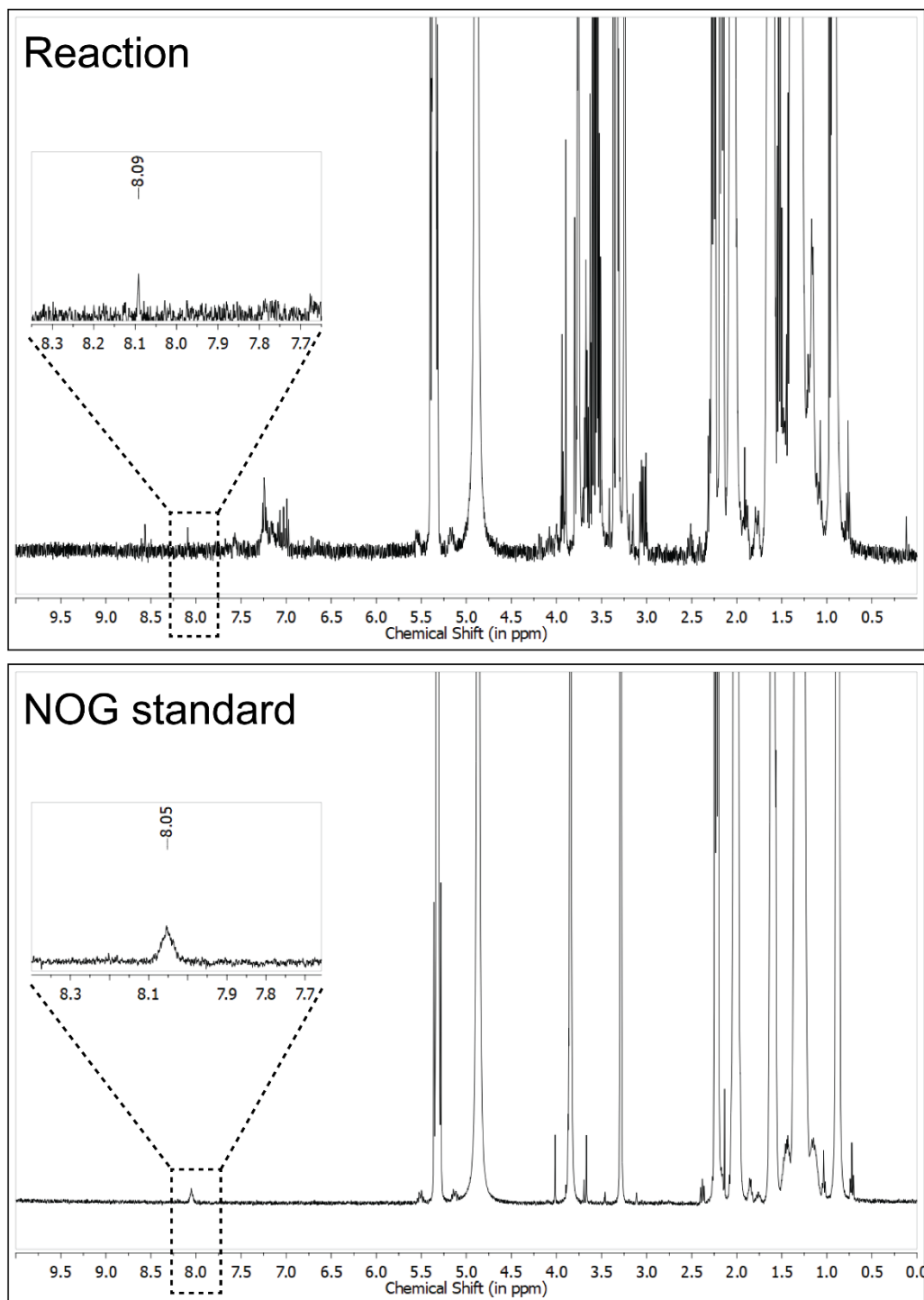
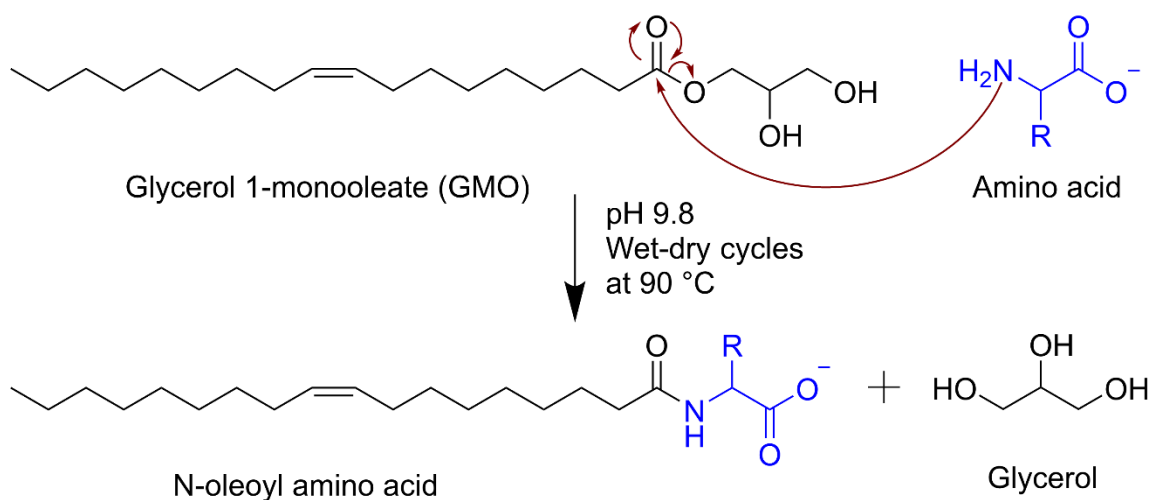


Figure 3.3 The ¹H NMR analysis of GMO + OA + Gly wet-dry cycling reaction. The ¹H NMR analysis of the final lipid content of the reaction (top panel) shows a signature peak for the amide hydrogen of NOG at 8.09 ppm (see inset), which is comparable to the one observed for the NOG standard (bottom panel) at 8.05 (see inset). The solvent used was methanol-d₄.

Scheme 3.1 A plausible mechanism for NAA synthesis from GMO and amino acid through an ester-amide exchange reaction.



3.3.2 NAAs can self-assemble into vesicles under acidic pH conditions

After showing NAA synthesis from amino acids and ester linkage-containing lipids under wet-dry cycles, we set out to understand whether these amphiphiles can assemble into vesicles on their own. This is one of the essential criteria that should be met before considering NAAs as model protocell membranes. Single-chain amphiphiles like fatty acids, which are also widely considered as protoamphiphile candidates, are known to form vesicles when the pH of the solution is around the apparent pKa (7-9) of their head group ($-\text{COOH}$) [27]. At this pH, both protonated and deprotonated species are present in relatively equal proportions, which come together to form a pseudo diacyl structure stabilized by hydrogen bonding, which overall has a cylindrical shape similar to phospholipids. This pseudo diacyl structure along with hydrophobic interactions, allows fatty acids to form vesicles. At pH values above and below their apparent pKa, fatty acids predominantly form micelles and oil droplets, respectively. NAAs, which are structurally similar to fatty acids, have been shown to get incorporated into preformed fatty acid and phospholipid vesicles, thereby enabling membrane growth [19,20]. However, whether NAAs could form vesicles on their own has not yet been explored systematically. Towards this, we checked the vesicle formation behavior of two commercially purchased NAAs, NOG and N-oleoyl serine (NOS). This was done by rehydrating a dry lipid film of these NAAs using an appropriate pH buffer, ranging from 4 to 10, to make a 6 mM NAA solution. Upon microscopic

analysis, we found that NOG readily assembled into vesicles at a slightly acidic pH range of 5 to 6, whereas NOS predominantly formed vesicles at pH 4 and 5 (Figure 3.4), with few vesicles observed even at pH 3. The lipid film rehydration method is known to generate different kinds of higher-order structures like micelles, droplets, and vesicles of varying size, shape, and lamellarity, which is also influenced by the pH of the medium. Therefore, we further confirmed the vesicular nature of these NAA aggregates by performing a calcein encapsulation experiment. Calcein, being a polar molecule, gets encapsulated within the aqueous lumen of the vesicles. Microscopic analysis showed that both NOG and NOS vesicles could readily encapsulate calcein within them (Figure 3.5).

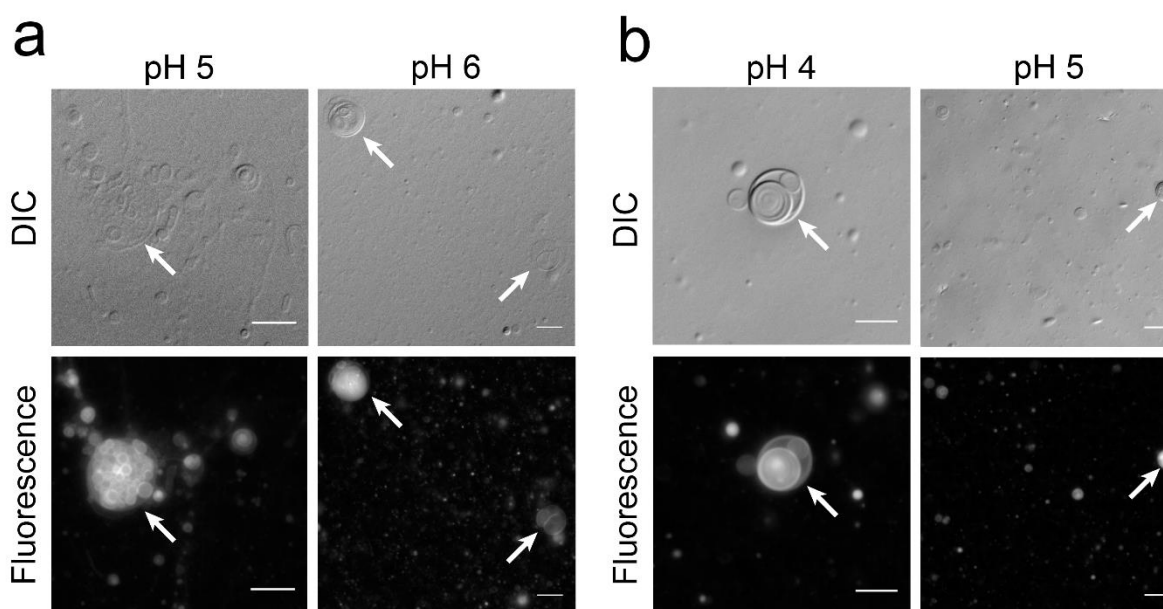


Figure 3.4 NAAs self-assemble into vesicles on their own under acidic conditions. (a) 6 mM of NOG forms vesicles in 200 mM acetate buffer at pH 5 (left panel) and in 200 mM MES buffer at pH 6 (right panel). (b) 6 mM NOS forms vesicles in 200 mM acetate buffer at pH 4 (left panel) and 5 (right panel). The observed vesicles (indicated by white arrows) typically vary in size, shape and lamellarity, some being unilamellar, multilamellar, and some even multivesicular in nature. Vesicle solutions were incubated at 60°C for 1 hour and immediately subjected to microscopy. For better visualization, vesicles were stained with 10 μ M of Octadecyl Rhodamine B Chloride (R18) dye and observed using differential interference contrast (DIC) and fluorescence microscopy. The scale bar is 10 μ m.

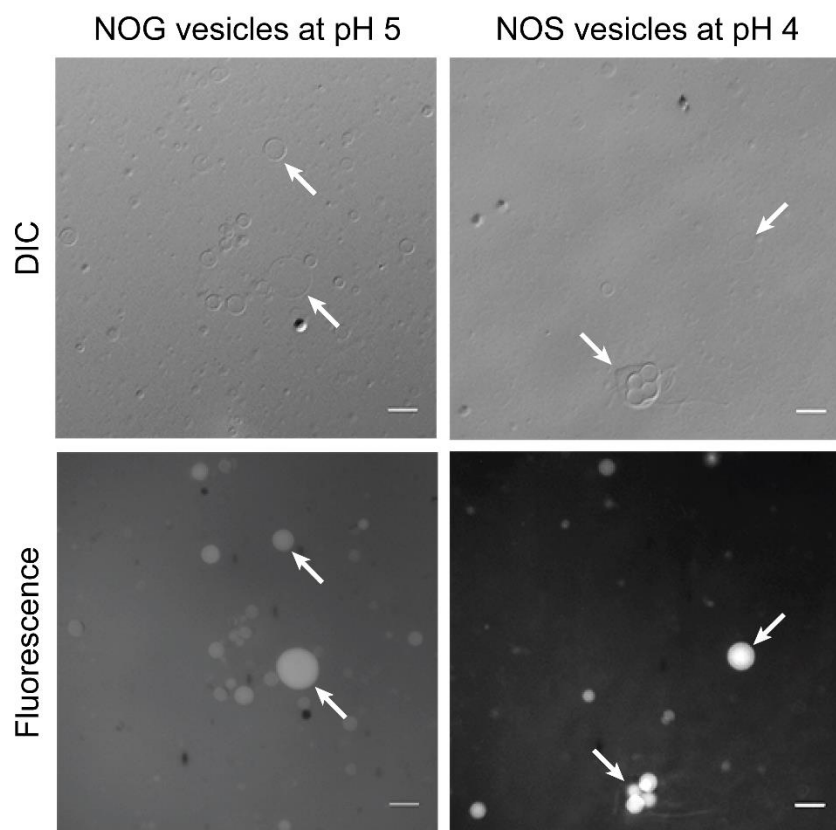


Figure 3.5 Encapsulation of calcein in NAA vesicles. Both NOG (left panel) and NOS (right panel) vesicles are able to encapsulate a fluorescent polar calcein molecule within them (indicated by white arrows), which confirms their vesicular nature. Vesicles were observed under both DIC and fluorescence microscopy. The calcein concentration used was 0.1 mM, which is below its self-quenching concentration. The scale bar is 10 μm .

In addition to pH, another important factor that influences fatty acid vesicle formation is the temperature of the system. Fatty acids show a thermo-responsive phase behavior, where they assemble into vesicles in aqueous solutions only above their chain-melting or transition temperature (T_m) and form crystals below this temperature [28,29]. We noticed a similar temperature-dependent phase behavior with NAAs too. During vesicle preparation, the NOG solution was incubated at 60 $^{\circ}\text{C}$ and immediately subjected to microscopy to image the resultant vesicles (see methods). However, as the solution remained at 18 $^{\circ}\text{C}$ over the course of microscopic analysis, this temperature variation induced the conversion of vesicles into fiber-like structures within a few minutes (Figure 3.6). A similar phenomenon was also observed with

NOS (Figure 3.6), although the nature of aggregates was different than the ones that were found in the case of NOG. Nevertheless, from a prebiotic point of view, this intriguing phenomenon is unlikely to come in the way of NAAs being able to serve as plausible protocell membranes because the early Earth temperature is thought to have been much higher than that of the contemporary Earth [30]. Also, high-temperature geochemical settings, like terrestrial hot springs and submarine hydrothermal vents, would have readily allowed NAAs to sustain themselves in vesicle form.

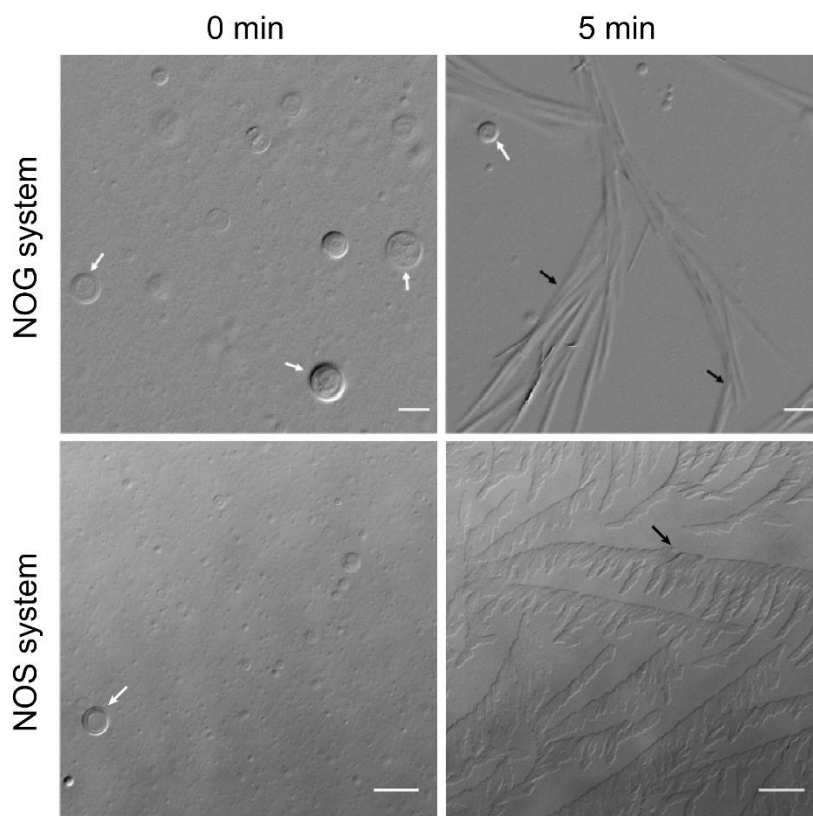


Figure 3.6 Temperature-dependent phase behavior of NOG and NOS. Both NOG and NOS solutions were incubated at 60°C for 1 hour to facilitate vesicle formation and immediately subjected to microscopy. A large number of vesicles (indicated by white arrows) were observed initially (0 min; left panels). However, as the microscopy was performed at room temperature, this decrease in the solution temperature over the course of microscopy induced the conversion of the vesicles into crystalline/fiber-like structures (indicated by black arrows) within a few minutes (right panels). Note the difference in the morphology of structures formed by NOG and NOS. Scale bar lengths are 10 μm and 20 μm for NOG and NOS images, respectively.

3.3.3 Vesicle formation by NOG-based amphiphile systems over a broad pH range

Most single-chain amphiphiles form vesicles only at a narrow pH range around the apparent pK_a of their head group, limiting their ability to form protocell membranes over a diverse pH range. Therefore, systematic efforts have been made to look for amphiphile systems that can generate vesicles over a broad pH range. Notably, the addition of surfactants like monoglycerides and fatty alcohols, which contain less readily dissociable polar hydroxyl group(s) in their head group region, have been shown to stabilize fatty acid vesicles by hydrogen bonding with their carboxyl head group [31,32]. This stabilizing effect is more prominent towards the alkaline pH range from the apparent pK_a of their head group that lies between pH 7 to 9 for most of the fatty acids. Consequently, these mixed fatty acid amphiphile systems form vesicles broadly in the neutral to alkaline pH range, but not at acidic pH, which constrains their ability to generate protocell compartments under a diverse pH regime. As shown in the previous section, NAAs like NOG can form vesicles on their own at an acidic range from pH 5 to 6, indicating that its apparent pK_a lies in this range. Since monoglycerides facilitate SCA vesicle formation towards the alkaline pH range from the apparent pK_a of these amphiphiles, we asked whether a mixture of NOG and GMO could form vesicles over a broad pH range spanning from acidic to neutral to alkaline pH. Indeed, the NOG + GMO mixed system (6 mM; 2:1 ratio) could generate vesicles from pH 4 to 11 (Figure 3.7).

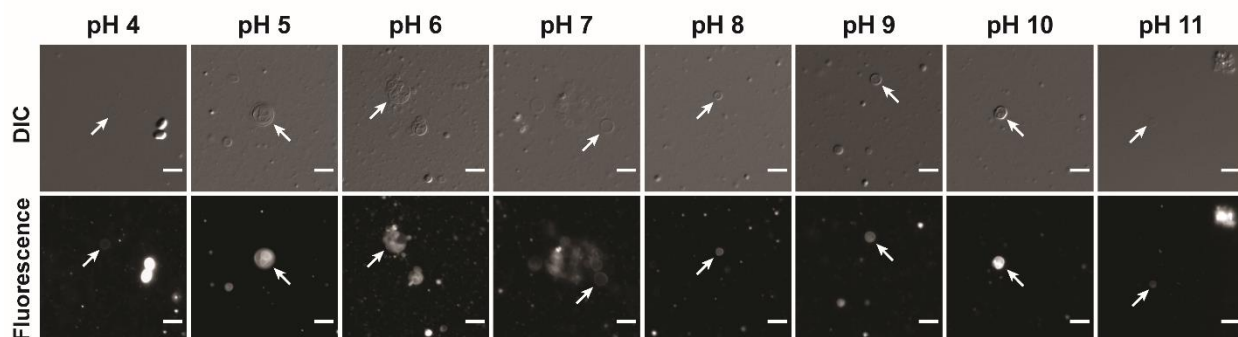


Figure 3.7 Vesicle formation by NOG + GMO mixed system. A mixture of NOG and GMO (6 mM; 2:1 ratio) from pH 4 to 11, as observed under differential interference contrast (DIC) and fluorescence microscopy. White arrows indicate vesicles. The scale bar is 10 μ m.

The hydroxyl groups in the glycerol moiety of GMO likely stabilize the deprotonated NOG species via hydrogen bonding, thereby allowing them to form vesicles over such a broad pH range. However, the overall vesicle formation propensity, as well as the size, shape and

lamellarity of the resultant vesicles, seem to vary across different pH values. Nevertheless, this result demonstrates the ability of monoglycerides to facilitate the membrane assembly of NAAs over a diverse pH range in addition to acting as a precursor for their synthesis (Figure 3.1).

Interestingly, the conversion of GMO to NOG in our reaction also led to a new heterogeneous amphiphile system at the end of the reaction, containing NOG and OA (Figure 3.1a). Exploring the vesicle formation behavior of this system constitutes an interesting study as both its components have their own optimum pH range for vesicle formation (NOG: pH 5 to 6, OA: pH 8 to 9). Moreover, from a prebiotic perspective, both NAAs and fatty acids would have been simultaneously present in a prebiotic soup and would likely have affected each other's self-assembly behavior. Therefore, we evaluated the vesicle formation behavior of the NOG + OA mixed system (6 mM; 1:1 ratio) at different pH values. Consistent with our earlier results and previously reported studies [31], homogenous NOG system (6 mM) formed vesicles at pH 5 and 6, whereas OA (6 mM) did so at pH 8 and 9. However, a mixed system of NOG and OA generated vesicles from pH 5 to 9 (Figure 3.8), notably even at the physiological pH range around 7, where both of its components were unable to self-assemble into vesicles on their own.

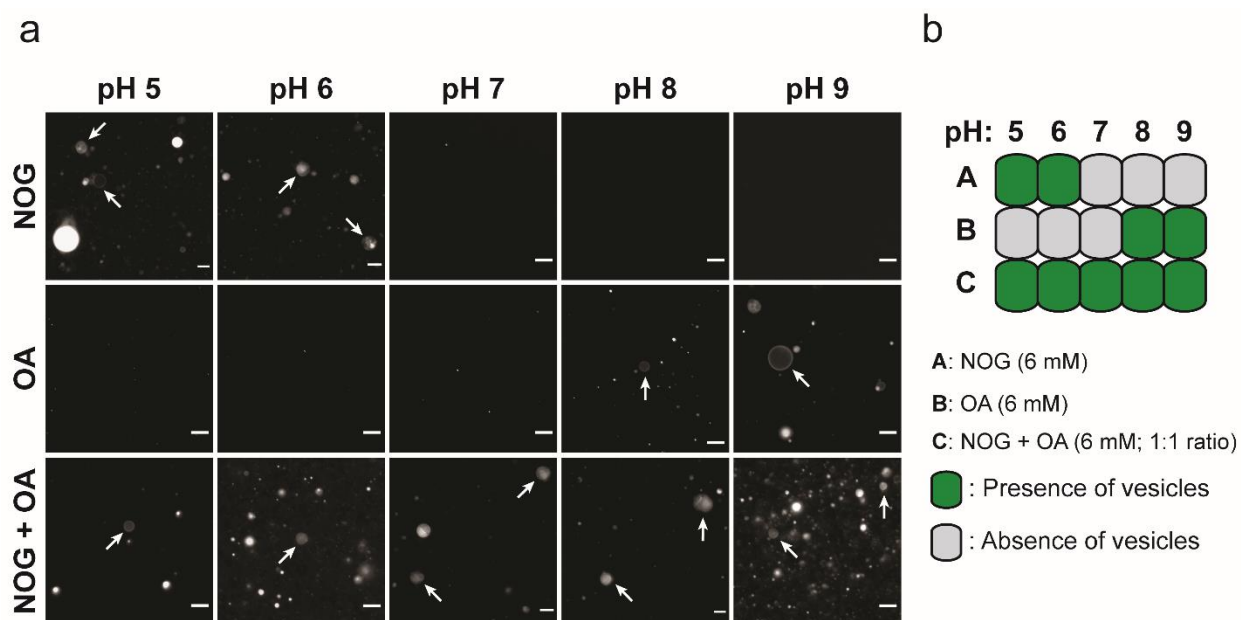


Figure 3.8 Vesicle formation behavior of the NOG + OA mixed system. (a) Fluorescence microscopy shows that NOG and OA by themselves generate vesicles at pH 5, 6, and pH 8, 9, respectively. However, the NOG + OA mixed system forms vesicles across pH 5 to 9. White arrows indicate vesicles. The scale bar is 10 μ m. (b) Schematic representation of the microscopy results that were shown in (a).

At this pH, the efficient hydrogen bonding between predominantly present deprotonated NOG and protonated OA species can generate pseudodiacyl structures that tend to favor bilayer formation. It nicely demonstrates how amphiphiles affect each other's physicochemical properties in a mixture that might also produce new emergent properties like vesicle formation at pH 7 in this particular case. Together, these results highlight the ability of NOG to generate robust membranes over a diverse pH range when mixed with amphiphiles like GMO and OA.

3.3.4 Metal ion stability of NOG-based vesicles

Along with temperature and pH, the ionic strength of the medium also significantly affects the formation and stability of SCA vesicles [10,13,33,34]. Particularly, fatty acid vesicles are extremely sensitive to metal ions (especially divalent ions like Mg^{2+}), which interact with their negatively charged carboxylate head groups and induce vesicle aggregation up to a certain concentration. Further, metal ions are required at a relatively high concentration for other prebiotically pertinent processes such as protometabolic reactions [35,36], ribozyme activity [37–40], and nonenzymatic template-directed replication of RNA [41,42]. Therefore, it is necessary to systematically evaluate the metal ion stability of vesicles generated by model protoamphiphile systems to characterize their compatibility with the functioning of other prebiotic processes. Towards this, we systematically evaluated the effect of divalent and monovalent metal ions on the stability of NAA-based vesicular systems using NOG-based model vesicles, and Mg^{2+} and Na^+ as the representative divalent and monovalent metal ions, respectively.

As 6 mM NOG in 200 mM acetate buffer pH 5 generates a large number of vesicles, we used these conditions to evaluate the effect of different metal ions on the stability of NOG vesicles. For a divalent cation like Mg^{2+} , it was observed that pure NOG vesicles could tolerate Mg^{2+} concentrations up to 1:1 molar ratio, beyond which magnesium ions induced a clumping of vesicles resulting in the formation of large-sized aggregates (Figures 3.9a). Overall, the behavior of the pure NOG system in the presence of increasing concentrations of Mg^{2+} followed three distinct phases (Figure 3.9c). A vesicular phase (up to 5 mM Mg^{2+}) contained only vesicles with no visible aggregates. It was followed by a transition phase (at 6 mM Mg^{2+}), where small aggregates started forming in the solution. Finally, an aggregate phase occurred (7 mM Mg^{2+} onwards), where the solution contained only large-sized magnesium-induced aggregates.

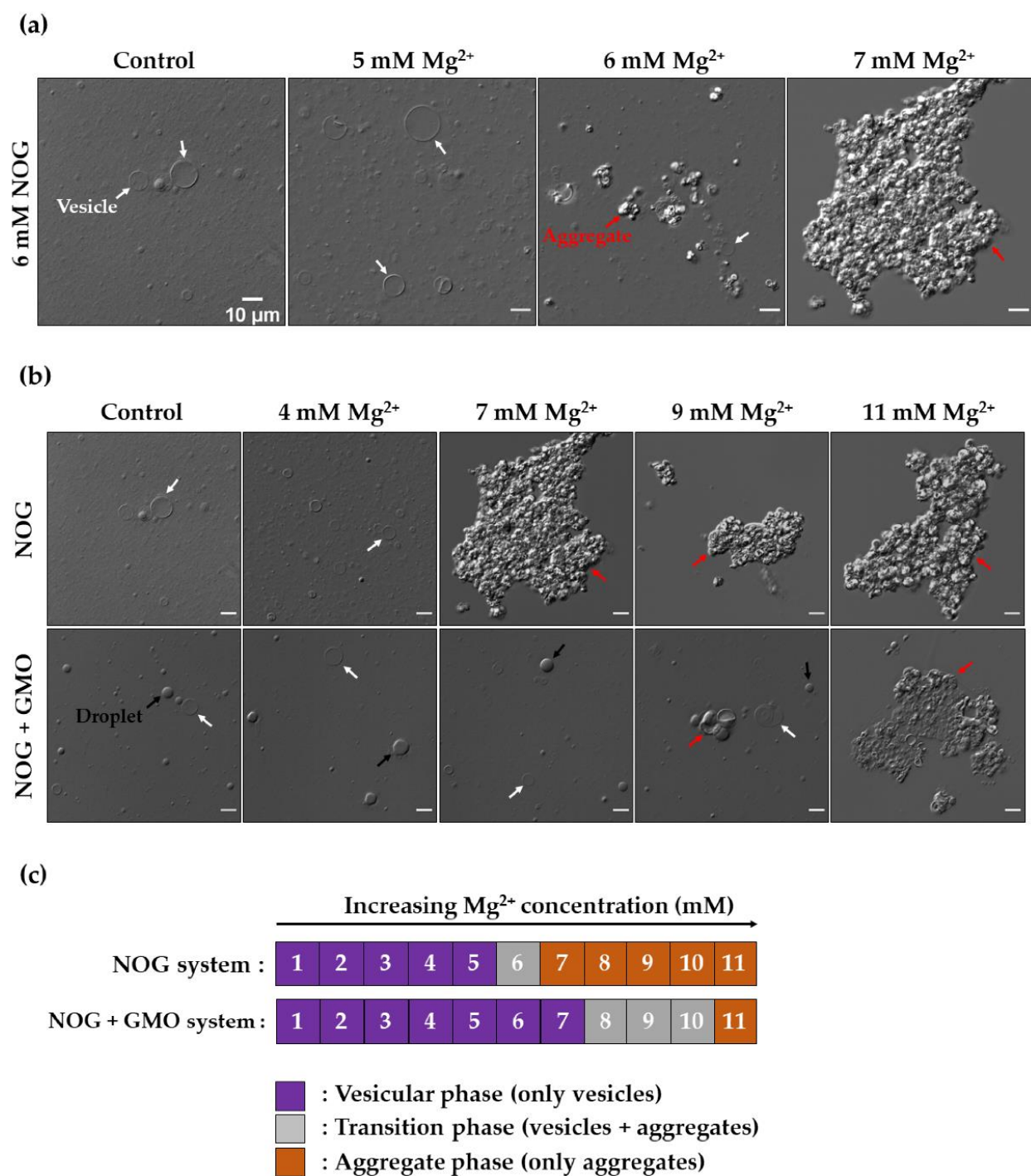


Figure 3.9 Effect of Mg²⁺ on pure NOG and NOG + GMO mixed vesicles. (a) Vesicles prepared from 6 mM NOG are stable in the control reaction (without Mg²⁺) and in the presence of 5 mM Mg²⁺. The metal ion-induced aggregates start forming at 6 mM Mg²⁺. At 7 mM Mg²⁺, vesicles completely collapse into large aggregates (b) Addition of GMO to the NOG system increases the stability of vesicles towards

Mg²⁺ ion. The NOG + GMO (6 mM; 2:1 ratio) mixed vesicles result in large magnesium-induced aggregates only at and above 11 mM Mg²⁺. The NOG + GMO mixture also generates a heterogeneous population of vesicles and droplets. Vesicles, droplets, and aggregates are indicated by white, black, and red arrows, respectively. Imaging was done using DIC microscopy. The scale bar is 10 μm for all images. (c) A distinct three-phase behavior of NOG-based vesicles is depicted with increasing concentrations of Mg²⁺. The vesicular phase (purple) contains only vesicles. It is followed by a transition phase (grey) where both free vesicles and small metal ion-induced aggregates are simultaneously present. Finally, the aggregate phase (orange) contains only large-sized aggregates.

Surfactants like monoglycerides are known to increase the stability of fatty acid vesicles towards metal ions [31,43]. Therefore, we sought to explore whether a similar effect is observed for a mixed amphiphile system containing NOG and a monoglyceride like GMO. Indeed the NOG + GMO (6 mM; 2:1 ratio) mixed vesicles were more stable in the presence of Mg²⁺, which could tolerate Mg²⁺ concentrations till 11 mM (Figure 3.9b). Notably, the addition of GMO also resulted in droplet formation along with vesicles. Hence, the resultant solution was a heterogeneous mixture of vesicles and droplets. Similar to the pure NOG system, this mixed system also showed a three-phase behavior in the presence of increasing Mg²⁺ concentrations (Figure 3.9c). However, the span of both the vesicular and transition phases of the NOG system increased after the addition of GMO to the system, which clearly indicated a stabilizing effect that was being conferred by the surfactant towards the metal ions. We also checked whether this aggregation phenomenon is reversible by adding magnesium chelating agents like EDTA to the solution containing magnesium-induced vesicle aggregates. It resulted in the disruption of aggregates and reappearance of vesicles in both the pure NOG and NOG + GMO mixed systems (Figure 3.10a). A similar effect was observed after the addition of a prebiotically-relevant chelating agent like citrate, where vesicles emerged from large aggregates (Figure 3.10b).

Next, we characterized the behavior of NOG-based vesicles in the presence of a monovalent cation like sodium (Na⁺). Previous studies have shown that fatty acid-based systems are more stable in the presence of monovalent cations than divalent ones [43]. We also observed similar behavior for NOG-based systems, where pure NOG vesicles formed aggregates only at and above 400 mM Na⁺ (Figure 3.11), which is about two orders of magnitude higher than that for Mg²⁺ (7 mM). The NOG + GMO mixed system was even more stable, resulting in aggregate formation only at 500 mM Na⁺ (Figure 3.11).

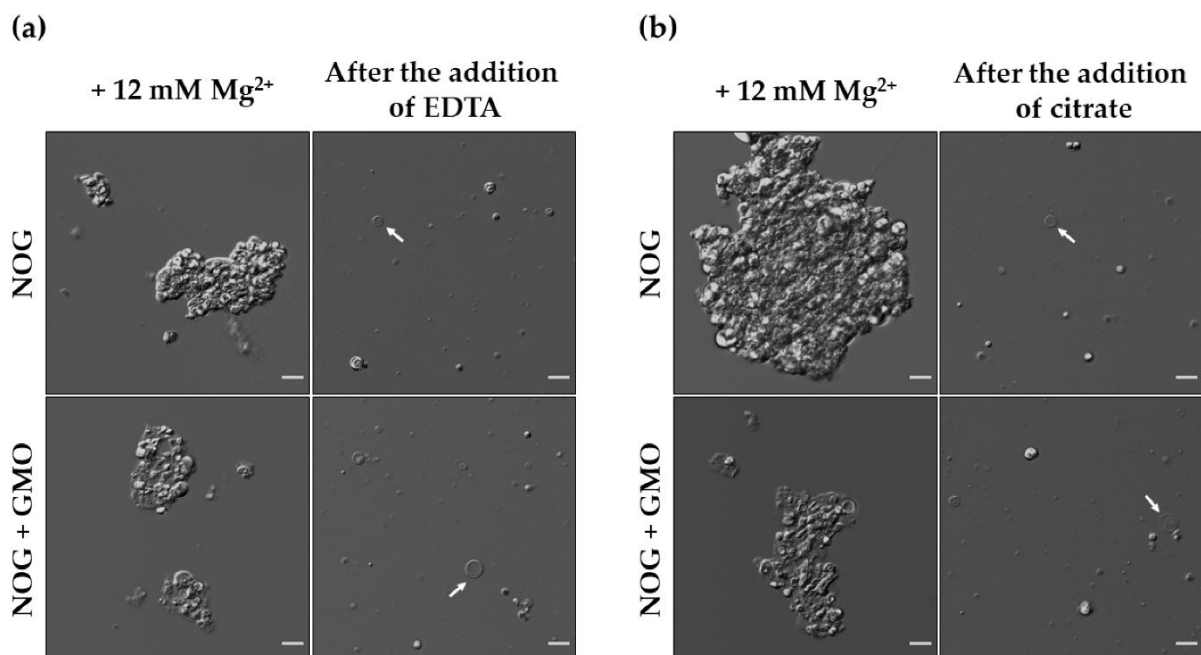


Figure 3.10 Re-formation of vesicles from magnesium-induced aggregates after the addition of a chelator. (a) Vesicles generated by both pure NOG (6 mM) and NOG + GMO (6 mM; 2:1 ratio) mixed systems (top and bottom panels, respectively) completely collapse into large aggregates in the presence of 12 mM Mg^{2+} . However, the addition of EDTA in 1:1 mole equivalents to that of Mg^{2+} results in the disassembly of aggregates with a concurrent reappearance of free vesicles (indicated by white arrows). (b) A similar effect is observed in the presence of citrate as a chelator, which was also added in 1:1 mole equivalents to that of Mg^{2+} . Imaging was done using DIC microscopy. The scale bar is 10 μ m.

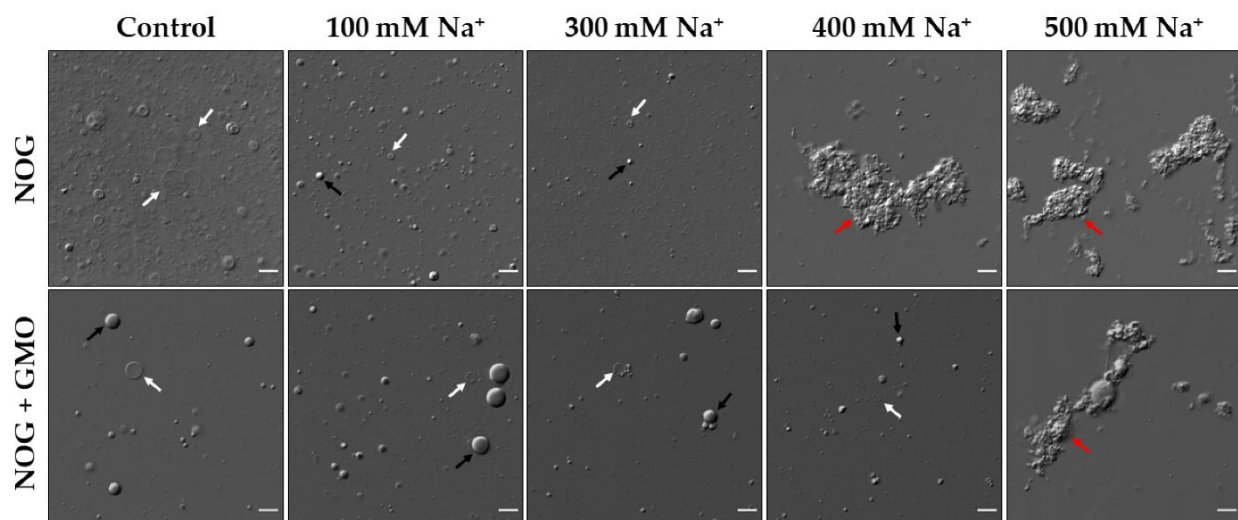


Figure 3.11 Effect of Na⁺ on the stability of NOG-based vesicles. 6 mM pure NOG vesicles (top panel) tolerate Na⁺ concentrations up to 300 mM, beyond which large metal ion-induced aggregates are formed. Also, the external addition of Na⁺ to the pure NOG vesicular system results in vesicle shrinkage and the formation of small droplets, as observed in the 100 mM and 300 mM Na⁺ reactions. The NOG + GMO (6 mM; 2:1 ratio) mixed system (bottom panel) forms a heterogeneous population of vesicles and droplets, which survives Na⁺ concentrations up to 400 mM, beyond which metal ion-induced aggregates are formed. White, black, and red arrows indicate vesicles, droplets, and aggregates, respectively. Imaging was done using DIC microscopy. The scale bar is 10 μm.

3.3.5 NOG acting as a substrate for peptide chain growth under wet-dry cycles

Another potential application of NAAs is their ability to act as a substrate for peptide synthesis under prebiotically-pertinent wet-dry cycling conditions, thereby generating N-acylated peptide amphiphiles (lipopeptides). Specifically, the addition of subsequent Gly or other amino acids on the carboxyl terminus of NOG, can produce N-acylated homo or heteropeptides, respectively (Figure 3.12, Scheme 3.2).

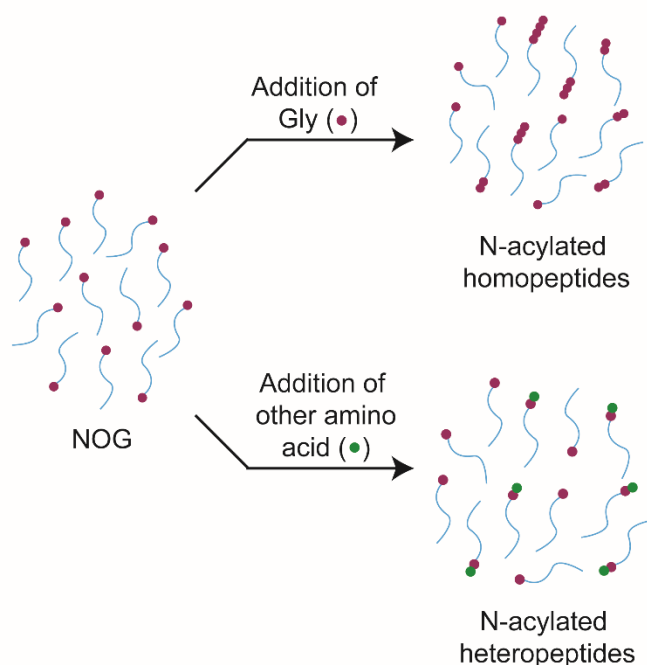
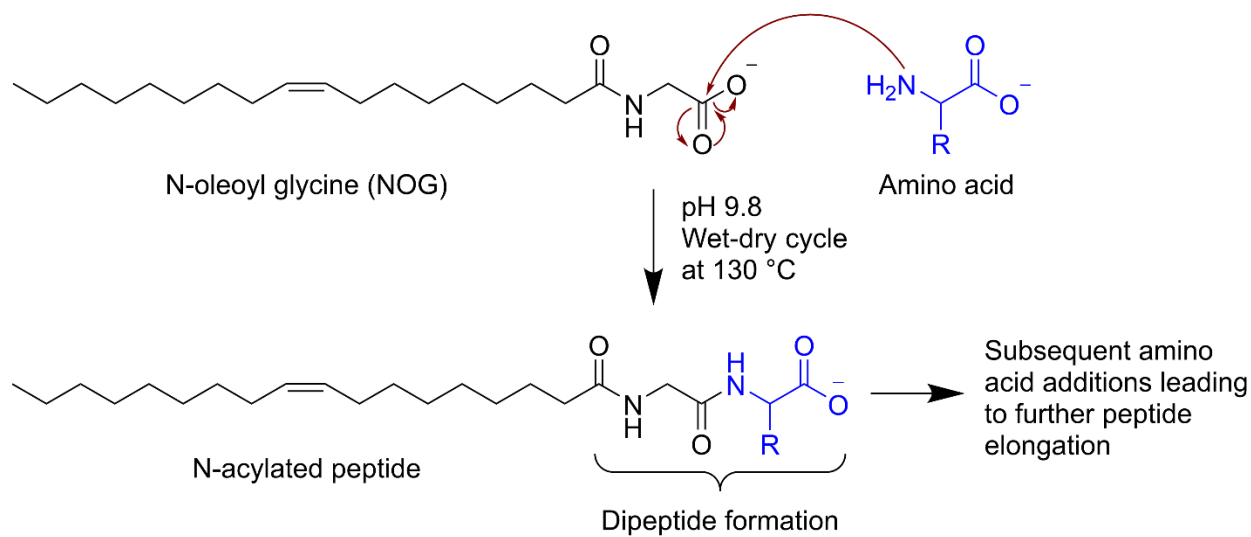


Figure 3.12 Schematic representation of the reaction of NOG with amino acids to form N-acylated peptide amphiphiles. The addition of Gly on the NOG terminus results in the formation homopeptides, whereas the addition of other amino acids on the Gly head group generated heteropeptides.

Scheme 3.2 Acid-amine coupling between NOG and amino acid, generating N-acylated peptides.



To test this, a mixture of 3 mM NOG and 200 mM Gly was subjected to a single wet-dry cycle at pH 9.8 and 130°C. This temperature, pH, and wet-dry cycling conditions are known to be suitable for peptide synthesis from non-activated Gly [3,21]. HRMS analysis showed the formation of lipopeptides with up to three Gly molecules added onto NOG (Figure 3.13).

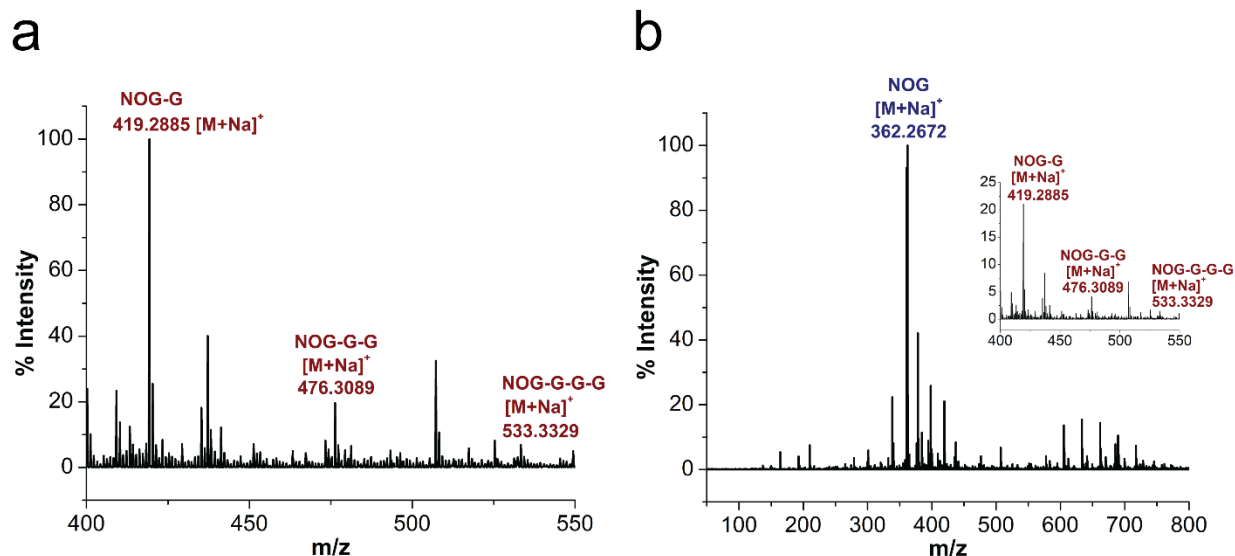


Figure 3.13 Formation of Gly-containing lipopeptides by the reaction between NOG and Gly. (a) A zoomed version of the mass spectrum generated from the HRMS analysis (positive mode) of the final lipid content of NOG + Gly wet-dry cycling reaction at 130 °C shows peaks for sodiated adducts of peptide chain extension products. Up to three Gly additions were observed on the NOG surface, which is indicated by NOG-G for a single addition (cal: 419.288; obs: 419.2885; mass error = 1.2 ppm), NOG-G-

G for two additions (cal: 476.3095; obs: 476.3089; mass error = - 1.3 ppm), and NOG-G-G-G-G for three additions (cal: 533.331; obs: 533.3329; mass error = 3.6 ppm). **(b)** Original HRMS spectrum of the same reaction, which also shows a peak for the unreacted NOG. Peptide chain extension products are shown in the inset.

Next, we evaluated if the maximum length of the peptide chain generated on the NOG head group is influenced by temperature. It was observed that the maximum number of Gly additions to the NOG increased with increasing temperature (Figure 3.14), with up to three additions observed at 130°C. A higher temperature of 140°C did not facilitate further peptide extension (Figure 3.14f). Finally, we checked whether NOG could react with other amino acids like alanine, serine, and lysine to generate N-acylated heteropeptides. We observed only a single amino acid addition in these reactions on the NOG head group (Figure 3.15). Although, the lipopeptide formation efficiency seemed to vary based on the amino acid type, the addition of lysine to the NOG head group was likely the most efficient one. As observed in the HRMS spectrum of NOG + Lys reaction (Figure 3.15d), NOG-Lys lipopeptide was the most abundant mass species, and the precursor NOG peak was absent, indicating almost a complete conversion of NOG to NOG-Lys lipopeptide. It possibly could be because of the favorable electrostatic interactions between the positively charged lysine and the negatively charged NOG at pH 9.8, allowing these two substrate molecules to come close to each other and react more efficiently. Overall, these results demonstrate NOG's ability to react with different amino acids under wet-dry cycles to generate a diverse set of lipopeptides.

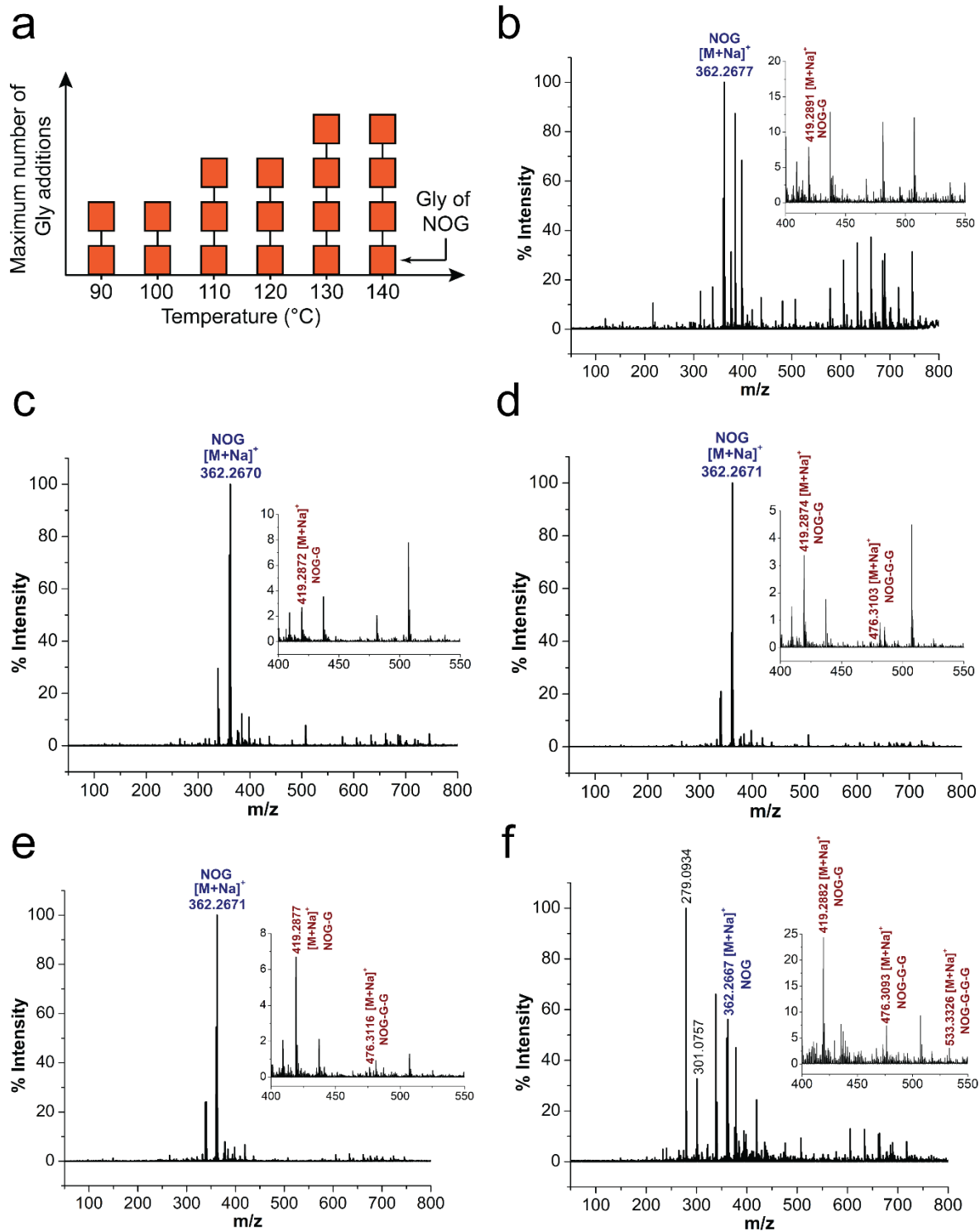


Figure 3.14 Effect of temperature on the maximum length of the peptide chain generated on the NOG head group. (a) A diagrammatic representation of the overall result shows that the maximum number of Gly additions increases with increasing temperature. Subsequent panels show the original mass spectrums obtained from the HRMS analysis (positive mode) of the final lipid content of the NOG + Gly

reaction performed at (b) 90 °C, (c) 100 °C, (d) 110 °C, (e) 120 °C, and (f) 140 °C. Inset shows the peptide chain extension product(s) in each of these spectrums. The data for the 130 °C reaction was used from the one reported in Figure 3.13. In the HRMS spectrum of the 140 °C reaction, some predominant stray peaks at 279.09 and 301.07 were detected, potentially indicating the breakdown of NOG at this temperature.

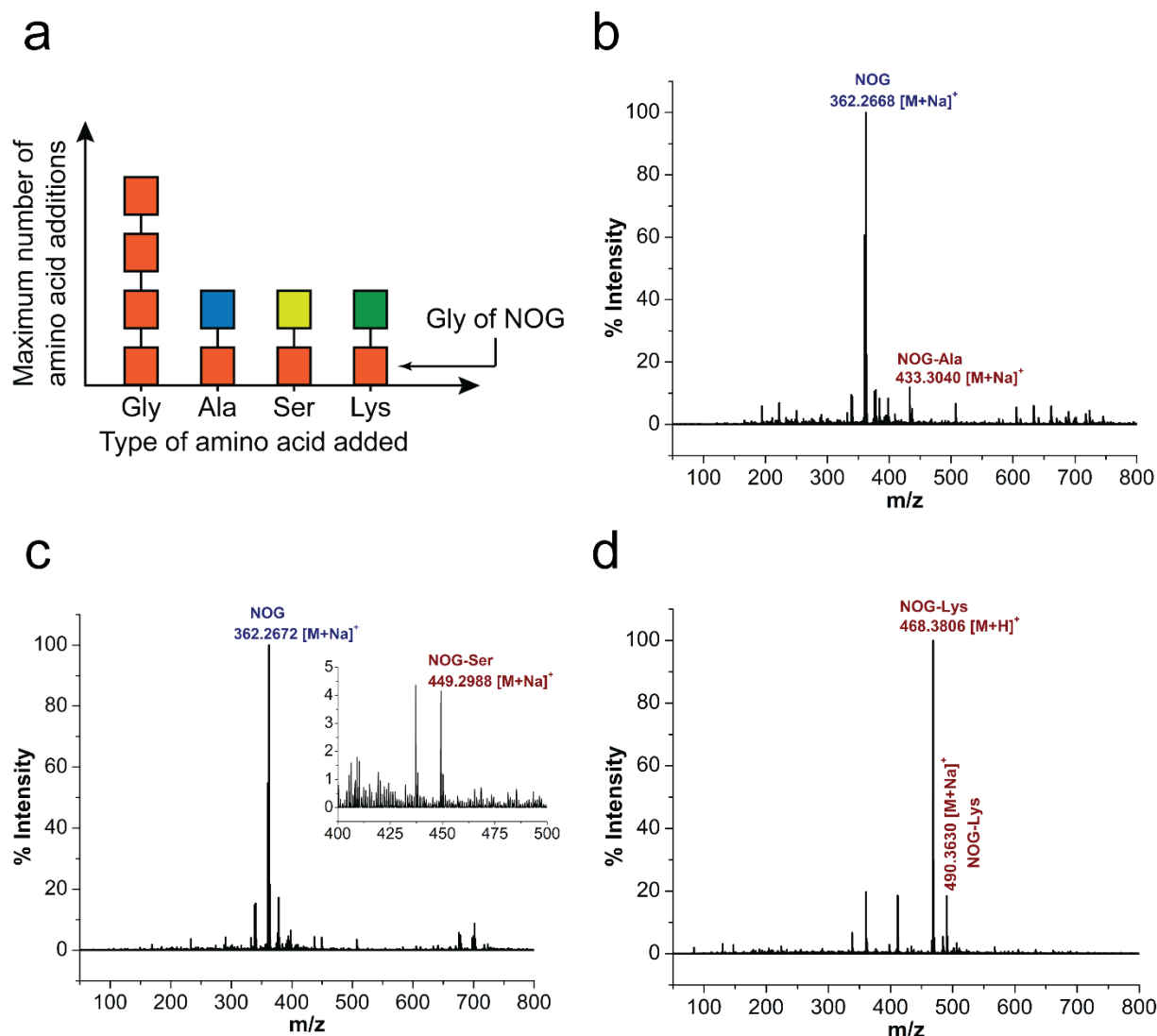


Figure 3.15 Reaction of NOG with an amino acid other than Gly results in the formation of N-acylated heteropeptides. (a) A diagrammatic representation of the overall result shows that reactions of NOG with alanine, serine, and lysine result in the generation of N-acylated heteropeptides containing corresponding amino acids. Although, unlike Gly, the addition of only a single amino acid is observed in these reactions. Subsequent panels show the original mass spectrums obtained from the HRMS analysis (positive mode) of the final lipid content of the corresponding reactions. (b) A reaction of NOG with

alanine generates NOG-Ala (cal: 433.3037; obs: 433.3040; mass error = 0.7 ppm). (c) A reaction of NOG with serine generates NOG-Ser (cal: 449.2986; obs: 449.2988; mass error = 0.4 ppm). (d) A reaction of NOG with lysine generates NOG-Lys. Unlike other amino acid extension products, for NOG-Lys, the most abundant peak was the protonated species ($[M+H]^+$; cal: 468.3796; obs: 468.3806; mass error = 2.1) followed by a sodiated adduct ($[M+Na]^+$; cal: 490.3615; obs: 490.3630; mass error = 3.1). Also, note that the peak for precursor NOG was not detected, which likely indicates the complete conversion of NOG to NOG-lys.

3.4 Discussion:

NAAs are naturally occurring lipids, which perform different functions in extant biology [44], and also have widespread commercial applications as biosurfactants [45] and in drug delivery [18]. However, their potential role in the origin of cellular life has been minimally explored. As mentioned earlier, they are hybrid molecules containing amino acid and fatty acid linked together via a stable amide linkage, thus having structural features of both lipids and amino acids (and even peptides). This unique combination of two centrally important molecules in a prebiotic context might have allowed NAAs to act as a connecting link between the lipid world and the peptide world. Notably, given their amphiphilic nature, these SCAs might have served as protoamphiphiles (prebiotically-plausible amphiphiles constituting early protocell membranes). In this study, we systematically characterized NAAs as a model protoamphiphile system.

The first and foremost thing while testing any amphiphile as a model protoamphiphile would be to justify its prebiotic availability. One way to do so is to check whether it can form under early Earth conditions from prebiotically-relevant molecules. We showed that NAAs could be synthesized from phospholipids and amino acids under prebiotically-pertinent wet-dry cycling conditions. However, phospholipids are structurally-complex diacyl lipids, which themselves depend on SCAs for their synthesis, both in extant biology[22] and some potentially prebiotic chemical reactions [23–26]. Moreover, phospholipids are mostly considered a product of biological evolution from simple SCAs [46–48]. Therefore, requiring phospholipids as a precursor for the synthesis of SCAs like NAAs might be perceived as going backward in the evolutionary trajectory of prebiotic lipids to biological lipids. To address this conundrum, we report a new prebiological route for synthesizing NAAs from an amino acid and a monoglyceride (a prebiotically-relevant ester-linkage containing SCA) under wet-dry cycling conditions. It

overcomes the dependence on structurally-complex diacyl lipids for the prebiotic synthesis of NAAs while strengthening their potential availability on early Earth. It will be interesting to test this reaction further using short-chain monoglycerides as a precursor, given the plausible prebiotic abundance of short-chain amphiphiles [5,6]. We also hypothesize that the synthesis of NAAs from monoglycerides and amino acids occurs via an ester-amide exchange reaction, which highlights the significance of this reaction in the prebiotic synthesis of protoamphiphiles (NAAs) in addition to that of protopeptides (depsipeptides) [49].

Another important feature that an amphiphile should possess to serve as a primary constituent of protocell membranes would be its ability to generate vesicles on its own. We showed that NAAs like NOG and NOS can readily self-assemble into vesicles under acidic pH conditions, demonstrating that NAAs are themselves capable of generating protocell compartments. Furthermore, our study also reveals several interesting features of the self-assembly behavior of NAAs. Firstly, it indicates that the apparent pKa of the head group of NOG and NOS would likely be in the acidic range, which is different from most fatty acids that have their apparent pKa values in the neutral to alkaline range. Although both fatty acids and NAAs have a carboxyl moiety at the terminal position of their head group, the presence of an amide linkage in NAA might lower the apparent pKa of its head group. Moreover, the pKa of NAA is also likely to get influenced by the nature of its amino acid component, as shown here with the example of NOG and NOS. The presence of an electron-withdrawing hydroxyl group in the side chain of the serine head group of NOS could make the terminal carboxyl group even more acidic, thereby decreasing the pH optimum (pH 4 to 5) for its vesicle formation as compared to that of NOG (pH 5 to 6). It will be interesting to check how the pH optimum of vesicle formation by other NAAs change based on their amino acid head group. This result also indicates that NAAs can be used as an amphiphilic system with a “tunable pH”. Furthermore, as most of the conventional fatty acid-based systems form vesicles only in the neutral to alkaline pH range [27], NAAs like NOG and NOS can provide an alternative protoamphiphile system with a vesicle forming-capability at acidic pH. This system could have a selective advantage over fatty acid-based systems in generating protocell membranes in acidic geothermal pool-like conditions. It also widens the possible environmental regimes where protocellular membranes could have formed on the early Earth.

After demonstrating the ability of NAAs to self-assemble into vesicles, we also checked whether increasing the heterogeneity of NAA-based amphiphile systems can allow them to form robust membranes under fluctuating environmental conditions. Studying the properties of such heterogeneous membranes also seems logical from a prebiotic perspective, given that the prebiotic soup might have possessed a large array of protoamphiphiles. Therefore, the protocellular membranes generated from these amphiphiles would likely be compositionally heterogeneous. Notably, increasing the compositional heterogeneity of fatty acid-based systems has been shown to be advantageous for generating stable vesicles under varied conditions of temperature, pH, and ionic strength [13,31,50]. Our study shows that this principle is applicable to NAA-based systems as well. When NOG is admixed with other amphiphiles like GMO or OA, the resultant heterogeneous amphiphile system can generate vesicles over a broad pH range, including acidic to highly alkaline pH regimes. We also showed that the addition of GMO increases the stability of NOG vesicles in the presence of both divalent and monovalent cations that play a crucial role in several prebiotic reactions [36–38,41]. Together, these results highlight the potential of NAA-based heterogeneous systems in generating robust protocell compartments, which could have supported a wide range of prebiotic reactions occurring at specific conditions of pH and metal ion concentrations.

Finally, we showed that, in addition to generating robust vesicles, NOG could also react with different amino acids under wet-dry cycling conditions to generate different N-acylated peptide amphiphiles/lipopeptides. It demonstrates the significance of NAAs in synthesizing newer peptide-based amphiphilic species with diverse head group types. Moreover, our study provides experimental evidence for the potential prebiotic availability of lipopeptides by demonstrating their synthesis under prebiotically-relevant conditions. Such membrane-anchored lipopeptides might have endowed early protocell membranes with new functions like catalytic activity [51]. Future research in this direction will contribute toward understanding how lipopeptides might have modulated the physicochemical properties and functionality of protocell membranes. Overall, our study establishes NAAs as a new promising model protoamphiphile system and underscores their pivotal role in shaping the emergence and evolution of protocell membranes on primitive Earth.

References

1. Sarkar, S.; Das, S.; Dagar, S.; Joshi, M.P.; Mungi, C. V.; Sawant, A.A.; Patki, G.M.; Rajamani, S. Prebiological Membranes and Their Role in the Emergence of Early Cellular Life. *J. Membr. Biol.* **2020**, *253*, 589–608.
2. Monnard, P.-A.; Walde, P.; Monnard, P.-A.; Walde, P. Current Ideas about Prebiological Compartmentalization. *Life* **2015**, *5*, 1239–1263.
3. Joshi, M.P.; Sawant, A.A.; Rajamani, S. Spontaneous emergence of membrane-forming protoamphiphiles from a lipid–amino acid mixture under wet–dry cycles. *Chem. Sci.* **2021**, *8*, 2970–2978.
4. Hargreaves, W.R.; Deamer, D.W. Liposomes from ionic, single-chain amphiphiles. *Biochemistry* **1978**, *17*, 3759–3768.
5. Lawless, J.G.; Yuen, G.U. Quantification of monocarboxylic acids in the Murchison carbonaceous meteorite. *Nature* **1979**, *282*, 396–398.
6. McCollom, T.M.; Ritter, G.; Simoneit, B.R. Lipid synthesis under hydrothermal conditions by Fischer-Tropsch-type reactions. *Orig. Life Evol. Biosph.* **1999**, *29*, 153–66.
7. Gibard, C.; Bhowmik, S.; Karki, M.; Kim, E.K.; Krishnamurthy, R. Phosphorylation, oligomerization and self-assembly in water under potential prebiotic conditions. *Nat. Chem.* **2018**, *10*, 212–217.
8. Fiore, M. The synthesis of mono-alkyl phosphates and their derivatives: an overview of their nature, preparation and use, including synthesis under plausible prebiotic conditions. *Org. Biomol. Chem.* **2018**, *16*, 3068–3086.
9. Apel, C.L.; Deamer, D.W. The Formation Of Glycerol Monodecanoate By A Dehydration Condensation Reaction: Increasing The Chemical Complexity Of Amphiphiles On The Early Earth. *Orig. Life Evol. Biosph.* **2005**, *35*, 323–332.
10. Rubio-Sánchez, R.; O’Flaherty, D.K.; Wang, A.; Coscia, F.; Petris, G.; Di Michele, L.; Cicuta, P.; Bonfio, C. Thermally Driven Membrane Phase Transitions Enable Content Reshuffling in Primitive Cells. *J. Am. Chem. Soc.* **2021**, *143*, 16589–16598.

11. Toparlak, Ö.D.; Wang, A.; Mansy, S.S. Population-Level Membrane Diversity Triggers Growth and Division of protocells. *JACS Au* **2021**, *1*, 560–568.
12. Jordan, S.F.; Nee, E.; Lane, N. Isoprenoids enhance the stability of fatty acid membranes at the emergence of life potentially leading to an early lipid divide. *Interface Focus* **2019**, *9*, 20190067.
13. Mansy, S.S.; Szostak, J.W. Thermostability of model protocell membranes. *Proc. Natl. Acad. Sci. U. S. A.* **2008**, *105*, 13351–5.
14. Chen, I.A.; Salehi-Ashtiani, K.; Szostak, J.W. RNA Catalysis in Model Protocell Vesicles. *J. Am. Chem. Soc.* **2005**, *127*, 13213–13219.
15. Chen, I.A.; Roberts, R.W.; Szostak, J.W. The emergence of competition between model protocells. *Science* **2004**, *305*, 1474–1477.
16. Battista, N.; Bari, M.; Bisogno, T. N-Acyl Amino Acids: Metabolism, Molecular Targets, and Role in Biological Processes. *Biomol.* *2019*, *Vol. 9*, Page 822 **2019**, *9*, 822.
17. Brady, S.F.; Clardy, J. Long-chain N-acyl amino acid antibiotics isolated from heterologously expressed environmental DNA [20]. *J. Am. Chem. Soc.* **2000**, *122*, 12903–12904.
18. M. Ziora, Z.; A. Blaskovich, M.; Toth, I.; A. Cooper, M. Lipoamino Acids as Major Components of Absorption Promoters in Drug Delivery. *Curr. Top. Med. Chem.* **2012**, *12*, 1562–1580.
19. Bonfio, C.; Russell, D.A.; Green, N.J.; Mariani, A.; Sutherland, J.D. Activation chemistry drives the emergence of functionalised protocells. *Chem. Sci.* **2020**, *11*, 10688–10697.
20. Izgu, E.C.; Björkbom, A.; Kamat, N.P.; Lelyveld, V.S.; Zhang, W.; Jia, T.Z.; Szostak, J.W. N-Carboxyanhydride-Mediated Fatty Acylation of Amino Acids and Peptides for Functionalization of Protocell Membranes. *J. Am. Chem. Soc.* **2016**, *138*, 16669–16676.
21. Rodriguez-Garcia, M.; Surman, A.J.; Cooper, G.J.T.; Suárez-Marina, I.; Hosni, Z.; Lee, M.P.; Cronin, L. Formation of oligopeptides in high yield under simple programmable conditions. *Nat. Commun.* **2015**, *6*, 8385.

22. Vance, J.E.; Vance, D.E. Phospholipid biosynthesis in mammalian cells. *Biochem. Cell Biol.* **2004**, *82*, 113–128.
23. Liu, L.; Zou, Y.; Bhattacharya, A.; Zhang, D.; Lang, S.Q.; Houk, K.N.; Devaraj, N.K. Enzyme-free synthesis of natural phospholipids in water. *Nat. Chem.* **2020**, *12*, 1029–1034.
24. Bonfio, C.; Caumes, C.; Duffy, C.D.; Patel, B.H.; Percivalle, C.; Tsanakopoulou, M.; Sutherland, J.D. Length-Selective Synthesis of Acylglycerol-Phosphates through Energy-Dissipative Cycling. *J. Am. Chem. Soc.* **2019**, *141*, 3934–3939.
25. Rao, M.; Eichberg, J.; Oró, J. Synthesis of phosphatidylethanolamine under possible primitive earth conditions. *J. Mol. Evol.* **1987**, *25*, 1–6.
26. HARGREAVES, W.R.; MULVIHILL, S.J.; DEAMER, D.W. Synthesis of phospholipids and membranes in prebiotic conditions. *Nature* **1977**, *266*, 78–80.
27. Monnard, P.-A.; Deamer, D.W. Preparation of Vesicles from Nonphospholipid Amphiphiles. *Methods Enzymol.* **2003**, *372*, 133–151.
28. Fameau, A.L.; Arnould, A.; Saint-Jalmes, A. Responsive self-assemblies based on fatty acids. *Curr. Opin. Colloid Interface Sci.* **2014**, *19*, 471–479.
29. Cistola, D.P.; Atkinson, D.; Hamilton, J.A.; Small, D.M. Phase Behavior and Bilayer Properties of Fatty Acids: Hydrated 1:1 Acid-Soaps. *Biochemistry* **1986**, *25*, 2804–2812.
30. Henderson-Sellers, A.; Meadows, A.J. Surface temperature of early Earth. *Nature* **1977**, *270*, 589–591.
31. Sarkar, S.; Dagar, S.; Verma, A.; Rajamani, S. Compositional heterogeneity confers selective advantage to model protocellular membranes during the origins of cellular life. *Sci. Rep.* **2020**, *10*, 1–11.
32. Rendón, A.; Carton, D.G.; Sot, J.; García-Pacios, M.; Montes, L.-R.; Valle, M.; Arrondo, J.-L.R.; Goñi, F.M.; Ruiz-Mirazo, K. Model Systems of Precursor Cellular Membranes: Long-Chain Alcohols Stabilize Spontaneously Formed Oleic Acid Vesicles. *Biophys. J.* **2012**, *102*, 278–286.

33. Maurer, S. The Impact of Salts on Single Chain Amphiphile Membranes and Implications for the Location of the Origin of Life. *Life* **2017**, *7*, 44.
34. Walde, P.; Namani, T.; Morigaki, K.; Hauser, H.; Namani, T.; Morigaki, K.; Hauser, H. Formation and Properties of Fatty Acid Vesicles (Liposomes). In *Liposome Technology*; CRC Press, **2018**; pp. 23–42.
35. Bonfio, C.; Godino, E.; Corsini, M.; Fabrizi de Biani, F.; Guella, G.; Mansy, S.S. Prebiotic iron–sulfur peptide catalysts generate a pH gradient across model membranes of late protocells. *Nat. Catal.* **2018**, *1*, 616–623.
36. Muchowska, K.B.; Varma, S.J.; Chevallot-Beroux, E.; Lethuillier-Karl, L.; Li, G.; Moran, J. Metals promote sequences of the reverse Krebs cycle. *Nat. Ecol. Evol.* **2017**, *1*, 1716–1721.
37. Bowman, J.C.; Lenz, T.K.; Hud, N. V.; Williams, L.D. Cations in charge: magnesium ions in RNA folding and catalysis. *Curr. Opin. Struct. Biol.* **2012**, *22*, 262–272.
38. Inoue, A.; Takagi, Y.; Taira, K. Importance of magnesium ions in the mechanism of catalysis by a hammerhead ribozyme: strictly linear relationship between the ribozyme activity and the concentration of magnesium ions. *Magnes. Res.* **2003**, *16*, 210–217.
39. Attwater, J.; Wochner, A.; Holliger, P. In-ice evolution of RNA polymerase ribozyme activity. *Nat. Chem.* **2013**, *5*, 1011.
40. Horning, D.P.; Joyce, G.F. Amplification of RNA by an RNA polymerase ribozyme. *Proc. Natl. Acad. Sci. U. S. A.* **2016**, *113*, 9786–9791.
41. Bapat, N. V.; Rajamani, S. Templated replication (or lack thereof) under prebiotically pertinent conditions. *Sci. Rep.* **2018**, *8*, 15032.
42. Bowler, F.R.; Chan, C.K.W.; Duffy, C.D.; Gerland, B.; Islam, S.; Powner, M.W.; Sutherland, J.D.; Xu, J. Prebiotically plausible oligoribonucleotide ligation facilitated by chemoselective acetylation. *Nat. Chem.* **2013**, *5*, 383–389.
43. Monnard, P.-A.; Apel, C.L.; Kanavarioti, A.; Deamer, D.W. Influence of Ionic Inorganic Solutes on Self-Assembly and Polymerization Processes Related to Early Forms of Life:

- Implications for a Prebiotic Aqueous Medium. *Astrobiology* **2002**, *2*, 139–152.
44. Bradshaw, H.B.; Rimmerman, N.; Hu, S.S. -J.; Burstein, S.; Walker, J.M. Chapter 8 Novel Endogenous N-Acyl Glycines: Identification and Characterization. *Vitam. Horm.* **2009**, *81*, 191–205.
 45. Clapés, P.; Infante, M.R. Amino acid-based surfactants: Enzymatic synthesis, properties and potential applications. *Biocatal. Biotransformation* **2002**, *20*, 215–233.
 46. Deamer, D.; David The Role of Lipid Membranes in Life's Origin. *Life* **2017**, *7*, 5.
 47. Mansy, S.S. Model protocells from single-chain lipids. *Int. J. Mol. Sci.* **2009**, *10*, 835–43.
 48. Mansy, S.S. Membrane transport in primitive cells. *Cold Spring Harb. Perspect. Biol.* **2010**, *2*, 1–15.
 49. Forsythe, J.G.; Yu, S.-S.; Mamajanov, I.; Grover, M.A.; Krishnamurthy, R.; Fernández, F.M.; Hud, N. V. Ester-Mediated Amide Bond Formation Driven by Wet-Dry Cycles: A Possible Path to Polypeptides on the Prebiotic Earth. *Angew. Chemie* **2015**, *127*, 10009–10013.
 50. Jordan, S.F.; Rammu, H.; Zheludev, I.N.; Hartley, A.M.; Maréchal, A.; Lane, N. Promotion of protocell self-assembly from mixed amphiphiles at the origin of life. *Nat. Ecol. Evol.* **2019**, *3*, 1705–1714.
 51. Reja, A.; Afrose, S.P.; Das, D. Aldolase Cascade Facilitated by Self-Assembled Nanotubes from Short Peptide Amphiphiles. *Angew. Chemie Int. Ed.* **2020**, *59*, 4329–4334.

Chapter 4

TESTING THE PREBIOTIC MEMBRANE ASSEMBLY PROCESS IN NATURAL, EARLY EARTH ANALOGUE HOT SPRING CONDITIONS

Adapted from: *Life* (2017) 7, 51 and *Life* (2021) 11, 1413

4.1 Introduction:

In this chapter, I will discuss a new and slightly unorthodox approach that we have adopted to better understand the origin of life conundrum. Several decades of research in the origin of life field have significantly advanced our understanding of how this transition from chemistry to biology might have occurred on early Earth. However, most results pertaining to this research are an outcome of experiments performed in the laboratory using highly pure reagents and solvents. Moreover, the reaction conditions are also stringently controlled to facilitate the reaction of interest while avoiding other cross-reactions. These studies are based on the implicit assumption that the reaction outcome will also be similar under natural conditions where life would have originated, which are incredibly complex geologically and diverse in their chemical composition. The question is, can this assumption be validated?

There are two possible ways to validate this assumption. One of them is to perform these experiments directly in the field, which is a challenging task for several practical reasons. As discussed by Prof. David Deamer in his insightful paper on testing ideas in prebiotic analogue conditions, there are several challenges associated with performing experiments in actual hot spring sites [1]. (i) Volume of the hot spring will play critical role while setting up the experiment and there is a risk of reactants and products getting diluted in the pool. Especially, larger hot springs will need hundreds of grams of starting reactants to perform these experiments even at millimolar scale and to get detectable yields of product. Therefore, performing such experiments will not be affordable. (ii) Many hot spring sites are in national parks and getting a permission to work there could be fairly complicated. Also many reaction products are unstable in nature and need to be analysed quickly, which might not be always possible given the limitations on accessing high-end instruments in the field. (iii) Also, there is a significant health risk associated with working at geothermal fields near active volcano sites because of the high temperature and presence of potentially toxic gases.

An alternative and pragmatic approach would be to bring samples from natural, early Earth analogue sites to the laboratory and perform experiments using these analogue samples. Such “analogue experiments” would give a more “realistic” sense of how prebiotically-pertinent

processes might behave under natural conditions compared to controlled laboratory conditions. Towards this, we tested the prebiotic membrane assembly process in actual water samples collected from active hot springs present in distinct locations of the world that have geological features presumably analogous to the early Earth. These experiments were performed with the following objectives:

- a) To get a realistic sense of how the membrane assembly process from prebiotically-relevant amphiphiles behaves under natural conditions –

The formation of membrane compartments would have been a crucial step during the emergence of protocells [2,3]. SCAs are considered plausible protoamphiphiles that would have constituted membrane compartments of early protocells. However, these SCAs are known to self-assemble into vesicles under a narrow set of reaction conditions, and these vesicles are generally susceptible to change in the surrounding environmental conditions [4,5]. Therefore, laboratory studies involving the prebiotic membrane assembly process are performed by carefully maintaining the pH, temperature, and ionic strength requirements for this process. However, natural conditions are likely to be more variable with respect to the above mentioned parameters. Therefore, we checked whether such prebiotically-plausible amphiphiles could generate vesicles under intrinsically variable natural conditions. It is also one of the crucial validations towards evaluating the potential of these SCAs as model protoamphiphiles.

- b) To check for the simultaneous effect of multiple ions on the vesicle formation process –

As discussed in chapter 3, ions are known to significantly affect the formation and stability of SCAs vesicles. Most studies in this regard check the effect of individual ions on SCA vesicles [6–11]. However, natural aqueous systems often possess multiple cations and anions in varying concentrations. Therefore, it is essential to evaluate the combined effect of multiple ions on the prebiotic membrane assembly process. However, mimicking such a natural system with a diverse ionic strength in the laboratory is difficult, as these ions are added in the form of salts, which invariably results in the excess addition of some counter ions while preparing such ionic mimics. In this context, hot spring water samples, possessing inherent diversity in their ionic compositions, could provide an excellent aqueous system to understand the simultaneous effect of multiple ions on the formation and stability of protoamphiphilic vesicles.

- c) To evaluate the conduciveness of terrestrial hot springs for the prebiotic membrane assembly process –

The influence of the overall ionic strength of an aqueous medium on prebiotic membrane assembly and stability also has implications for discerning the plausible niche(s) where life might have originated on the early Earth [12]. Deep-sea hydrothermal vents and terrestrial hot springs are the two widely considered niches for the origin of life on Earth [13,14]. However, the high salinity of seawater would have been detrimental to the prebiotic compartmentalization process [6]. In contrast, terrestrial freshwater bodies, such as hot springs and lakes, with their overall low ionic strengths, would have provided a more conducive environment for the membrane assembly of protoamphiphiles [2,15]. Several decades of laboratory experiments with fatty acid vesicles using low ionic strength buffers provide a proof of concept to this notion. Therefore, studying the prebiotic membrane assembly in actual hot spring water samples could provide a direct validation of the potential of these niches to support this process, as it would have been crucial for the emergence of life on Earth.

We studied the vesicle formation behavior of both fatty acid-based and NAA-based amphiphile systems in water samples that were collected from early Earth analogue hot spring sites. Samples were collected from the hot spring origin sites, specifically from regions that lacked any visible microbial mats and vegetation, to avoid interference from biological activity to the extent feasible. Furthermore, all samples were also filtered at the collection site through a 200 nm Whatman syringe filter to avoid microbial contamination. In all, for the fatty acid-based systems, different combinations of fatty acids and their derivatives readily formed vesicles in laboratory buffered conditions. However, in hot spring water samples, only a binary system of fatty acid and monoglyceride was able to generate vesicles. These results were consistent across different fatty acid systems of varying chain length and saturation and also with different hot spring samples. Subsequently, we performed similar experiments with the NAA-based system, where both pure NOG and NOG + GMO mixed systems could self-assemble into vesicles in the hot spring samples tested.

4.2 Materials and methods:

4.2.1 Materials:

All fatty acids and their derivatives were purchased from Nu-Chek-Prep (USA), except for 1-Decanoyl-rac-glycerol, which was purchased from Sigma-Aldrich (India). N-oleoyl glycine (NOG) and N-oleoyl serine (NOS) were purchased from Avanti polar lipids (USA). The rest of the reagents and chemicals were bought from Sigma-Aldrich (India). All the reagents and chemicals used in this study were of the highest commercially available grade and used without further purification.

4.2.2 Methods:

4.2.2.1 Vesicle formation by fatty acid-based amphiphile systems in hot spring water samples

- **Collection of Water Samples from Hot Springs**

The water samples were collected from Puga (PU), Chumathang (CH), and Panamic (PA) hot springs at Ladakh, which is an astrobiologically-relevant and early Earth analogue site in India. This collection was done as a part of an expedition under the aegis of the NASA Spaceward Bound program [16]. The samples were collected from both origin and run-off sites. However, only the samples collected from the origin sites were used for this study, as these sites lacked any obvious microbial mats and vegetation, thus reducing concerns of biological contamination. Also, there was less human interference at these sites than at run-off sites. Furthermore, all samples were filtered at the collection site through a 200 nm Whatman syringe filter to avoid microbial contamination, if any, and their temperature and pH were recorded on site. The pH was re-analyzed in the laboratory for all the water samples before being used for the experiment. All the hot spring samples had a pH in the neutral to alkaline range.

- **Geochemical Analysis of Hot Spring Water Samples**

The water samples that were collected from the three different hot springs were analyzed to detect and quantify major ions present in these samples. These measurements were carried out following standard protocols [17]. Briefly, the alkalinity of the samples was measured using an auto-titrator Titrino plus 877 (Metrohm, Switzerland). The concentrations of the major cations (Na^+ , K^+ , Ca^{2+} , Mg^{2+} , and Li^+) and anions (Cl^- ,

SO₄²⁻) were measured using the ion chromatography instrument Compact IC plus 882 (Metrohm, Switzerland). The accuracy and precision of these analyses were regularly monitored and were found to have average values of ±4%. The net inorganic charge balance (NICB) for these samples was within ±10%, thus ensuring good data quality.

- **Formation of fatty acid vesicles in hot spring water samples**

In a typical reaction, the fatty acid alone, or in combination with the pertinent derivative, was first melted by heating above their melting temperature. Appropriate concentrations were then dissolved in chloroform, and the chloroform was evaporated under a vacuum to form a fatty acid film. The desired solvent volume was then added to this film and mixed by vortexing and pipetting. The solvent was either 200 mM bicine buffer pH 8.5 or the hot spring water of comparable pH. Importantly, the solvent was preheated above the melting temperature of the system before adding to the lipid film. Different higher-order structures formed in the resultant solution were visualized under DIC microscopy (AxioImager Z1, Carl Zeiss, Germany), using 40X objective (NA = 0.75).

4.2.2.2 Vesicle formation by NAA-based amphiphile systems in hot spring water samples

- **Collection of water samples from hot springs**

The collection of hot spring water samples for this part of the study was done in collaboration with Luke Steller and Prof. Martin J. Van Kranendonk (UNSW, Australia). Water samples (denoted by TIKB and TIKC) were collected directly from two hot spring pools at Hells Gate Geothermal Reserve, Tikitere, New Zealand. These samples were filtered with a 0.22 µm polyethersulfone membrane filter (rinsed with 20 ml of the sample) and stored in acid-washed high-density polyethylene bottles until further use. These water samples had a pH of around 7-7.5.

- **Geochemical analysis of hot spring water samples**

The collected water samples were analysed to identify and quantify different ions present in them. These measurements were performed following standard protocols as reported earlier [17]. Briefly, the concentrations of the major cations (Na⁺, K⁺, Ca²⁺, Mg²⁺, and NH₄⁺) and anions (Cl⁻, F⁻, SO₄²⁻, and NO₃⁻) were measured using the ion chromatography instrument Compact IC plus 882 (Metrohm, Herisau, Switzerland). Moreover, the alkalinity of the samples was measured using an auto-titrator Eco Titrator (Metrohm, Switzerland). The dissolved Silica concentrations were measured by a

conventional molybdenum-blue method using a double beam UV-VIS Spectrophotometer (M.D.T. INTERNATIONAL, India). The accuracy and precision of these analyses were monitored regularly, with an average value of $\pm 4\%$. The net inorganic charge balance (NICB) for these samples was around 1, indicating good data quality.

- **Formation of NAA-based vesicles in hot spring water samples**

Dry lipid films of pure NOG and mixed systems containing NOG + GMO in a 2:1 ratio were prepared as described in the previous chapter. These lipid films were hydrated with 50 μL of hot spring water sample (TIKB/TIKC) to get a total amphiphile concentration of 6 mM. The solution was further incubated at 60 °C for 1 hour with constant shaking at 500 rpm, with intermittent mixing by vortexing and pipetting to facilitate the vesicle formation process. The initial pH of the hot spring water samples was 7–7.5, which decreased to 5–5.5 after the amphiphile addition, likely because of the acidic nature of NOG. The formation of vesicles was checked by DIC and epifluorescence microscopy by following a similar procedure to that mentioned in section 3.2.3 of chapter 3.

4.3 Results

4.3.1 Vesicle formation behavior of fatty acid-based amphiphile systems in hot spring water

We started these “analogue” experiments by looking at the self-assembly of fatty acid-based systems (Figure 4.1) in hot spring water samples collected from three hot springs in Ladakh (India), namely PU, CH, and PA. All these water samples had a pH of around 8.3 to 8.65, which is known to be suitable for vesicle formation by oleic acid (OA; C18:1). The experiment was performed using four different combinations of OA and its alcohol (OOH) and glycerol derivatives (GMO) as follows: 1) only OA (6 mM); 2) OA + OOH (6 mM; 2:1 ratio); 3) OA + GMO (6 mM; 2:1 ratio); 4) OA + OOH + GMO (6 mM; 4:1:1 ratio). These oleic acid-based amphiphile systems have been widely used for studying the effect of different parameters on the formation and stability of plausible prebiotic membranes [8,18,19]. We used 200 mM bicine buffer pH 8.5 as a laboratory positive control, which is known to favor vesicle formation by all the above combinations of OA and its derivatives. Note that the pH of this laboratory control is comparable to that of the hot spring samples used in the study.

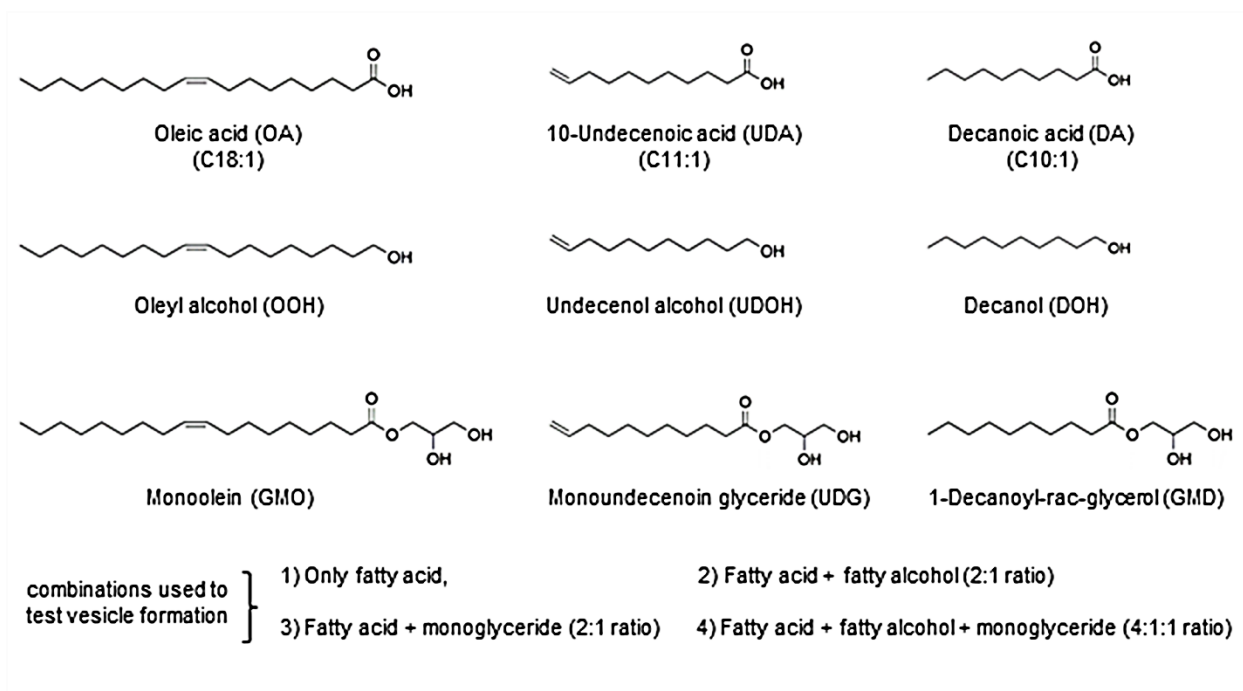


Figure 4.1 Different fatty acids and their derivatives used in fatty acid-based experiments. Different combinations of a particular fatty acid and its derivatives that were tested for their vesicle-forming ability in hot spring water samples are also indicated.

As expected, all the four combinations of OA and its derivatives readily formed vesicles in bicine buffer pH 8.5 (Figure 4.2a). However, when shifted to natural water samples, out of the four combinations, only a binary system of OA + GMO generated vesicles in PU hot spring water (Figure 4.2b). The rest of the combinations mainly resulted in shiny oil droplets. The results were consistent in CH and PA water samples (Figure 4.3). However, the number of vesicles formed by the OA + GMO system was seemingly more in PU followed by CH and PA, possibly owing to the differences in their ionic compositions and the individual concentrations of these ions. Most of the resultant vesicles were large multilamellar or multivesicular vesicles. In the case of PA, a white precipitate was observed on the walls of the reaction container, which dissolved and resulted in vesicles only after prolonged heating (75 °C for three hours). Additionally, the OA + GMO system always resulted in a mixture of vesicles and oil droplets in all three hot spring samples. Under DIC microscopy, vesicles appear as donut-shaped structures having less contrast when compared with the surrounding medium. Contrarily, oil droplets typically appear as shiny convex circles. Also, vesicles preferentially stay in the aqueous solution

and are detected as moving objects under a microscope, whereas oil droplets appear as non-moving objects adhered to the glass surface of the slide.

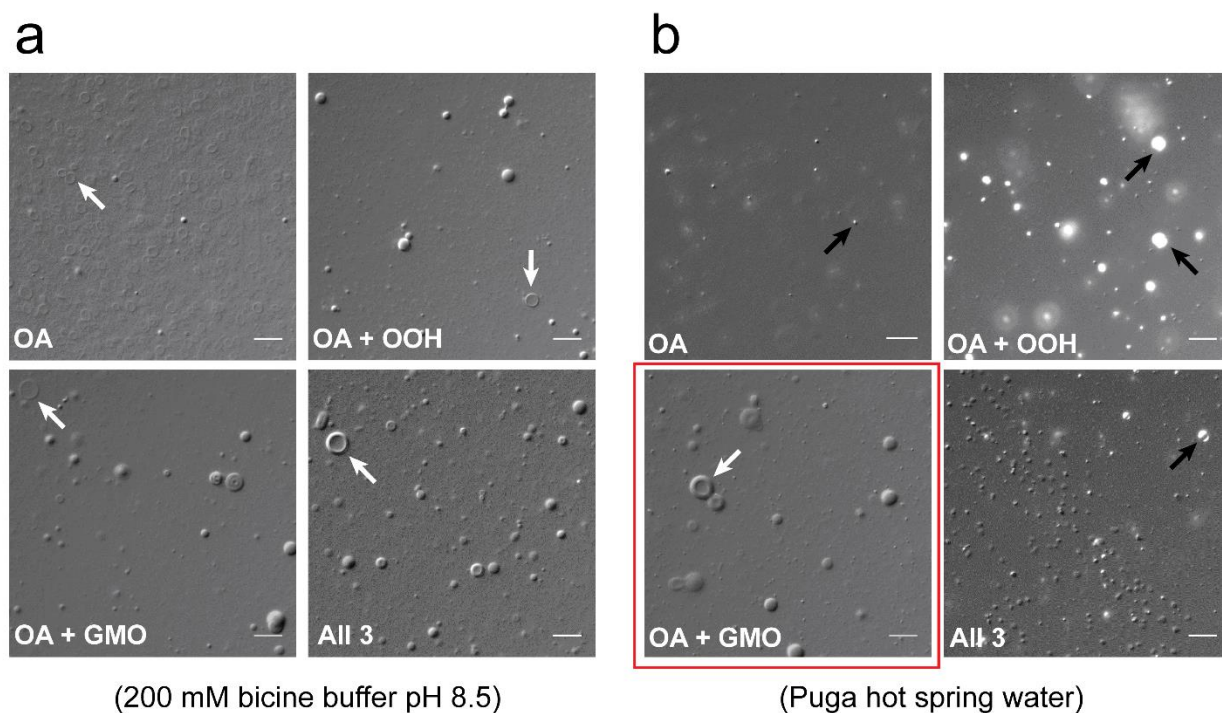


Figure 4.2 Vesicle formation behavior of oleic acid-based amphiphile systems in the laboratory “buffered” versus “natural” hot spring water sample as monitored under DIC microscopy. (a) All four combinations of OA and its derivatives form vesicles in 200 mM bicine buffer pH 8.5 (laboratory positive control). **(b)** However, only a binary system of OA + GMO (panel highlighted with a red square box) generates vesicles in Puga hot spring water sample (pH 8.48). The rest of the combinations mainly result in shiny oil droplets. Vesicles and oil droplets are denoted by white and black arrows, respectively. The scale bar is 20 μm .

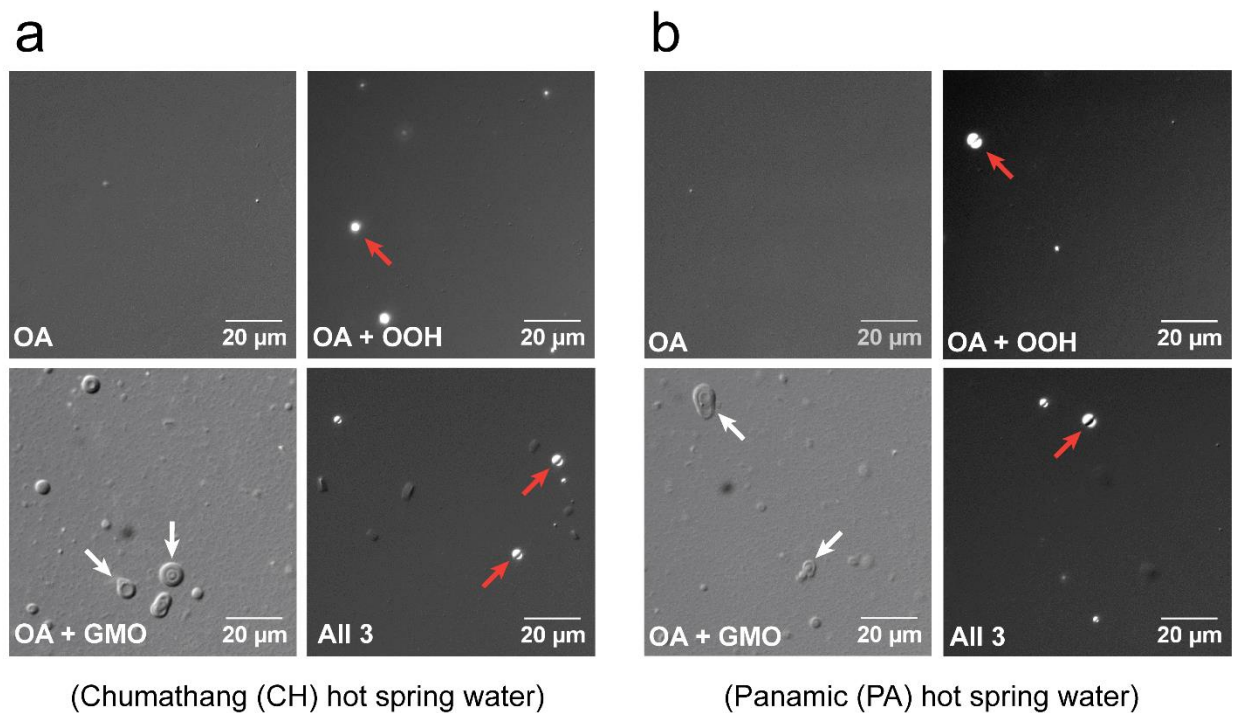


Figure 4.3 Vesicle formation behavior of oleic acid-based amphiphile systems in (a) CH and (b) PA hot spring water samples as observed under DIC microscopy. Consistent with the PU hot spring results, only a binary system of OA + GMO generates vesicles in CH and PA water samples. The rest of the combinations either do not form any higher-order structures or generate oil droplets. Vesicles and oil droplets are denoted by white and orange arrows, respectively.

4.3.2 Effect of chain length and unsaturation on the vesicle-forming ability of fatty acid and its derivatives in the hot spring water samples

Small-chain fatty acids (C8–C12) are thought to have been present more abundantly on early Earth as compared to long-chain ones because they have been detected in higher yields in prebiotically-plausible lipid synthesis reactions [17] and meteorites samples [18,19]. Therefore, we also investigated the vesicle formation behavior of small-chain fatty acid-based systems in hot spring water samples. Firstly, we used a fatty acid system based on 10-Undecenoic acid (UDA; C11:1) to study the effect of reducing the chain length on vesicle formation ability while keeping the unsaturation constant as that in oleic acid (C18:1). A total amphiphile concentration of 90 mM was used in these experiments to account for the higher critical vesicle concentration (CVC) of UDA. CVC is the concentration above which a particular amphiphile forms vesicles. The overall results for the UDA system were comparable to that of the oleic acid system, where

only a mixture of UDA and its glycerol derivative (UDG) (90 mM; 2:1 ratio) resulted in vesicle formation in all the hot spring samples (Figure 4.4). Although, in the case of the PA sample, only oil droplets were present initially, which eventually transformed into vesicles upon prolonged heating. Rest of the combinations; UDA alone (90 mM), or UDA + undecanoyl alcohol (UDOH) (90 mM; 2:1 ratio), or UDA + UDOH + UDG (90 mM; 4:1:1 ratio), did not form vesicles in hot spring waters. Even in this fatty acid system, all of the four combinations of UDA and its derivatives readily formed vesicles in 200 mM bicine buffer pH 8, which served as the positive control.

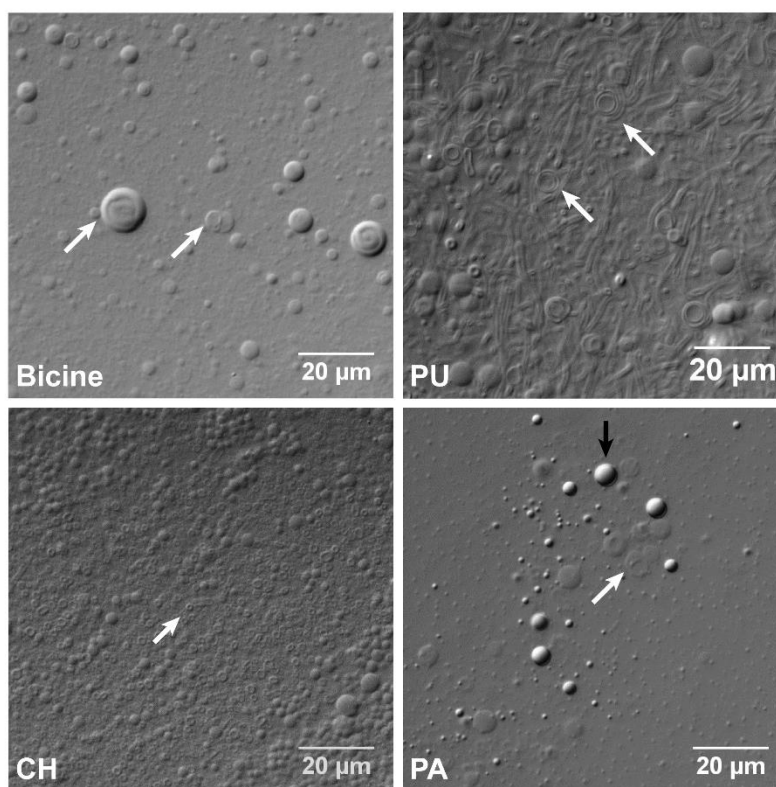


Figure 4.4 UDA + UDG binary system generates vesicles in all hot spring water samples. A binary system of 10-Undecenoic acid (UDA; C11:1) and its glycerol derivative (UDG) (90 mM; 2:1 ratio) is able to generate vesicles (denoted by white arrows) in all hot spring water samples (PU, CH, and PA), along with the 200 mM bicine buffer pH 8 control. PA sample, which initially had only oil droplets, showed the formation of vesicles after 3 hours of heating at 75 °C. The above image from PA shows a mixture of droplets (black arrows) and vesicles (white arrows) that were observed after heating.

Subsequently, we focused on the decanoic acid (DA; C10:0) system, which allowed us to evaluate how the vesicle formation behavior in hot spring water gets affected when shifted from an unsaturated system (UDA) to a saturated one (DA). DA is one of the most extensively studied small-chain amphiphilic systems that is widely considered a plausible precursor of prebiotic membranes [23]. In the case of the DA system also, we observed comparable results to those mentioned for the above two systems (OA and UDA), where a binary combination of DA and its glycerol derivative (GMD) (60 mM; 2:1 ratio) readily formed vesicles in all hot spring samples (Figure 4.5). DA alone (60 mM), or its combination with decanol (DOH) (60 mM; 2:1 ratio), did not form vesicles in any hot spring water.

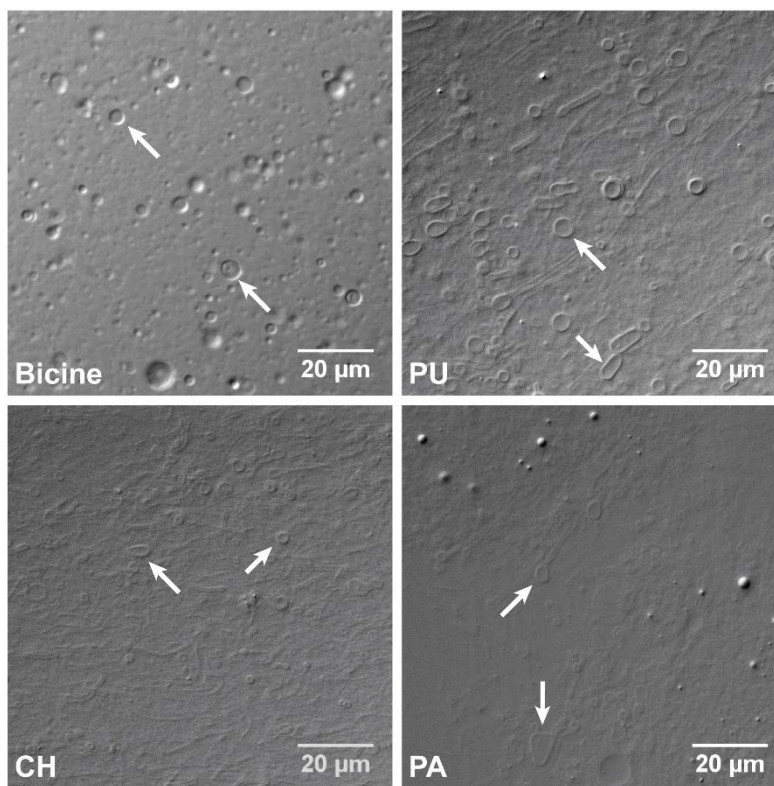


Figure 4.5 DA + GMD binary system generates vesicles in all hot spring water samples. A binary system of decanoic acid (DA; C10:0) and its glycerol derivative (GMD) (60 mM; 2:1 ratio) is able to generate vesicles (denoted by white arrows) in all hot spring water samples (PU, CH, and PA), along with the 200 mM bicine buffer pH 8 control.

Interestingly, a tertiary system comprising DA + DOH + GMD (60 mM; 4:1:1 ratio) also resulted in vesicle formation in PU water (Figure 4.6). However, this tertiary system generated some peculiar structures in CH and PA water, where vesicles were typically seen surrounding a central lipid aggregate (Figure 4.6). This aggregate possibly could be rich in DOH that might get excluded from the vesicle-forming components in the form of the oil droplet. As consistent with previous results, all the four combinations of DA and its derivatives readily self-assembled into vesicles in bicine buffer laboratory control. The vesicle formation behavior of all fatty acid systems that were studied has been summarized in table 4.1.

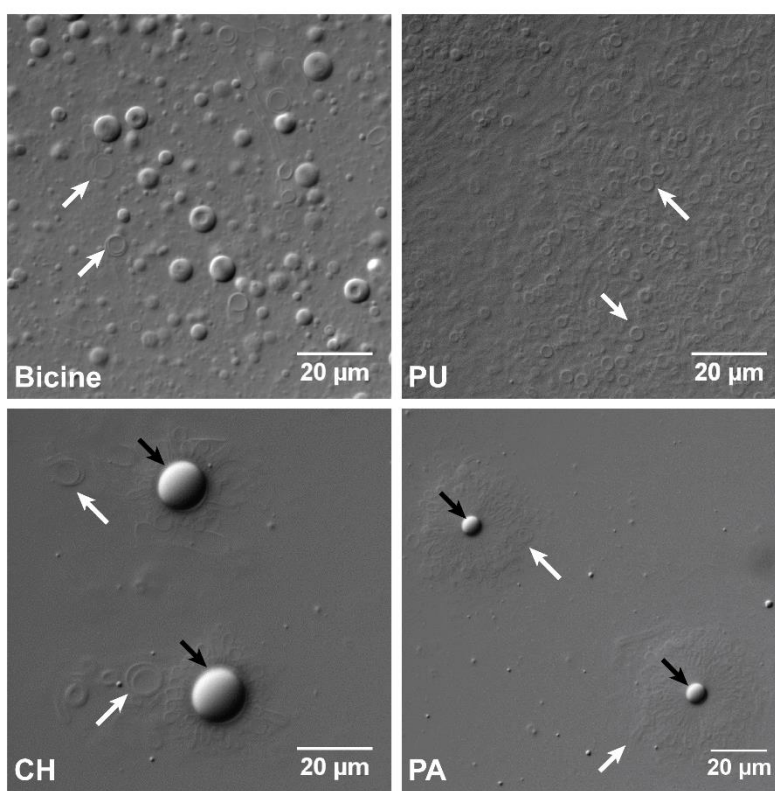


Figure 4.6 Vesicle formation behavior of DA + DOH + GMD tertiary system in the laboratory buffered versus hot spring water samples. A tertiary system of decanoic acid (DA), decanol (DOH), and the glycerol derivative of decanoic acid (GMD) (60 mM; 4:1:1 ratio) formed vesicles (denoted by white arrows) in 200 mM bicine buffer pH 8 and also in Puga (PU), as indicated in the top two panels. Interesting structures were observed in the Chumathang (CH) and Panamic (PA) systems (bottom two panels), in which vesicles were present surrounding a central lipid aggregate, as indicated by white and black arrows, respectively.

Table 4.1 A summary of the vesicle formation behavior of different fatty acid-based systems in bicine buffer (laboratory positive control) and different hot spring water samples.

(Green color indicates the presence of vesicles, while the orange color indicates their absence)

Vesicle formation checked in	Fatty acid system	Combination of fatty acid and its derivatives			
		Only fatty acid	Fatty acid + Fatty alcohol (2:1 ratio)	Fatty acid + monoglyceride (2:1 ratio)	Fatty acid + Fatty alcohol + monoglyceride (4:1:1 ratio)
200 mM bicine buffer*	OA (C18:1)				
	UDA (C11:1)				
	DA (C10:0)				
Puga (PU)	OA (C18:1)				
	UDA (C11:1)				
	DA (C10:0)				
Chumathang (CH)	OA (C18:1)				
	UDA (C11:1)				
	DA (C10:0)				
Panamic (PA)	OA (C18:1)				
	UDA (C11:1)				
	DA (C10:0)				

*Bicine buffer pH was 8.5 for the OA system and 8 for UDA and DA systems

4.3.3 Geochemical analysis of the PU, CH, and PA hot spring water samples

We hypothesized that a peculiar self-assembly behavior of fatty acid systems across different hot spring waters might be an outcome of the variable ionic strengths of these water samples. Therefore, we performed a systematic geochemical analysis of these hot spring samples, where we detected multiple ions in varying concentrations (table 4.2). However, the overall ionic strength of PU was higher than that of CH, followed by PA, which shows a positive correlation with the overall vesicle-forming propensity trend in these samples (PU > CH > PA). The chemistry of the hot spring samples analysed in this study is dominated by monovalent cations (Na⁺ and K⁺) and anions (HCO₃⁻ and Cl⁻). However, concentrations of major divalent (Mg²⁺, Ca²⁺) and monovalent (Na⁺, K⁺) cations were lower (even in PU) than what has been reported to disrupt vesicle formation [6]. In this previous study, these ions had been individually tested for their vesicle disruption ability. However, not much is known about their combined

effect on vesicle stability. These multiple ions in varying concentrations could exert a combinatorial effect on the vesicle formation by fatty acid-based systems in hot spring water samples, allowing only certain combinations to form vesicles. Interestingly, this effect was seen across all tested fatty acid systems. Additionally, the possibility of the presence of organic compounds in these hot spring waters cannot be excluded, which could have also affected the vesicle formation process.

Table 4.2 Geochemical analysis of hot spring water samples used in fatty acid-based experiments.

The overall ionic strength decreases from Puga to Panamic. TZ^+ and TZ^- indicate the sum of cations and anions, respectively, in microequivalent units. TZ^+ / TZ^- indicates net inorganic charge balance (NICB).

Hot spring water	pH	Major cations					Major anions			TZ^+	TZ^-	TZ^+/TZ^-
		Na ⁺	K ⁺	Ca ²⁺	Mg ²⁺	Li ⁺	HCO ₃ ⁻	Cl ⁻	SO ₄ ²⁻			
		All values in mM								μE		
Puga	8.48	26.14	2.08	0.89	0	1.26	14.57	11.83	1.27	31258	28936	1.08
Chumathang	8.64	15.54	0.55	0.22	0.005	0.44	10.2	2.99	2.53	16980	18248	0.93
Panamic	8.37	6.76	0.14	0.36	0.002	0.05	5.68	0.26	0.99	7665	7918	0.97

4.3.4 NAA-based amphiphile systems also readily form vesicles in hot spring water samples

The intriguing vesicle formation behavior of fatty acid-based systems in natural hot spring water samples motivated us to evaluate the behavior of our novel NAA-based protoamphiphilic system under such natural conditions. In this study, we used N-oleoyl glycine (NOG) as a representative NAA. Water samples used in these analogue experiments were

collected from two hot spring sites in Tikitere, New Zealand, abbreviated as TIKB and TIKC. These samples were chosen because of their slightly acidic to neutral pH, which is suitable for vesicle formation by NOG-based systems. Although, it should be noted that merely having a favorable pH for vesicle self-assembly does not assure vesicle formation in hot spring samples, as observed in the case of fatty acid-based systems. Therefore, it is essential to experimentally check the self-assembly behavior of these SCAs in natural water samples, to understand how these systems behave under natural conditions.

Towards this, we firstly analyzed the ionic content of TIKB and TIKC water samples (Table 4.3), given the influence of ionic strength on the self-assembly behavior of these amphiphiles. It was observed that the ionic makeup of both TIKB and TIKC was dominated by NH_4^+ and SO_4^{2-} ions. Although, several other cations (Na^+ , K^+ , Ca^{2+} , Mg^{2+}) and anions (Cl^- , F^- , NO_3^- , HCO_3^-) were also detected in varying concentrations, highlighting the ionic diversity that such natural aqueous systems possess. Notably, similar to Ladakh hot spring samples, the concentrations of both monovalent and divalent cations in these water samples were much below the level at which they generally induce vesicle aggregation.

Table 4.3 Geochemical analysis of the hot spring water samples used in NAA-based experiments.

Hot spring sample	Major cations					TZ ⁺	Major anions					TZ ⁻	TZ ⁺ /TZ ⁻	
	NH ₄ ⁺	Na ⁺	K ⁺	Ca ²⁺	Mg ²⁺		NO ₃ ⁻	F ⁻	Cl ⁻	HCO ₃ ⁻	SO ₄ ²⁻		SiO ₂	
	All values in μM					μE	All values in μM					μE	μM	
TIKB [†]	2756	743	285	98	31	4043	24	45	122	29	2550	5319	1128	0.76
TIKC [†]	3296	1007	301	167	27	4991	14	48	150	1458	2312	6294	1019	0.79

[†]The initial pH of TIKB and TIKC was 7-7.5, which decreased to 5-5.5 after the addition of amphiphiles (likely because of the acidic nature of NOG).

These hot spring samples were used to check the vesicle formation behavior of pure NOG (6 mM) and NOG + GMO (6 mM; 2:1 ratio) mixed systems. It was observed that both pure and mixed NOG systems readily assembled into vesicles in both TIKB and TIKC samples (Figure 4.7). The resultant vesicle population was heterogeneous in terms of the size, shape, and lamellarity of vesicles. Therefore, these vesicles were stained using R18 dye (an amphiphilic dye that readily partitions into membranes) and observed under epifluorescence microscopy for

better visualization of such higher-order structures. These fluorescence microscopy images further delineated the lamellarity of these vesicles (Figure 4.7).

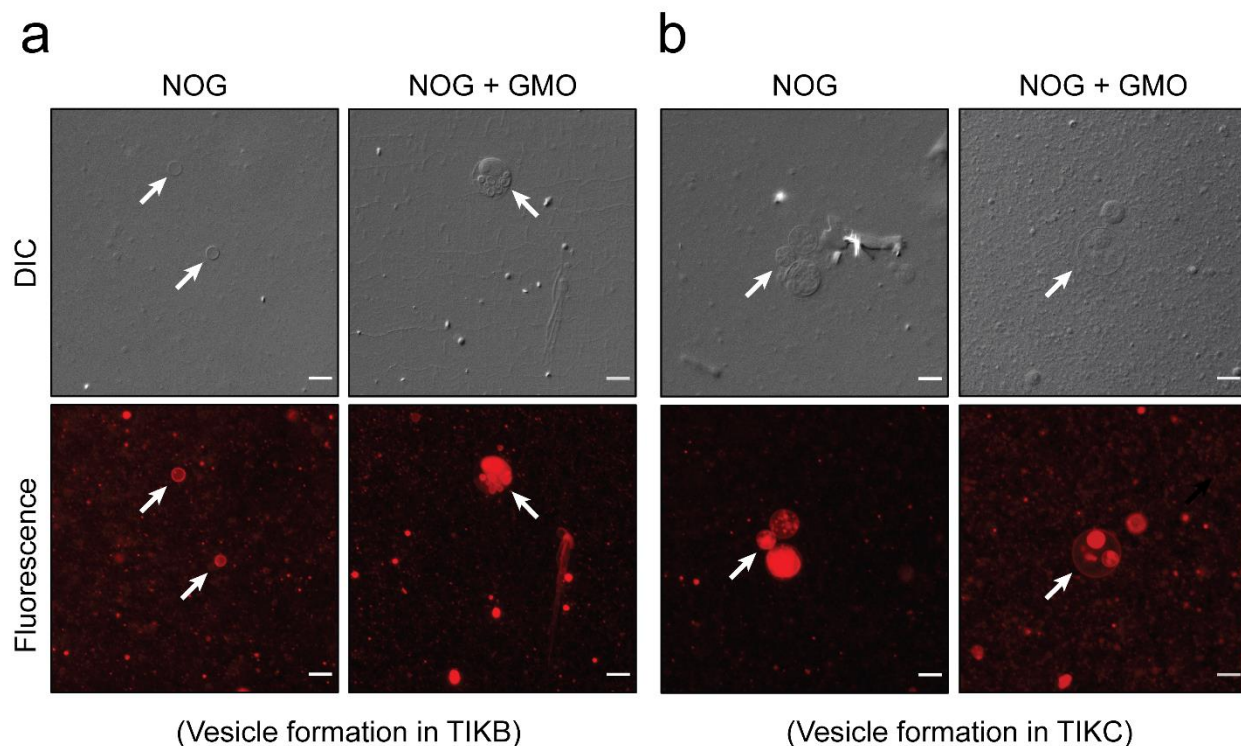


Figure 4.7 Vesicle formation behavior of NOG-based amphiphile systems in hot spring water samples. Both pure NOG (6 mM) and NOG + GMO (6 mM; 2:1 ratio) mixed systems readily form vesicles (denoted by white arrows) in (a) TIKB and (b) TIKC hot spring water samples. Vesicle morphology varies from unilamellar to multivesicular vesicles that were visualized under DIC (top panels) and fluorescence (bottom panels) microscopy. For fluorescence imaging, vesicles were stained with an amphiphilic dye named octadecyl rhodamine-B chloride (R18). Fluorescence images are pseudocolored for better visualization. The scale bar is 10 μm .

We also evaluate the vesicle formation behavior of the NOG + OOH (6 mM; 2:1 ratio) mixed system in these hot spring water samples, which could readily form vesicles in TIKC but not in TIKB (Figure 4.8). Although the lipid film hydration method generates a morphologically diverse set of vesicles in a pH-dependent manner, the variety of ions and their relative concentrations in these hot spring samples could further affect both the self-assembly and the morphology of such vesicles. It could also be a likely reason for the intriguing behavior of the NOG + OOH mixed system in these hot spring samples.

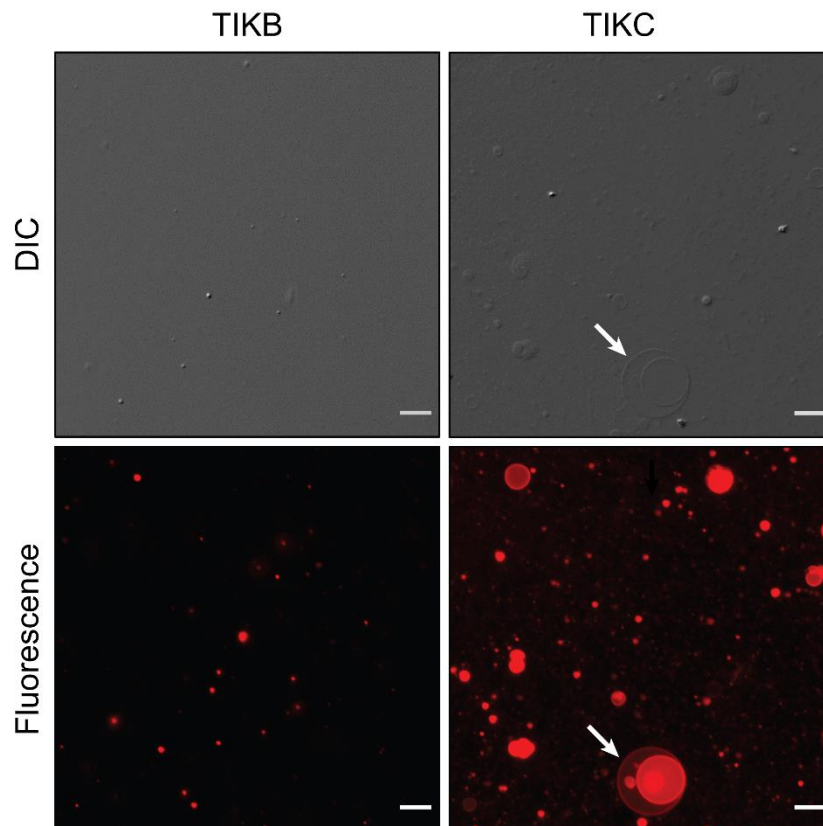


Figure 4.8 Vesicle formation behavior of NOG + OOH mixed system in hot spring water samples. NOG + OOH (6 mM; 2:1 ratio) system readily formed vesicles (indicated by white arrows) in TIKC (right panel) but not in TIKB (left panel) water. Vesicles were imaged by both DIC and fluorescence microscopy. For fluorescence imaging, vesicles were stained with an amphiphilic dye named octadecyl rhodamine-B chloride (R18). Fluorescence images are pseudocolored for better visualization. The scale bar is 10 μm .

4.4 Discussion

Our study highlights the importance of validating laboratory outcomes under natural conditions to get a more “realistic” sense of how prebiotically-pertinent reactions would actually behave in nature. In this proof-of-concept study, we systematically evaluated the membrane assembly behavior of two prebiotically-relevant SCAs systems in natural water samples collected from different hot spring sites. In the case of fatty acid-based systems, we observed that different combinations of fatty acids and their derivatives readily formed vesicles in laboratory buffered conditions. However, in hot spring waters, only a mixed system containing fatty acid and monoglyceride was able to generate vesicles. This binary system formed vesicles in all three

hot spring samples under study, which had a difference in their ionic strengths. Furthermore, these results were consistent across all the tested fatty acid systems, independent of varying chain length and unsaturation. These results demonstrate how prebiotically-pertinent processes could behave differently in “laboratory” versus “natural” conditions. We also evaluated the self-assembly behavior of our newly introduced NAA-based protoamphiphilic systems in hot spring water samples, using NOG as a representative. It was observed that NOG on its own and in combination with GMO could readily form vesicles in hot spring samples. It demonstrates the ability of NAAs to generate vesicles even in natural aqueous systems with varying ionic strengths, which further substantiates their candidature as model protocell membranes.

Shifting from a “controlled” laboratory setup to a more diverse natural setting would introduce additional factors that might influence the reaction of interest, shaping the final reaction outcome. The variation in the ionic strength of natural aqueous systems, in terms of the type of ions present and also their relative concentrations, would be one such crucial factor. Notably, geochemical analysis of the different hot spring water samples used in these experiments showed the intrinsic diversity associated with hot springs in terms of their ionic content. Therefore, the characteristic vesicle formation behavior of different SCA systems in hot spring water samples might be attributable to a combinatorial effect of multiple ions present in varying concentrations in these samples.

Nonetheless, a stabilizing effect provided by monoglycerides to SCA vesicles under hot spring conditions was found to be a more generalized phenomenon, which was consistently observed for both fatty acid- and NAA-based systems, and, importantly, across different hot spring samples. Notably, such a stabilizing effect was also observed in a recent study that evaluated the membrane assembly of fatty acid-based systems in hot spring water samples, although from a different analogue site [24]. The authors report that the binary system of fatty acid and a monoglyceride readily formed vesicles in two hot spring samples differing in their pH and ionic strength values. Together, these results support the hypothesis that mixed SCA systems, with a stabilizing counterpart like monoglycerides, could have generated robust protocell membranes capable of tolerating the fluctuating environmental conditions prevalent on the early Earth.

Finally, our study provides direct evidence for the ability of terrestrial hot springs to support the membrane assembly process from prebiotically-plausible SCAs. With their overall low ionic strength, these freshwater aqueous systems would have provided a more conducive environment for the formation of protocell compartments as compared to salt-rich marine environments. Furthermore, our results with fatty acid-based systems also indicate that these geothermal fields might have also provided a “selection mechanism,” allowing only certain amphiphile systems to form vesicles, depending on the physicochemical constraints at play in that specific niche. Together, these results suggest a potential bipartite role played by terrestrial hot springs during the origin of life on Earth; these geological settings would not only have acted as a supportive niche for the life’s origin, but also provided pertinent selection pressures to shape its early evolution.

References

1. Deamer, D. Where Did Life Begin? Testing Ideas in Prebiotic Analogue Conditions. *Life* **2021**, Vol. 11, Page 134 **2021**, 11, 134.
2. Deamer, D.; David The Role of Lipid Membranes in Life’s Origin. *Life* **2017**, 7, 5.
3. Segré, D.; Ben-Eli, D.; Deamer, D.W.; Lancet, D. The Lipid World. *Orig. Life Evol. Biosph.* **2001**, 31, 119–145.
4. Formation and Properties of Fatty Acid Vesicles (Liposomes). *Liposome Technol.* **2016**, 23–42.
5. Monnard, P.A.; Deamer, D.W. Preparation of Vesicles from Nonphospholipid Amphiphiles. *Methods Enzymol.* **2003**, 372, 133–151.
6. Monnard, P.-A.; Apel, C.L.; Kanavarioti, A.; Deamer, D.W. Influence of Ionic Inorganic Solutes on Self-Assembly and Polymerization Processes Related to Early Forms of Life: Implications for a Prebiotic Aqueous Medium. *Astrobiology* **2002**, 2, 139–152.
7. Namani, T.; Deamer, D.W. Stability of Model Membranes in Extreme Environments. *Orig. Life Evol. Biosph.* **2008**, 38, 329–341.
8. Sarkar, S.; Dagar, S.; Verma, A.; Rajamani, S. Compositional heterogeneity confers

- selective advantage to model protocellular membranes during the origins of cellular life. *Sci. Rep.* **2020**, *10*, 1–11.
9. Dalai, P.; Ustriyana, P.; Sahai, N. Aqueous magnesium as an environmental selection pressure in the evolution of phospholipid membranes on early earth. *Geochim. Cosmochim. Acta* **2018**, *223*, 216–228.
 10. Jin, L.; Kamat, N.P.; Jena, S.; Szostak, J.W. Fatty Acid/Phospholipid Blended Membranes: A Potential Intermediate State in Protocellular Evolution. *Small* **2018**, *14*, 1704077.
 11. Toparlak, Ö.D.; Karki, M.; Egas Ortuno, V.; Krishnamurthy, R.; Mansy, S.S. Cyclophospholipids Increase Protocellular Stability to Metal Ions. *Small* **2019**, 1903381.
 12. Maurer, S. The Impact of Salts on Single Chain Amphiphile Membranes and Implications for the Location of the Origin of Life. *Life* *2017*, *Vol. 7*, Page 44 **2017**, *7*, 44.
 13. Baross, J.A.; Hoffman, S.E. Submarine hydrothermal vents and associated gradient environments as sites for the origin and evolution of life. *Orig. Life Evol. Biosph.* **1985**, *15*, 327–345.
 14. Damer, B.; Deamer, D. The hot spring hypothesis for an origin of life. *Astrobiology* **2020**, *20*, 429–452.
 15. Deamer, D.W.; Georgiou, C.D. Hydrothermal Conditions and the Origin of Cellular Life. *Astrobiology* **2015**, *15*, 1091–1095.
 16. Ansari, A.; SINGH, V.; Ahmad, S.; A report on the expedition of nasa spaceward bound india programme, ladakh, india, 09th august – 19th august, 2016. **2016**;
 17. Tripathy, G.R.; Goswami, V.; Singh, S.K.; Chakrapani, G.J. Temporal variations in Sr and $^{87}\text{Sr}/^{86}\text{Sr}$ of the Ganga headwaters: estimates of dissolved Sr flux to the mainstream. *Hydrol. Process.* **2010**, *24*, 1159–1171.
 18. Sarkar, S.; Dagar, S.; Rajamani, S. Influence of Wet-dry Cycling on the Self-Assembly and Physicochemical Properties of Model Protocellular Membrane Systems. *ChemSystemsChem* **2021**, *3*, e2100032.

19. Rendón, A.; Carton, D.G.; Sot, J.; García-Pacios, M.; Montes, L.-R.; Valle, M.; Arrondo, J.-L.R.; Goñi, F.M.; Ruiz-Mirazo, K. Model Systems of Precursor Cellular Membranes: Long-Chain Alcohols Stabilize Spontaneously Formed Oleic Acid Vesicles. *Biophys. J.* **2012**, *102*, 278–286.
20. McCollom, T.M.; Ritter, G.; Simoneit, B.R. Lipid synthesis under hydrothermal conditions by Fischer-Tropsch-type reactions. *Orig. Life Evol. Biosph.* **1999**, *29*, 153–66.
21. Lawless, J.G.; Yuen, G.U. Quantification of monocarboxylic acids in the Murchison carbonaceous meteorite. *Nature* **1979**, *282*, 396–398.
22. Schmitt-Kopplin, P.; Gabelica, Z.; Gougeon, R.D.; Fekete, A.; Kanawati, B.; Harir, M.; Gebefuegi, I.; Eckel, G.; Hertkorn, N. High molecular diversity of extraterrestrial organic matter in Murchison meteorite revealed 40 years after its fall. *Proc. Natl. Acad. Sci. U. S. A.* **2010**, *107*, 2763–8.
23. Black, R.; Blosser, M. A Self-Assembled Aggregate Composed of a Fatty Acid Membrane and the Building Blocks of Biological Polymers Provides a First Step in the Emergence of Protocells. *Life* **2016**, *6*, 33.
24. Milshteyn, D.; Damer, B.; Havig, J.; Deamer, D. Amphiphilic Compounds Assemble into Membranous Vesicles in Hydrothermal Hot Spring Water but Not in Seawater. *Life* **2018**, *8*, 11.

Chapter 5

Summary and conclusions

The origin of life on Earth is thought to have followed a fundamental step of protocell formation. This process would have been influenced by a dynamic interplay between membrane assembly and abiotic synthesis of peptides and nucleic acids. Towards this, we studied the effect of phospholipids as model membrane-forming amphiphiles on the abiotic peptide synthesis from glycine, under prebiotically-pertinent wet-dry cycling conditions. It was observed that peptides do form in the presence of lipids, albeit at a lower yield. A systematic investigation in this regard led to the serendipitous discovery of N-acyl amino acids (NAAs) in the reaction. Thus, a mixture of phospholipids and amino acids under wet-dry cycles resulted in two competing processes, simultaneously forming peptides and NAAs from a common set of reactants. Moreover, the synthesis of NAAs was observed with other amino acids and ester-linkage containing phospholipids, indicating the generality of this reaction. The NAA synthesis likely follows an ester-amide exchange mechanism, which is the first experimental demonstration of this process in a lipid-amino acid system under prebiotically-plausible conditions.

NAA is a hitherto uncharacterized class of protoamphiphiles that might have generated membrane compartments of protocells. Therefore, we systematically explored different properties of NAAs to assess their potential as a model protoamphiphile system. Firstly, we demonstrated a new prebiological route for their synthesis under wet-dry cycles, from amino acids and an ester-linkage containing SCA like GMO. It supports their potential availability on the early Earth. Subsequently, we evaluated the membrane assembly behavior of NAAs, which is a crucial property for them to act as model protocell membranes. NAAs like NOG and NOS, were found to self-assemble into vesicles at acidic pH, contrary to fatty acids (conventional model protoamphiphiles) that form vesicles at neutral to alkaline pH conditions. Furthermore, heterogeneous amphiphile systems containing NOG and GMO/OA, were able to generate vesicles over a broad pH range. Particularly, the blended vesicles made from NOG and GMO were also stable in the presence of metal ions. Together, these results demonstrate the potential of such heterogeneous amphiphilic systems in generating robust protocell compartments, which could have supported a wide range of prebiotic reactions occurring at specific conditions of pH and metal ion concentrations. Notably, NOG was also able to act as a substrate for peptide chain growth under wet-dry cycling conditions, wherein the amino acid head group moiety reacted with amino acids, resulting in the formation of lipopeptides. Such lipopeptides might have had implications for the functionalization of protocell membranes. Altogether, these results establish

NAAAs as a new model protoamphiphile system and highlight their putative role in shaping the emergence and evolution of functional protocell membranes on primitive Earth.

Finally, to get a more “realistic” sense of how prebiotic membrane assembly processes would materialize under natural conditions, we studied the vesicle formation by fatty acid and NAA-based amphiphile systems, in actual water samples collected from different hot spring sites. Pertinently, terrestrial hot springs are considered one of the plausible niches for life’s origin and also provide an excellent aqueous system to evaluate the simultaneous effect of multiple ions on the prebiotic processes like that of membrane assembly. For fatty acid-based systems, although different combinations of fatty acid and its derivatives readily formed vesicles in laboratory buffered conditions, only a mixture of fatty acid and monoglyceride was able to generate vesicles in hot spring water samples. Also, there was a positive correlation between the overall vesicle-forming propensity and the ionic strength of different hot spring samples. These results were consistent irrespective of the fatty acid chain length and the presence of unsaturation. In the case of NAA-based amphiphile systems, both pure NOG and NOG + GMO mixed systems were able to self-assemble into vesicles in hot spring samples. These results illustrate how prebiotically-pertinent processes could materialize differently in “laboratory” versus “natural” conditions, thus highlighting the importance of validating laboratory outcomes in a natural environment. Our results also demonstrate how terrestrial freshwater bodies such as hot springs could support the prebiotic membrane assembly process with their overall low ionic strength. Furthermore, as observed with fatty acid-based systems, such geochemical settings might also provide different selection pressures, under which certain amphiphile combinations preferentially form vesicles over the others. It signifies a potential dual role played by terrestrial hot springs in modulating the early events during life’s origin; providing a conducive environment for protocell formation while also exerting different selection pressures, thereby shaping their evolution.

PUBLICATIONS

- Joshi, M. P., Steller, L., Van Kranendonk, M. J., & Rajamani, S. (2021). Influence of Metal Ions on Model Protoamphiphilic Vesicular Systems: Insights from Laboratory and Analogue Studies. *Life*, 11(12), 1413. [Link](#)
- Joshi, M. P., Sawant, A. A., & Rajamani, S. (2021). Spontaneous emergence of membrane-forming protoamphiphiles from a lipid–amino acid mixture under wet–dry cycles. *Chemical Science*, 12(8), 2970-2978. [Link](#)
- Sarkar, S., Das, S., Dagar, S., Joshi, M. P., Mungi, C. V., Sawant, A. A., Patki, G.M., & Rajamani, S. (2020). Prebiological Membranes and Their Role in the Emergence of Early Cellular Life. *The Journal of Membrane Biology*, 253(6), 589-608. [Link](#)
- Joshi, M. P., Samanta, A., Tripathy, G. R., & Rajamani, S. (2017). Formation and stability of prebiotically relevant vesicular systems in terrestrial geothermal environments. *Life*, 7(4), 51. [Link](#)

ARCHIVES

- Joshi MP, Uday A, Rajamani S. Elucidating N-acyl amino acids as a model protoamphiphilic system. *ChemRxiv*. Cambridge: Cambridge Open Engage; 2022
DOI: [10.26434/chemrxiv-2022-wxxtq](https://doi.org/10.26434/chemrxiv-2022-wxxtq)

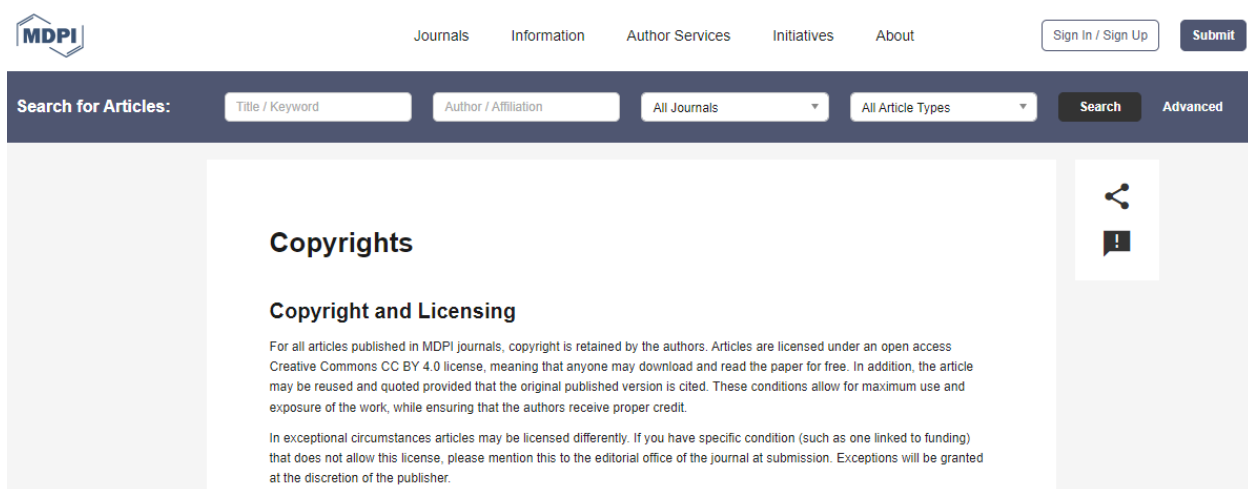
COPYRIGHT LICENSCE PERMISSIONS

Permission for reuse of –

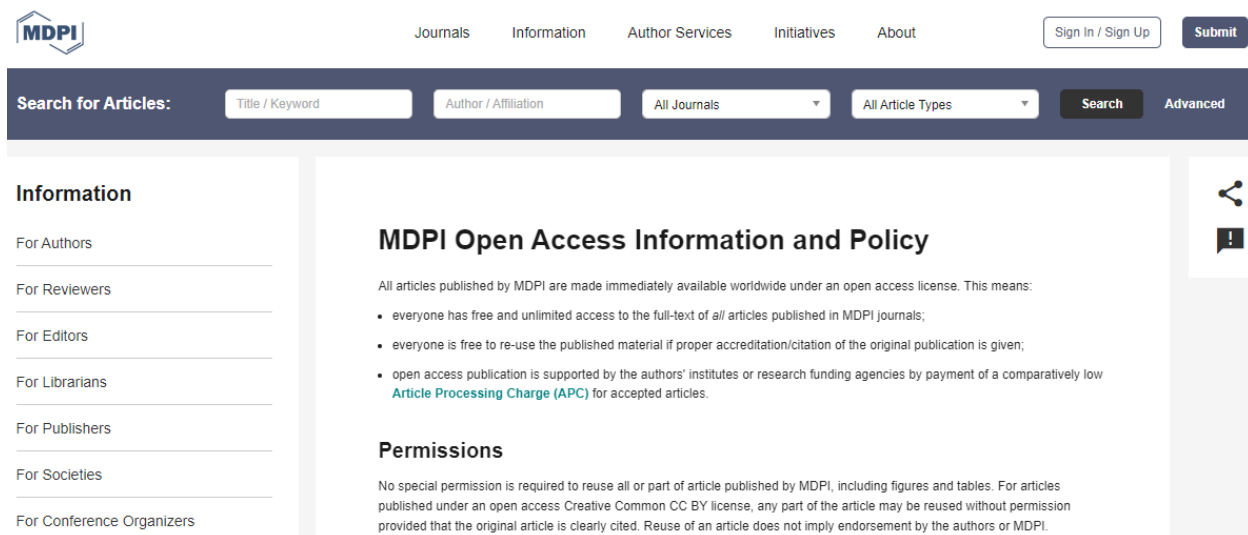
- Joshi, M. P., Steller, L., Van Kranendonk, M. J., & Rajamani, S. (2021). Influence of Metal Ions on Model Protoamphiphilic Vesicular Systems: Insights from Laboratory and Analogue Studies. *Life*, 11(12), 1413

AND

- Joshi, M. P., Samanta, A., Tripathy, G. R., & Rajamani, S. (2017). Formation and stability of prebiotically relevant vesicular systems in terrestrial geothermal environments. *Life*, 7(4), 51



The screenshot shows the MDPI website's 'Copyrights' page. At the top, there is a navigation bar with the MDPI logo on the left and links for 'Journals', 'Information', 'Author Services', 'Initiatives', and 'About' in the center. On the right side of the navigation bar are 'Sign In / Sign Up' and 'Submit' buttons. Below the navigation bar is a search bar with the text 'Search for Articles:' and four input fields: 'Title / Keyword', 'Author / Affiliation', 'All Journals' (with a dropdown arrow), and 'All Article Types' (with a dropdown arrow). To the right of these fields are 'Search' and 'Advanced' buttons. The main content area has a light gray background. On the left, there is a vertical sidebar with a 'Share' icon and an 'Alert' icon. The main text area is titled 'Copyrights' and 'Copyright and Licensing'. The text states: 'For all articles published in MDPI journals, copyright is retained by the authors. Articles are licensed under an open access Creative Commons CC BY 4.0 license, meaning that anyone may download and read the paper for free. In addition, the article may be reused and quoted provided that the original published version is cited. These conditions allow for maximum use and exposure of the work, while ensuring that the authors receive proper credit. In exceptional circumstances articles may be licensed differently. If you have specific condition (such as one linked to funding) that does not allow this license, please mention this to the editorial office of the journal at submission. Exceptions will be granted at the discretion of the publisher.'



The screenshot shows the MDPI website's 'MDPI Open Access Information and Policy' page. The layout is similar to the previous screenshot, with the same navigation bar and search bar. The main content area has a light gray background. On the left, there is a vertical sidebar with a 'Share' icon and an 'Alert' icon. The main text area is titled 'MDPI Open Access Information and Policy'. The text states: 'All articles published by MDPI are made immediately available worldwide under an open access license. This means:'. Below this are three bullet points: 'everyone has free and unlimited access to the full-text of all articles published in MDPI journals;', 'everyone is free to re-use the published material if proper accreditation/citation of the original publication is given;', and 'open access publication is supported by the authors' institutes or research funding agencies by payment of a comparatively low Article Processing Charge (APC) for accepted articles.' Below the bullet points is a section titled 'Permissions' with the text: 'No special permission is required to reuse all or part of article published by MDPI, including figures and tables. For articles published under an open access Creative Common CC BY license, any part of the article may be reused without permission provided that the original article is clearly cited. Reuse of an article does not imply endorsement by the authors or MDPI.'

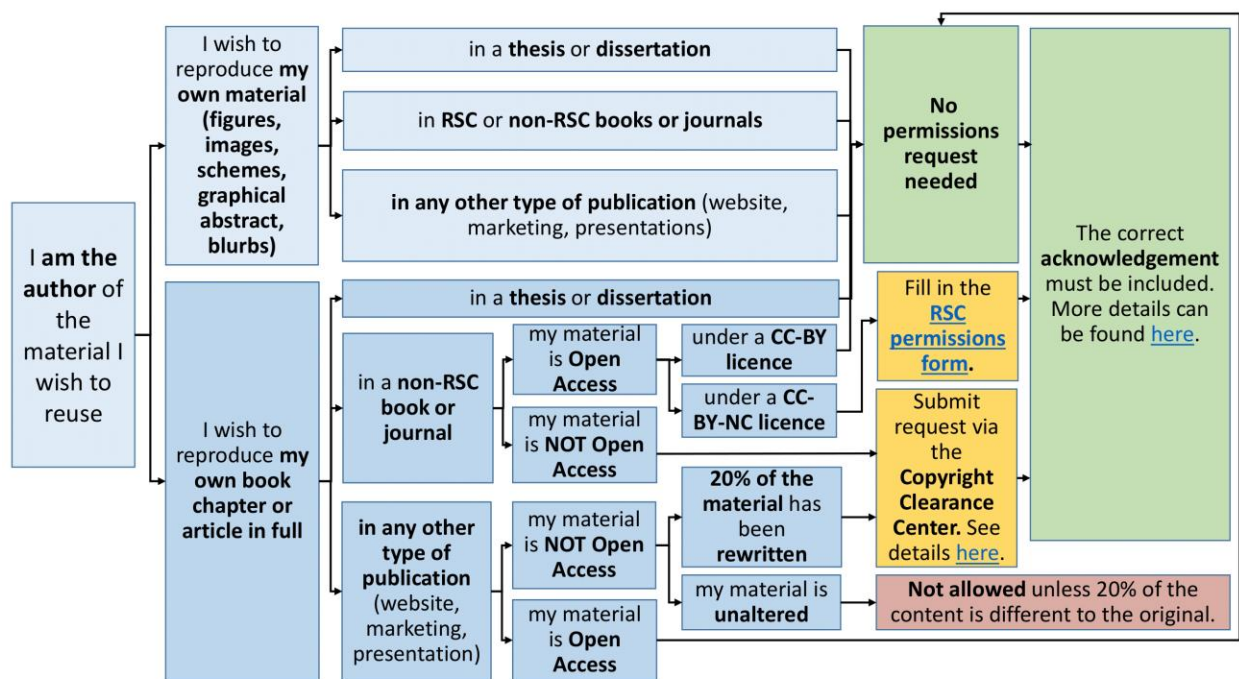
Permission for reuse of –

- Joshi, M. P., Sawant, A. A., & Rajamani, S. (2021). Spontaneous emergence of membrane-forming protoamphiphiles from a lipid–amino acid mixture under wet–dry cycles. *Chemical Science*, 12(8), 2970–2978.

Reusing Royal Society of Chemistry material

Reuse permissions requests

Material published by the Royal Society of Chemistry (RSC) and other publishers is subject to all applicable copyright, database protection and other rights. The graphic below outlines the steps to obtain permission to reuse RSC materials, where required:



Author reusing their own work published by the RSC

You do not need to request permission to reuse your own figures, diagrams, tables, or images that were originally published in an RSC publication. However, permission should be requested for use of the whole article or chapter except if reusing it in a thesis. If you are including an article or book chapter published by the RSC in your thesis please ensure that your co-authors are aware of this.

Reuse of material that was published originally by the RSC must be accompanied by the appropriate acknowledgement of the publication. The form of the acknowledgement is dependent on the journal in which it was published originally, as detailed in the ['Acknowledgements' section](#).